LASER INDUCED FLUORESCENCE STUDIES OF JET-COOLED AROMATIC AMINES

by

Rachel Howell

Submitted in partial fulfilment for the degree of

Doctor of Philosophy

to

Imperial College of Science Technology and Medicine

University of London

1990

ABSTRACT

This thesis is concerned with laser induced fluorescence studies of aromatic amines cooled in a supersonic jet expansion. A general introduction is given and the experimental techniques employed are outlined.

LIF excitation and emission spectra of jet cooled 4-N,N-dimethylaminobenzonitrile, 4-N,N-dimethylaminoethylbenzoate and 4-N,N-dimethylaminomethylbenzoate. These molecules are of interest because in polar solvents, in addition to emission from the locally excited state they exhibit an anomalous red shifted fluorescence which has been attributed to emission from a TICT state. The data obtained here reveal a red shifted emission band, however it is assigned as emission arising from formation of a ground state dimer which undergoes reorganisation in the excited state to give excimer emission. LIF emission spectra of DMABN complexed with various solvents are also presented and similar emission is observed, which is assigned in terms of fluorescence from solvated monomer and dimer species.

The theme of ground state dimers is continued with a study of the jet cooled N-ethylcarbazole dimer. This molecule, unlike the dimer of DMABN, exhibits structured fluorescence spectra characteristic of emission from the initially excited dimer state.

The jet cooled LIF excitation and emission spectra of the molecule N-(4-cyanophenyl)carbazole are presented for the first time. This molecule is of interest in the context of this thesis as it exhibits only emission from the TICT state in polar solvents. The spectra are assigned and discussed in terms of the related molecules carbazole and benzonitrile.

ACKNOWLEDGEMENTS

Firstly, I would like to express my gratitude to my supervisor Professor David Phillips for his encouragement and advice throughout the course of this work.

I am also grateful to all members of Prof. Phillip's group both at the Royal Institution and Imperial College, especially Wim Bouwman and Evelyn Joslin, who created a friendly and enthusiastic atmosphere in which to study. In particular I wish to thank Dr. Alan Taylor and Dr. Anita Jones for their friendship and guidance during this project.

I would also like to acknowledge Professor Keitaro Yoshihara and Dr Hrvoje Petek for their help during my time in Okazaki.

It is appropriate that I thank the SERC for financial support to pursue this project.

Finally, I would like to thank Mum and Dad for their unfailing patience and support.

CONTENTS

LIST OF FIGURES

LIST OF TABLES

CHAPTER ONE: GENERAL INTRODUCTION

1.1 Introduction

Laser induced fluorescence studies of the molecules 4-N,N-dimethylaminobenzonitrile, 4-N,N-dimethylamino ethyl- and methyl- benzoate, N-(4-cyanophenyl)carbazole and the dimer of N-ethylcarbazole are presented in this thesis. An introduction to each molecule and a summary of previous studies are given in the relevant chapters, so the aim here is to introduce very briefly some general concepts used throughout this thesis.

Two photophysical processes are fundamental to this thesis: absorption of electromagnetic radiation by a molecule and the subsequent dissipation of energy by fluorescence, these are illustrated in figure 1.1. Fluorescence is defined simply as the spontaneous electric dipole transition from an excited to a lower electronic state of the same multiplicity, usually the ground electronic state.

1.2 Solvent effects

Most absorption and fluorescence studies are carried out in the presence of a solvent medium. When an aromatic molecule is placed in a solvent environment it experiences short and long range forces that affect the absorption and emission spectra of the absorbing species. These solvent interaction forces such as hydrogen bonding, dipole-dipole, dipole-induced dipole interactions and other higher order interactions within the solvent, tend to affect the energy

Figure 1.1 Schematic diagram showing solvent relaxation

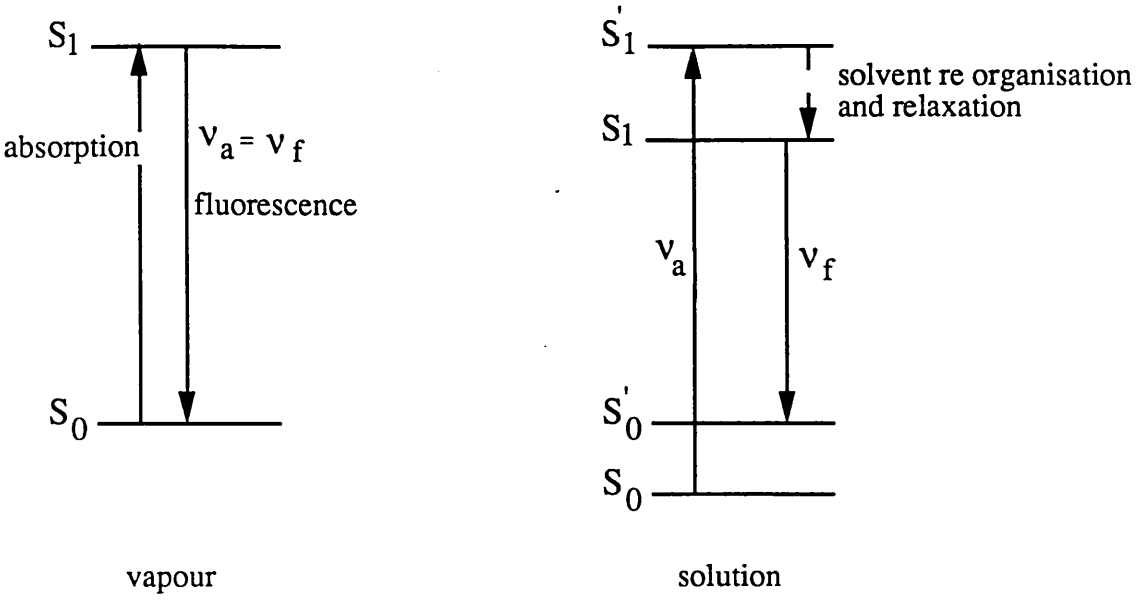

Figure 1.2 The origin of the observed spectral shift of a gas phase complex

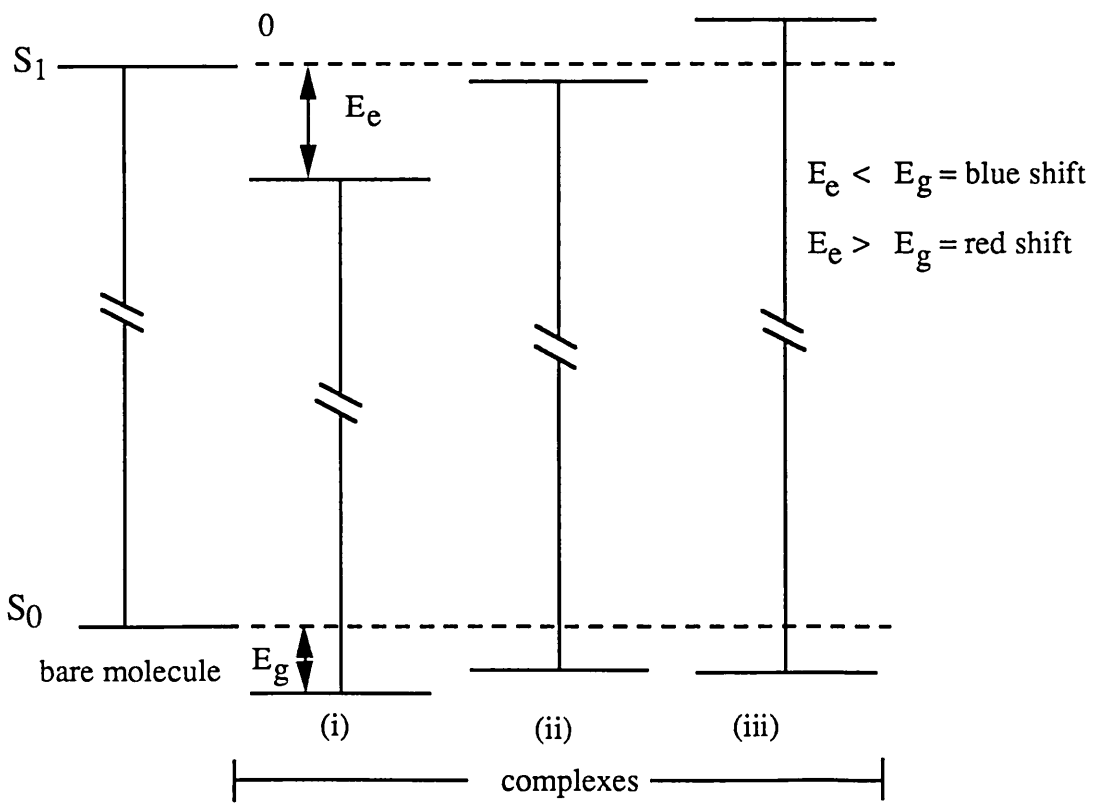

difference between the ground and excited states of the absorbing species, and the observed spectra are therefore characteristic of the molecule in its solvent environment rather than of the isolated molecule. The general effect of the solvent relaxation is illustrated in figure 1.1. In the vapour phase the 0-0 tansitions in the absorption and fluorescence of a molecule are identical, however in the presence of a solvent these bands are no longer coincident. From Onsager theory the difference in the energy of the 0-0 bands in absorption and emission is given by[1]:

$$\Delta\nu = \frac{2(\mu_1 - \mu_0)^2}{hca^3}\left[\frac{(\epsilon-1)}{(2\epsilon+1)} - \frac{(n^2-1)}{(2n^2+1)}\right] \qquad (1)$$

Where

μ_0 and μ_1 are the solute dipole moments in the ground and excited states respectively, ϵ = solvent dielectric constant, n = solvent refractive index, a = Onsager cavity radius, c = speed of light and h = Planck's constant.

For non polar solvents $n^2 \approx \epsilon$, and no shifts are observed; for polar solvents the magnitude of the shift can be large and is dependent on the extent to which the dipole moment changes on excitation, the solvent dipole moment and the extent of the solute - solvent interaction.

Electronic transitions from one state to another by absorption of photons are assumed to be much faster than molecular motions therefore it is the solvent cage around the ground state molecule that determines the initial perturbation of the excited state. However, the mobility of

the solvent cage in the condensed phase allows stabilisation forces to re-arrange the solvent shell before emission can occur (see figure 1.1), any energy changes for this being provided by the motions of the surrounding medium. Fluorescence from this re-arranged state is assumed rapid, producing a new ground state solvent cage.

In general for $\pi\pi^*$ transitions the higher energy electronic state is such that the electron cloud is more dispersive and polarisable, therefore experiencing greater dispersive interactions from the solvent than the ground state, and hence enhanced stabilisation, giving rise to a bathochromic shift.

In the solution phase bulk solvent properties are thought to dominate over specific solvent - solute interactions, although these interactions may also occur, being of a similar nature to those occurring within the solvent environment.

In this thesis all experiments are performed in a supersonic jet environment, therefore there is no possibility of chromophores diffusing together in the expansion as can occur in the solution phase; any contact between chromophores occurs in the initial stages of the expansion and as such any solvent - solute complexes and dimers are formed in the ground state prior to electronic excitation. In the supersonic jet environment it is possible to envisage several types of behaviour, namely the formation of isolated un-solvated molecules, or specific solute - solvent complexes of well defined structure and low stoichiometry, or ill defined clusters of the solute with larger numbers of solvent

molecules. In the latter situation, the forces involved include solvent - solvent and solvent - solute interactions. If an aromatic molecule interacts with a solvent molecule exothermically then the energy of the ground state will be lowered. If they were to react in such a way that there was an increase in energy then they would not form a complex in the jet - cooled environment. The presence of the solvent molecule can also perturb the energy of the excited state, and three types of behaviour can be envisaged(as illustrated in figure 1.2.):

i) The attractive interaction between the molecules is stronger in the excited state, resulting in a shift of the origin transition to lower energy than for the unsolvated molecule, known as a red or bathochromic shift.

ii) There is an attractive interaction upon excitation though not as strong as in the ground state, resulting in a shift of the complex transition to higher energy than for the unsolvated molecule, i.e. a blue or hypsochromic shift.

iii) The interaction is repulsive in the excited state, resulting in a hypsochromic shift from the unsolvated molecule origin transition.

Well defined complexes are characterised by appropriately well defined spectra whereas larger clusters exhibit bulk solvent - like behaviour. The transition between these two cases is difficult to establish without the benefit of mass resolution, as demonstrated for carbazole - argon mixed expansions[2].

1.3 Self Complexation

In the supersonic jet environment many weakly bound species may be formed that are unstable under normal conditions. One such type of species that may be formed at high sample 'concentrations' is a ground state self complex of the sample under investigation. It is not possible to determine the stoichiometry of such complexes in this work, however under the conditions used a dimeric species is considered to be the most likely. Upon excitation of this ground state dimer to the S_1 state two types of excited state dimers can be envisaged. Classically the term excimer is used to describe any excited state dimer[3], however in the course of this work the terms molecular dimer and excimer are used to describe two different types of emission behaviour from the excited state dimer, these two cases are depicted in figure 1.3. Molecular dimer refers to emission from the directly excited dimer state, and is typically characterised by a perturbed monomer spectrum, as seen for the dimer of carbazole[4]. The term excimer is used to describe a state of the excited dimer that lies close in energy to the initially excited state and results from some reaction of the dimer along the intermolecular coordinates such that the Franck-Condon overlap with the ground state is different from the initially excited state, as is the case for the fluorene dimer[5] This overlap is typically with the repulsive 'wall' of the ground state potential surface, giving rise to emission that is broad, structureless and red shifted from the excitation energy. Transformation to this excimer state

Figure 1.3. A model of the potential surfaces for the two types of excited state dimer behaviour.

a) Molecular dimer.

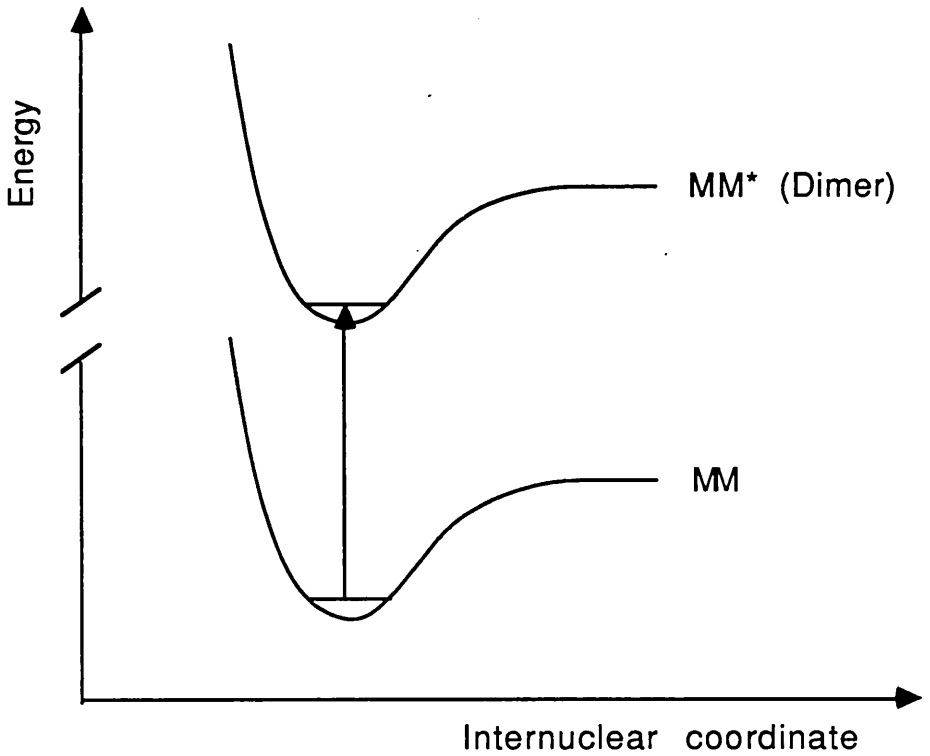

b) Coupled Excimer.

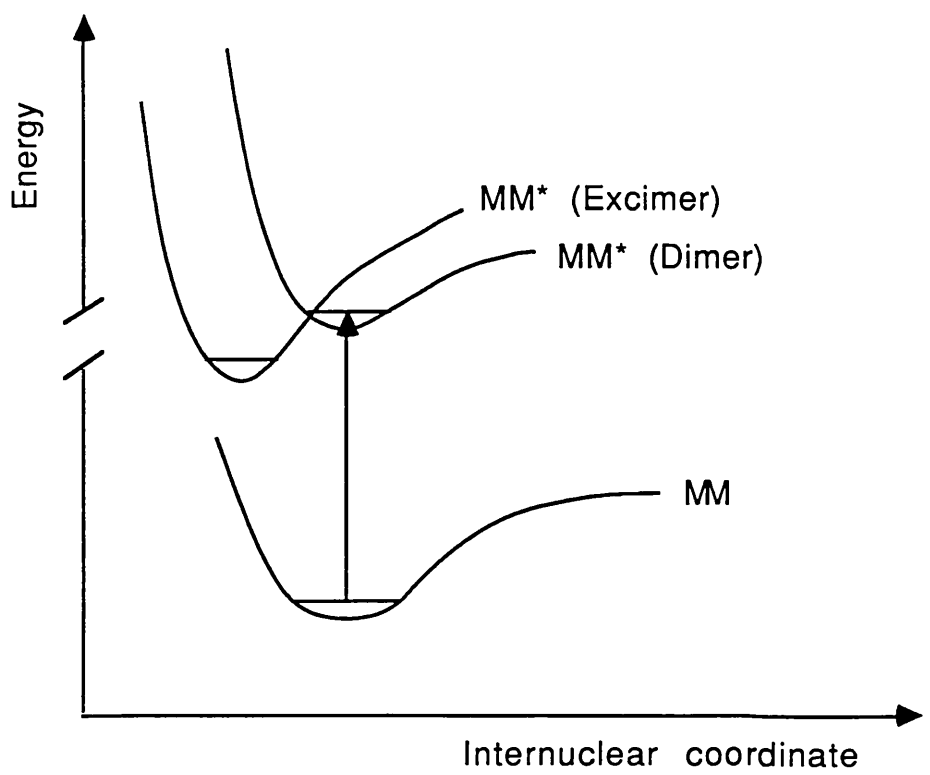

may in some cases be barrierless or have a small but finite barrier: in some cases this barrier is such that excimer formation is precluded.

1.4 Charge Transfer State Phenomena

Excited state charge transfer is a commonly observed phenomenon. Intermolecular charge transfer can occur between two aromatic molecules or between one molecule and its solvent environment giving rise to a specific low stoichiometry exciplex (excited state complex) as is the case for anthracene exciplexes with dimethylaniline[6]. In the context of this thesis it is *intra*molecular charge transfer that is of principle importance. Many of the molecules studied consist of a donor moiety and an acceptor moiety and so have the possibility of intramolecular charge transfer. In most of the cases considered here charge transfer is facilitated by twisting of the bond connecting the two moieties and solvent relaxation then stabilises the polar charge transfer state. Formation of such a twisted intramolecular charge transfer state[7] gives rise to red shifted emission which is typically broad and structureless even under jet cooled conditions. In chapter three the twisted intramolecular charge transfer state is discussed in more detail.

1.5 Terminology

The term origin transition is used in this thesis to describe that electronic transition which, upon the interaction of a molecule with electromagnetic radiation, results in the excitation from the vibrationless ground state to the vibrationless zero point level of an excited state. As such it does not result in any change in vibrational quantum number.

The following terminology has been adopted for assignment of spectra: 0(0,0) represents the origin transition, and for example ß(0,1) represents a transition from zero quanta of a ground state bending vibration to one quantum of the first electronic excited state bending vibration.

In the tables of relative energies presented in this thesis all spectral shifts are quoted as positive values. It is worth noting here that in the case of excitation spectra a positive value indicates a hypsochromic shift from the electronic origin transition, and in the case of emission spectra a positive value denotes a bathochromic shift from the resonance band (i.e. that emission band in resonance with the excitation energy).

As previously stated, the aim here was to introduce very briefly some of the key concepts used in this thesis, more complete discussions of these concepts are given in subsequent chapters.

1.6 References

1 S.R.Meech,
PhD thesis, University of Southampton (1983)

2 S.Leutwyler and J.Bösiger,
Faraday Discuss. Chem. Soc. 86 (1988) paper.

3 J.B.Birks,
"Photophysics of Aromatic Molecules,
Wiley-Interscience, New York (1970)

4 A.G.Taylor, A.C.Jones and D.Phillips,
Chem. Phys. 138 (1989) 413.

5 H.Saigusa and M.Itoh,
J. Phys. Chem 89 (1985) 5486.

6 M.Castella, A.Tramer and F.Piuzzi,
Chem. Phys. Letters 129 (1986) 112.

7 W.Rettig,
Angew. Chem. Int. Ed. Engl. 25 (1986) 971.

CHAPTER TWO - EXPERIMENTAL METHODS

2.1 Introduction

The purpose of this chapter is to outline the experimental techniques employed in order to obtain the data presented in this thesis. A discussion of the salient points of supersonic jet spectroscopy will be given in section 2.2, and the experimental apparatus used to record the laser induced fluorescence excitation and emission spectra will be briefly described in section 2.3.

2.2 The Supersonic Jet

The use of a supersonic free jet expansion as a means of preparing internally cold isolated gas phase molecules was originally investigated by Kantrowitz and Grey[1] and has over many years become a widely accepted technique. The use of such a technique in spectroscopic investigations is now well established and there have been many review articles published in the literature[2-6]. A major advantage gained by using such a technique is the simplification of gas phase spectra of polyatomic molecules,since when recorded under supersonic jet expansion conditions these are generally free from sequence congestion, hot bands, as well as solvent and lattice effects.

2.2.1 Basic Concepts

A supersonic free jet expansion is produced when a sample molecule is seeded into an inert gas at relatively high pressure P_0 and then allowed to expand through a small orifice of diameter D, into a region of lower pressure,P_1. In the experiments presented in this thesis the orifice was in the form of a small circular hole in a thin wall.

In the initial stages of the expansion, downstream of the nozzle, a series of binary collisions take place between the inert carrier gas atoms and the seeded sample molecules. These collisions result in narrowing the distribution of translational velocities of the beam constituents, and hence confining their translational energy to a very narrow distribution. An inert atomic gas such as helium has no rotational or vibrational degrees of freedom, and consequently has a low heat capacity which makes it an ideal carrier gas for producing large temperature decreases in the expansion.

As the translationally cold carrier gas atoms undergo further collisions with the sample molecules, there is subsequent energy transfer from the molecular rotational and vibrational degrees of freedom to the 'translational bath' of the carrier gas atoms.This results in cooling of the vibrational and rotational degrees of freedom of the sample molecules. Rotational and vibrational degrees of freedom transfer energy with differing efficiency, the cross section for rotational energy transfer being higher than that for vibrational transfer. This results in the population of the rotational

states of the molecules being consistent with lower temperatures than their vibrational counterparts.Rotational simulation work on the contours of aniline [7] (figure 2.1) suggest that under the expansion conditions described in section 2.2.3, the rotational temperature is approximately 2.5K, whilst the persistence of hot bands in the excitation spectra of carbazole recorded in this laboratory suggests that the vibrational temperature for some molecules is somewhat higher, approximately 50K[8].

As the expansion proceeds the sample number density decreases, and eventually becomes too low for further collisions to occur, at which point no further energy can flow from the internal degrees of freedom to the 'translational bath'. The system is effectively frozen in the state in which it enters this collision free region .The molecules do not undergo any further collisions until they have proceeded so far downstream of the nozzle that the expansion becomes 'aware' of the presence of background gases in the expansion chamber.

It is the collision free region of the expansion that is interrogated in spectroscopic investigations since the energy of the system cannot change without interaction with a source of energy such as a photon.

2.2.2 Theoretical Considerations

An expansion into free space proceeds as an initially cylindrical flow followed by flow as if from a virtual point source, after which point the expansion can be considered to

Figure 2.1 Rotational simulation of the aniline origin band contour

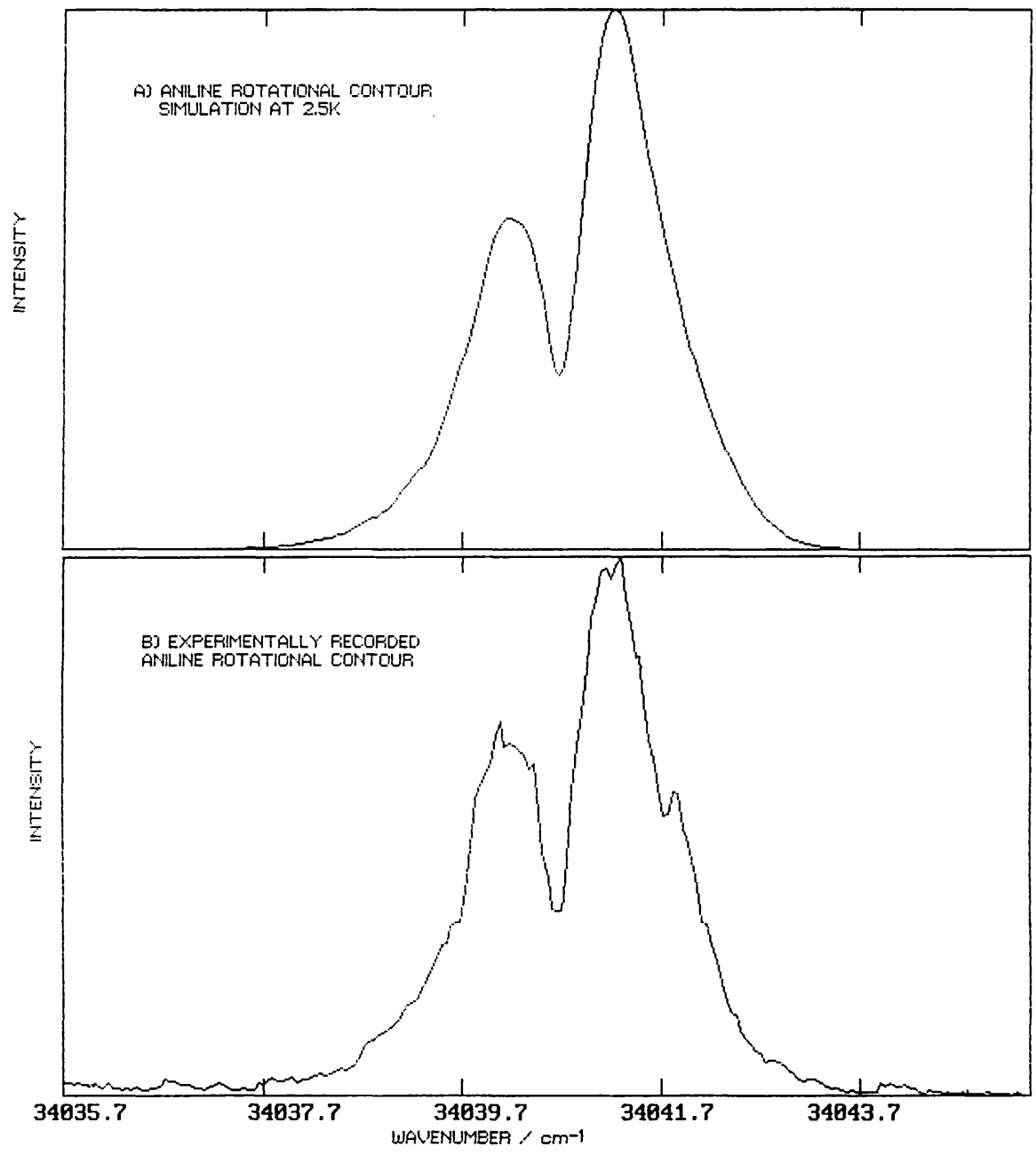

be approximately isentropic[9]. During this expansion the translational temperature decreases due to the initially random thermal motion of the beam constituents being restricted to mass flow in one direction. The velocity of the beam constituents along this directed flow path increases. Variation of the temperature of the expansion can be expressed in simple thermodynamic terms by the equation[10]:

$$\frac{T_o}{T} = 1 + \left[\frac{(\gamma - 1)}{2}\right] M^2 \qquad ...(1)$$

where:

T_o= Temperature of gas in nozzle prior to expansion

γ= Gas constant per unit mass, given by Cp / Cv, where Cp is the heat capacity at constant pressure per unit mass, and C_v is the heat capacity at constant volume.

M = Mach number, given by:

$$M = u/a \qquad ....(2)$$

where u is the velocity of the gas along the directed flow path and a is the local velocity of sound.The local velocity of sound is given by the expression:

$$a = (\gamma r T)^{1/2} \qquad ....(3)$$

(where r = Cp-Cv)

and hence decreases at lower temperatures, for example at 393K a=367ms^{-1} and at 10K a= 58.7ms^{-1}.

The Mach number in a supersonic jet is greater than unity, hence the beam constituents can be said to travel at 'supersonic' velocities, but this is due to the low velocity of sound rather than high particle velocities.

The Mach number, and hence cooling of the expansion,is dependent on the distance from the nozzle, and can be approximated by the expression[11]:

$$M = A\ (X/D)^{\gamma-1} \qquad ....(4)$$

X = distance downstream from nozzle

D = diameter of nozzle

A = constant (related to γ , empirically determined as 3.26 for argon)

There are limitations to the accuracy of equation (2), in the fact that it only describes the region of the expansion where the density of beam constituents is high enough for binary collisions to take place. As the expansion proceeds too few collisions take place to affect the translational velocity distribution, hence a terminal Mach number is obtained [12], which can be expressed as:

$$M_t = \epsilon(L_o/D)^{(1-\gamma)/\gamma} \qquad ....(5)$$

where L_o is the mean free path of the atoms in the expansion, and ϵ.is an experimentally determined constant, characteristic for a particular gas.

For Argon;

$$M_t = 133(P_oD)^{0.4} \quad ....(6)$$

where:

P_o = Backing pressure of carrier gas

D = diameter of nozzle

Thus the terminal Mach number, and hence degree of cooling is solely dependent on the backing pressure, P_o, and the diameter of the nozzle D.The terminal translationl temperature can be obtained by substitution of (6) into (4):

For Argon:

$$T_o/ T = 1+ 5896 (P_oD)^{0.8} \quad ....(7)$$

At a certain distance downstream of the nozzle, background gases present in the vacuum chamber begin to interact with the free molecular flow of the expansion. A transition from free flow to that influenced by the chamber takes place[13], and a shock boundary known as a Mach disc is encountered. The axial position of this disc can be determined by:

$$X_m = 0.67D(P_0/P_1)^{1/2} \quad ....(8)$$

Where:

X_m = distance of Mach disc from nozzle

P_1 = background pressure in expansion chamber

The useful region of the expansion for spectroscopic study lies between the distance from the nozzle at which terminal Mach number is reached (X_t) and the Mach disc is reached (X_m). A value for X_t can be found from equations (4) and (6) Using a 200 micron nozzle and argon carrier gas at 0.08bar the useful range of study is 1.2mm< X <4.2mm. In most cases using a 100micron nozzle and helium carrier gas at 4bar whilst investigating the beam 4mm downstream of the nozzle no features attributable to the Mach disc were observed.

For an isentropic expansion, the density of the gas falls proportionally with X^2, where X is the distance from the nozzle. The sample density variation can be expressed as:

$$\frac{\rho}{\rho_o} = \left[\frac{X_t}{X}\right]^2 \left[\frac{T}{T_o}\right]^{(1/\gamma-1)} \qquad \ldots.(9)$$

for $X_{min} < X < X_o$

where:

X_{min} = 2.5D for argon

X_o = axial virtual origin - point at which flow is no longer cylindrical.

ρ = density of expansion

ρ_o = density of reservoir

X_t can be found from M_t given by equations (4) and (6) and T can be found from M_t and equation (1). By using argon carrier gas and X=4mm, the ratio ρ/ρ_o is approximately 8.2×10^{-4}. The sample vapour pressure is approximately 1mB, hence , assuming perfect gas law, the sample density at 4mm is ~ 2×10^{16} per litre, which is equivalent to an effective concentration of ~3×10^{-8} Molar.

The introduction of small partial pressures of polyatomic molecules into the expansion is thought to have a negligible effect on cooling because of the large number of collisions undertaken before the terminal Mach number is reached.

2.2.3 Experimental Procedure

The supersonic jet apparatus used in all experiments except those relating to DMABN produced a continuous flow expansion. The apparatus is depicted in figure 2.2 and has been discussed in detail elsewhere[6].

The sample of interest is heated in a stainless steel oven using resistive heater elements to give sufficient vapour pressure. The oven / nozzle assembly , which is supported by the top flange of the expansion chamber, is shown in figure 2.3. The sample vapour is then mixed with helium carrier gas at a backing pressure of typically 4bar, and the resultant mixture allowed to expand through a continuous flow nozzle of diameter 100-200microns into the expansion chamber. The nozzle is made from 1/4" OD stainless steel cylinder, 1/8" internal diameter, which has a small orifice drilled into the 0.005" thick end wall.

The expansion chamber is maintained at a pressure of less than 0.01mbar by a vapour booster pump(Edwards 18B4A,throughput capacity 4000ls^{-1} at 10^{-4} mbar) backed up by a rotary pump (Edwards EM275, throughput capacity 100ls^{-1} at 1mbar pressure, typical input pressure of booster pump). To allow access to the chamber without letting the pumps up to atmospheric pressure, a large baffle valve is incorporated

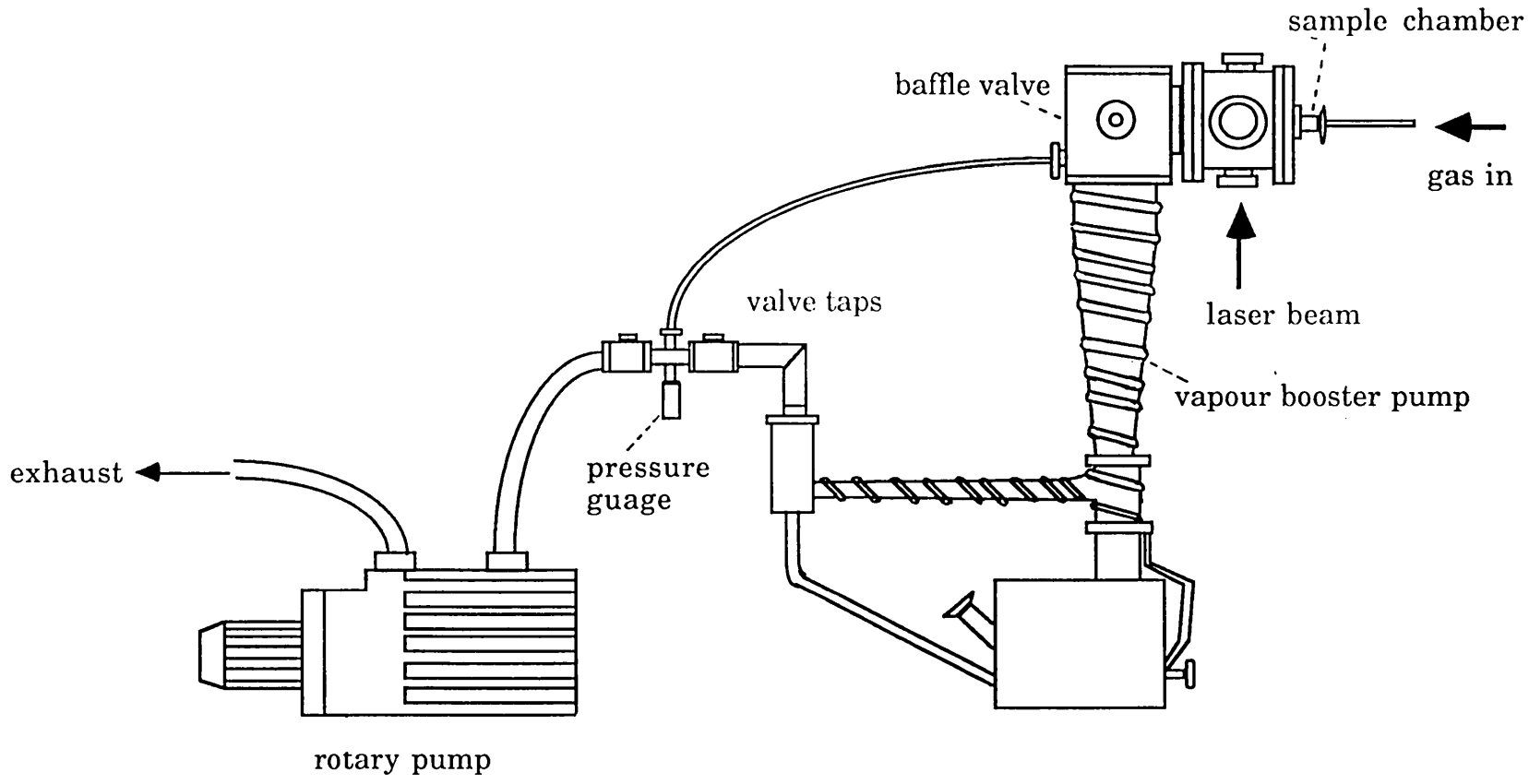

Figure 2.2 Diagram of supersonic jet apparatus

Figure 2.3 Cross section of nozzle / oven assembly

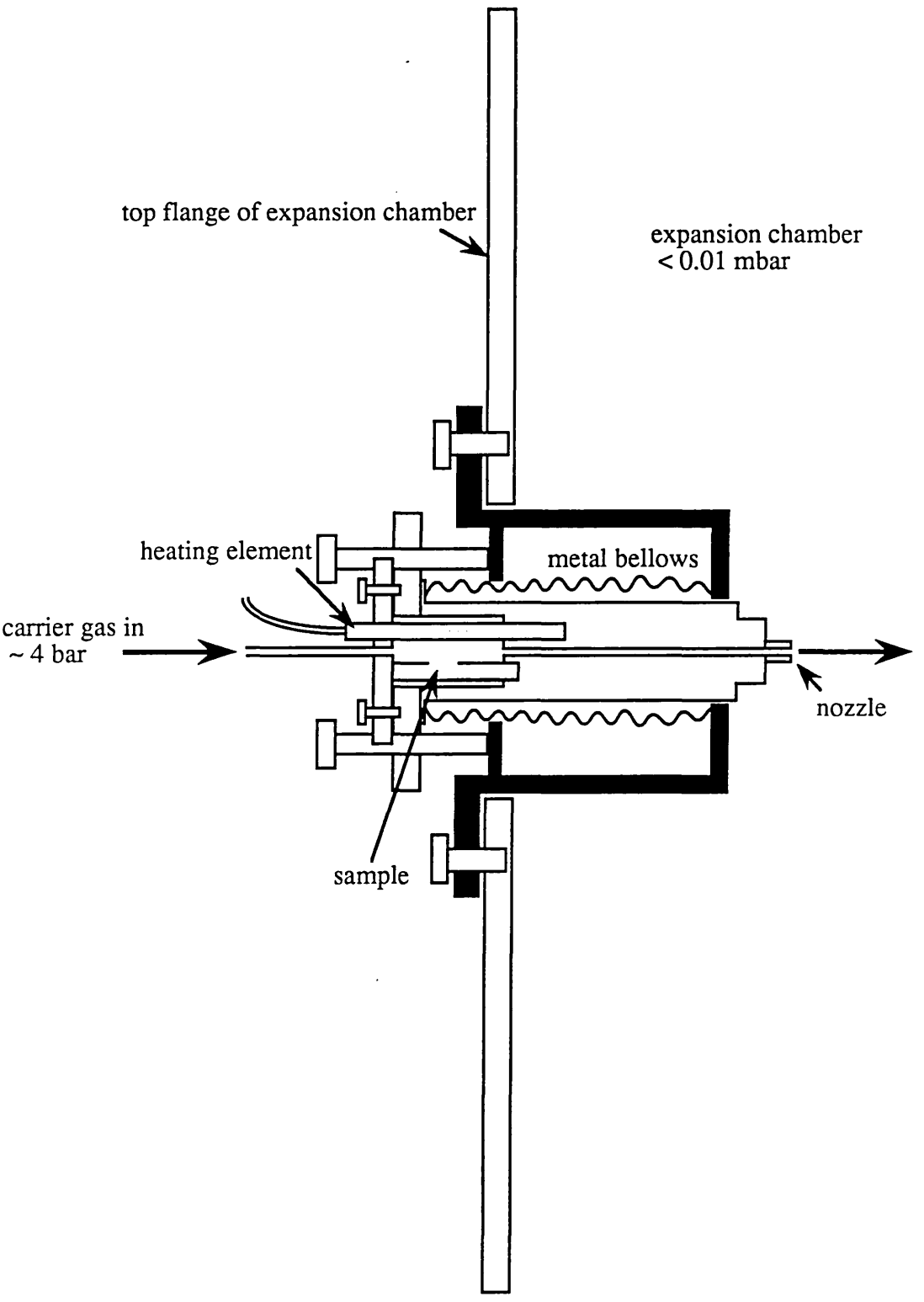

into the expansion chamber, which is operated by compressed nitrogen.

For experiments concerning DMABN , the system used, incorporating a pulsed nozzle assembly, has been described elsewhere[14,15] . The sample was contained in a trough drilled in the bottom flange next to the orifice of the pulsed molecular beam valve, and was heated between 50-130^{o}C using microprocessor controlled heaters to provide sufficient sample vapour. This was then seeded with helium carrier gas at pressures up to 3000torr. The mixture was allowed to expand through the 0.5mm orifice of the pulsed valve during the 300 - 400 microsecond opening time of the nozzle, into the chamber, which was maintained at typically 10^{-5}torr by the use of a turbo molecular pump(Rigaku RTP - 500, throughput 500ls^{-1}) and a rotary pump (Anelva, throughput 260ls^{-1}). Nozzle opening was controlled using a home built controller and was timed relative to the laser pulse by the synchronous output of the laser, the delay between nozzle opening and laser pulse was typically 0.2ms. As for the previously described apparatus, a valve was incorporated to allow access to the chamber without affecting the pump.

2.2.4 Complex Formation

A major advantage of a supersonic expansion is the ability to form van der Waals complexes. Complexes can be formed which have weak intermolecular forces and would not exist at room temperature, but under these conditions their very small

binding energies exceed the internal energy of the molecules from which they are formed and therefore they become stable. The seeded molecule can form complexes with either solvent molecules introduced into the expansion, the carrier gas or, under some conditions, with itself.

Usually the formation of complexes with the carrier gas is undesirable as red shifted features often appear in the excitation spectra. With argon, complexes are readily formed at backing pressures >1atm., so adequate cooling could not be achieved without the formation of aromatic amine - argon complexes of varying stoichiometry. The preferred carrier gas throughout these experiments was helium since although it has been shown to form such complexes[5] it does so much less readily than argon and no evidence for this was observed during these experiments.

Complexes of the aromatic amines with various solvents were formed by passing the helium carrier gas through a reservoir containing the solvent of choice prior to mixing with the sample vapour. The mixture of solvent, solute and carrier gas was then expanded across the nozzle. Both the solvent and solute molecules become internally cooled and may collide with each other to form stable ground state complexes in an exothermic reaction. The excess energy released may be removed from the system by a third body in a three body collision,or may be redistributed amongst the internal vibrational degrees of freedom of the complex in such a manner that the vibrations along the dissociation co-ordinate are not sufficiently populated that the complex falls apart. Further cooling may occur during subsequent two body

collisions of the van der Waals complex and the carrier gas atoms.

Under the conditions employed in these experiments the expansion studied was a mixture of bare solvent molecules, bare solute molecules, solvent - solute complexes, solvent aggregates and solute aggregates, and the precise stoichiometry of these complexes cannot readily be determined. It was possible to vary the amount of sample self aggregates by increasing the partial pressure of sample in the expansion. This was achieved by raising the temperature of the sample oven and hence increasing the sample vapour pressure prior to the expansion.

2.3 Spectroscopic Technique

The technique of laser induced fluorescence can be summarised as the study of fluorescence from an excited electronic state which has been populated through irradiation by a laser rather than by any other monochromatic source.

2.3.1 The Excitation Source

The excitation source in all LIF excitation and dispersed fluorescence experiments, except those relating to the molecule DMABN, was a commercially available excimer pumped dye laser system (Lambda Physik EMG103MSC / FL2002). The system was operated as described in the instrument manual provided by the manufacturers. The wavelength controller unit was interfaced via a Stanford Research Systems model SR250

gated integrator and boxcar averager to an IBM compatible personal computer.

The principal advantage of this laser system is the ability to provide tuneable radiation in the spectral range 270 - 900nm by the selection of appropriate laser dye solutions and the use of second harmonic generation.

For experiments relating to the molecule DMABN the excitation source used for recording LIF excitation spectra was a Lambda physik EMG104MSC/FL2003 excimer pumped dye laser system which differed from the above system only by the dye laser having an intrinsic microprocessor grating controller as opposed to a separate unit for the FL2002 dye laser. For dispersed fluorescence spectra of DMABN the excitation source was a Coherent Antares Nd:YAG pumped 702-1 hybridly mode locked Rhodamine 6G dye laser with a DODCI saturable absorber, the system was amplified using a Quantel RG60-10 regenerative amplifier and a PTA-10 dye amplifier. A schematic representation of this laser system is shown in figure 2.4. In table 2.1 the typical output characteristics of these laser systems are presented.

2.3.2 Measurement of Fluorescence Excitation Spectra

Excitation spectra were recorded by scanning the wavelength of the dye laser whilst monitoring the total unfiltered fluorescence from the excited state aromatic amine. If the excitation energy exactly matched that of an allowed vibronic transition, light was absorbed and a fluorescence signal was

Figure 2.4 Schematic representation of laser system used for DMABN dispersed fluorescence measurements

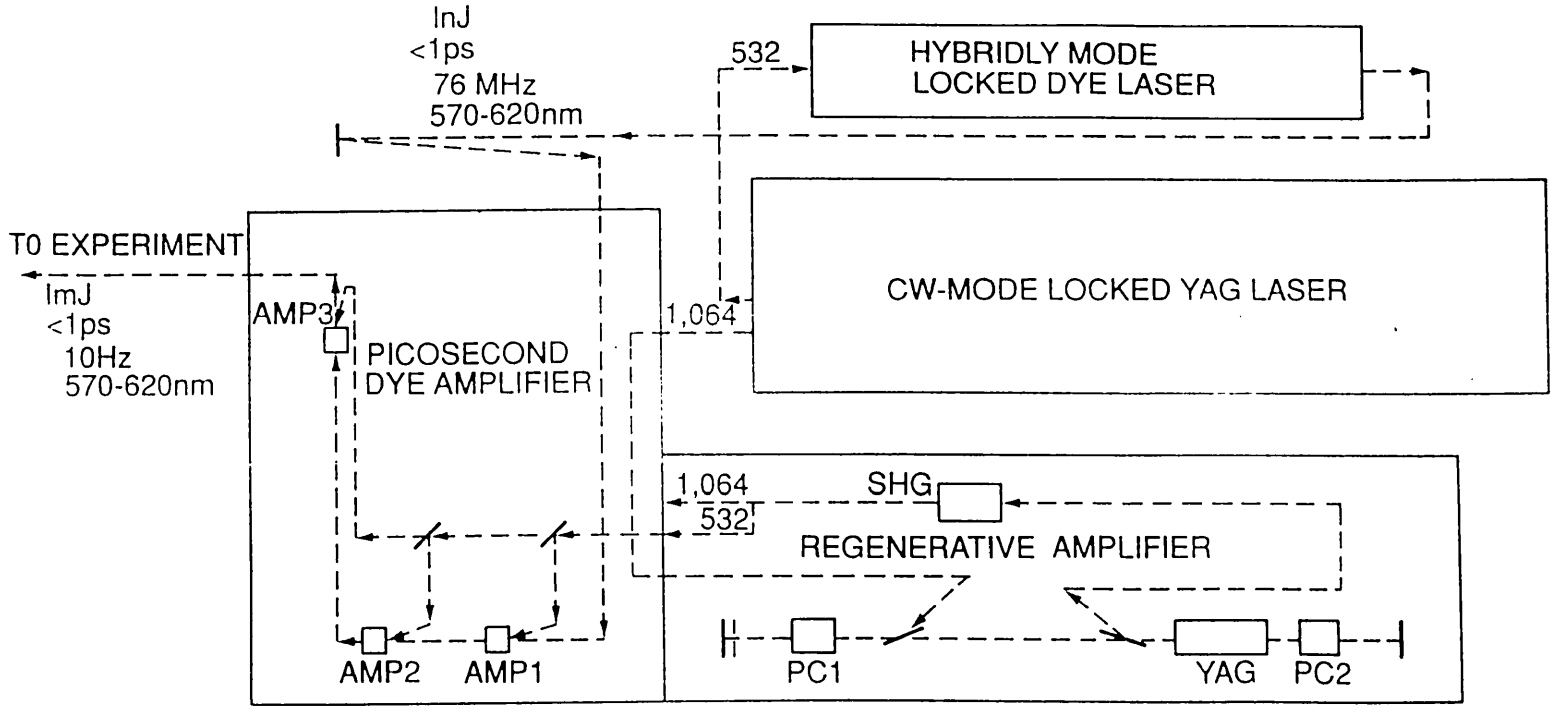

Table 2.1 Typical output characteristics of the Excitation source used

1) Excimer pumped dye laser system

EMG103MSC

Excimer	XeCl
Energy / pulse	100mJ / pulse
Pulse duration	17ns
Laser wavelength	308nm
Repetition rate	30Hz

EMG104MSC

Excimer	XeCl
Energy / pulse	100mJ / pulse
Pulse duration	17ns
Laser wavelength	308nm
Repetition rate	10Hz

FL2002/2003 dye laser

energy / pulse (fundamental)	10-16mJ / pulse
pulse duration	17ns
energy / pulse (U.V)	< 1mJ
Bandwidth (fundamental)	< 0.2 cm^{-1}

Table 2.1 cont....

2) Nd YAG pumped dye laser system

Nd:YAG laser

Laser wavelength	1064nm	532nm
Average power	20W	1.2W
Pulse duration	100ps	70ps
Repetition rate	76MHz	76MHz

Regenerative amplifier

Laser wavelength	532nm
Energy/pulse	25mJ
Pulse duration	7ps
Repetition rate	10Hz

Dye laser

Laser wavelength	570 - 620nm
Energy/pulse	1nJ
Pulse duration	<1ps
Repetition rate	76MHz

Dye Amplifier fundamental and doubled output

Laser wavelength	570 - 620nm	285 - 310nm
Energy/pulse	1mJ	200μJ
Pulse duration	<1ps	<1ps
Repetition rate	10Hz	10Hz

Figure 2.5 Schematic diagram of apparatus used for measurement of LIF excitation spectra

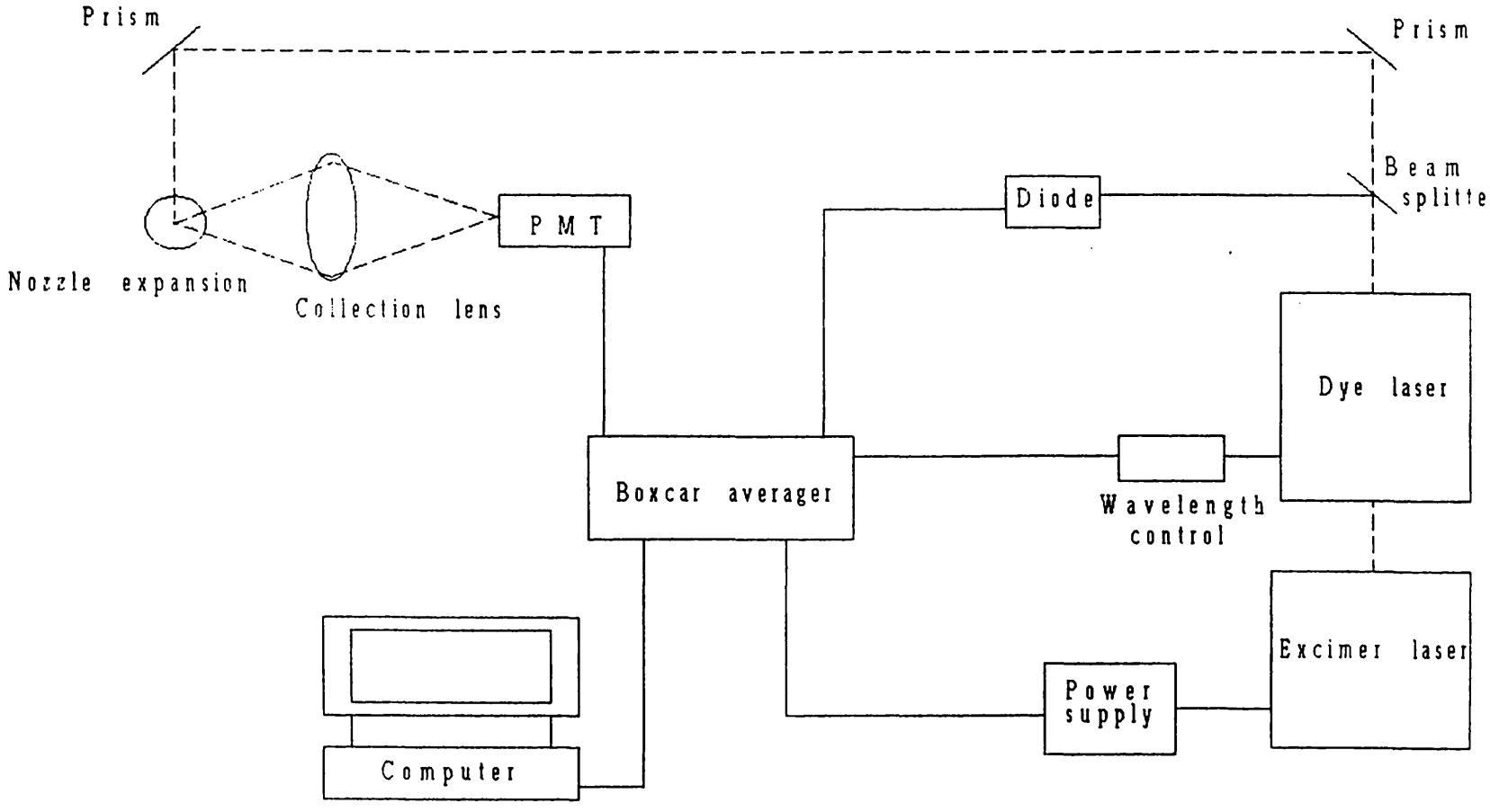

detected in cases where the absorption of the chromophore had an appreciable fluorescence quantum yield.

A schematic representation of the experimental system employed in these experiments is shown in figure 2.5. The laser beam (the frequency doubled output of an excimer pumped dye laser) was steered towards the supersonic jet apparatus and upwards into the expansion chamber by the use of two quartz prisms which enabled accurate adjustment of the beam position. The intensity of the beam was heavily attenuated by the use of neutral density filters in order to reduce the amount of scattered light detected, prevent the more intense fluorescence signals from saturating the photomultiplier tube, and also to prevent saturation of the excited transition. Reduction of scattered light detected is an important factor in the measurement of high quality spectra. Just prior to entering the expansion chamber the laser beam was focussed using a quartz lens so that it crossed the molecular beam at right angles to the expansion and reached tight focus in the expansion at a position 4mm downstream from the nozzle. To assist in accurate alignment, and also to reduce scattered light, the laser beam passed through a series of irises prior to crossing the molecular beam.The beam then diverged into a further series of irises and into a woods horn. Figure 2.6 depicts the region of interrogation in these experiments.

Fluorescence was detected mutually perpendicular to both the laser and molecular beams using an 8cm focal length quartz lens of diameter 8cm placed inside the chamber. The light collected by the lens was spatially filtered outside the

Figure 2.6 Area of interrogation inside expansion chamber

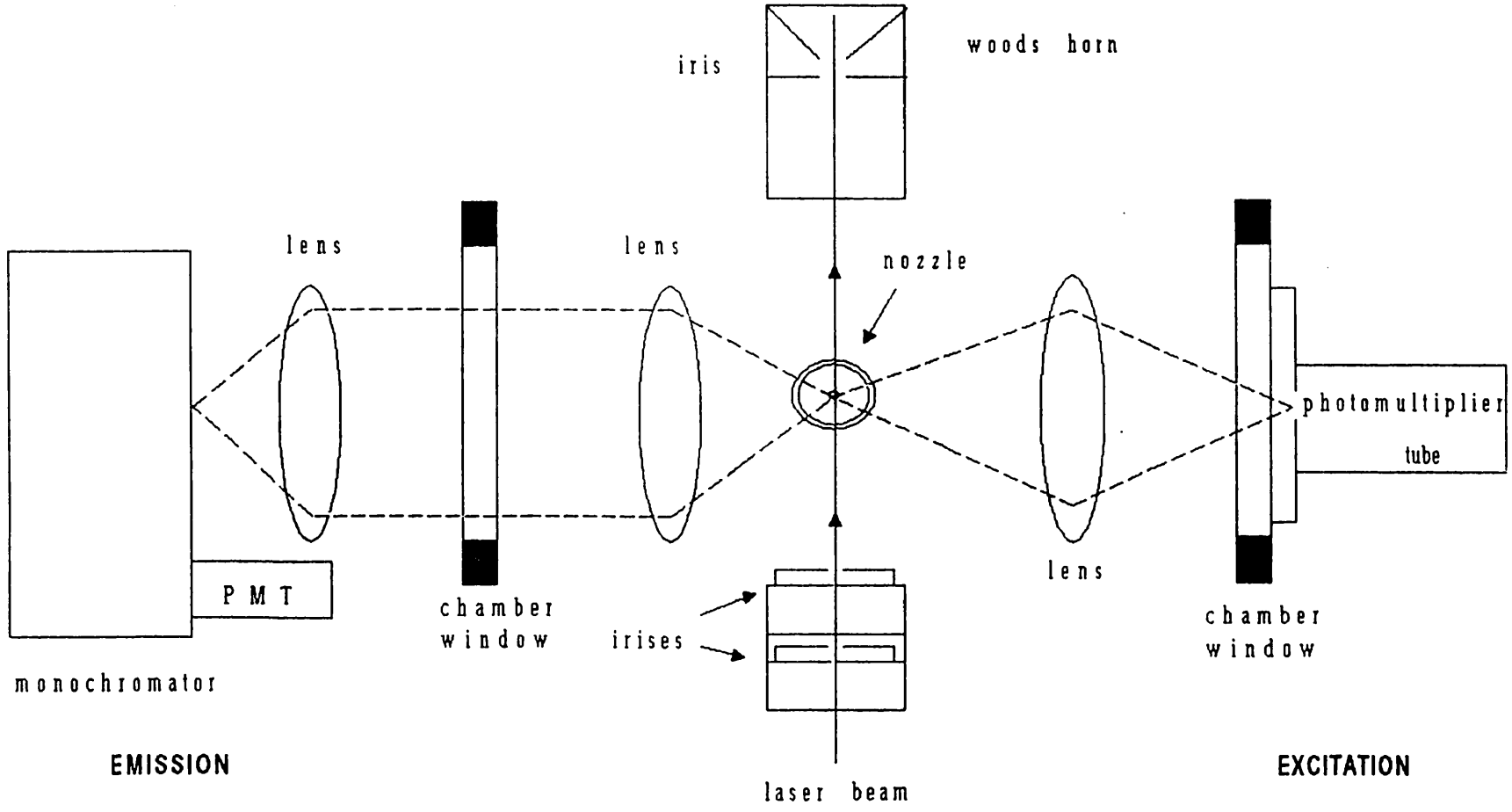

chamber using an iris and focussed onto a photomultiplier tube (Philips XP2020Q adjusted for high gain). Correct alignment of the output lens and photomultiplier tube(PMT) was achieved before the experiment by placing a ground quartz scatter plate in front of the molecular beam and ascertaining that the scattered laser light traversed the centre of the output window and was focussed onto the photocathode of the PMT. The PMT outputs an electrical pulse when a photon strikes the photocathode and the analogue signal from the PMT was fed into a boxcar averaging unit.

A correction was made for variations in laser intensity by splitting off a small fraction(20%) of the laser light, prior to it entering the chamber, using a beam splitter. After considerable attenuation this light was focussed onto a photodiode (Hamamatsu S17722-02). The signal from the diode was fed into a second boxcar averaging unit. Correction for laser intensity is necessary as when tuning the wavelength over an entire "dye tuning curve" large changes in laser intensity occur.

The signal fed into both boxcar averaging units was sampled during a specific time gate of approx. 100ns which was timed relative to the laser pulse by feeding the synchronous output of the excimer laser into the boxcar averager and delaying the gate relative to this signal. The signal sampled was then averaged over 30 laser shots at each wavelength step during the scan. The boxcar unit was interfaced to an American Research Corporation personal computer and a Stanford Research systems software package was used to initialise scans and control data acquisition. The photomultiplier

output was divided by the diode signal to give spectra corrected for variations in laser intensity.

Excitation spectra of DMABN were recorded using the excitation source depicted in figure 2.4. The doubled output of this was selected using an appropriate cut off filter and steered into the molecular beam apparatus using two quartz prisms as shown in figure 2.7. Intensity of the laser light was carefully controlled with neutral density filters. The laser light was focussed to intersect the expansion at a position 7-10mm downstream of the nozzle using a 50mm focal length f/1 CaF_2 lens. Fluorescence was collected mutually perpendicular to both beams using f/1 optics and detected by a Hamamatsu Photonics R758 photomultiplier tube. The contribution from scattered laser light was reduced by placing the appropriate optical filter in front of the PMT.The output signal from the PMT was amplified by 25 - 125 times in a 300MHz amplifier and the signal was stored and averaged in an NEC micro computer. THe spectra were generally obtained by averaging over 10 laser shots for each scan interval. Simultaneously the excitation output power was monitored by a photodiode whose signal was fed into the computer and used to normalize spectra with respect to fluctuations in laser intensity.

2.3.3 Measurement of Dispersed Fluorescence Spectra

For measurement of dispersed fluorescence spectra the excitation source was fixed at a particular absorption

Figure 2.7 Diagram of detection layout used for DMABN experiments

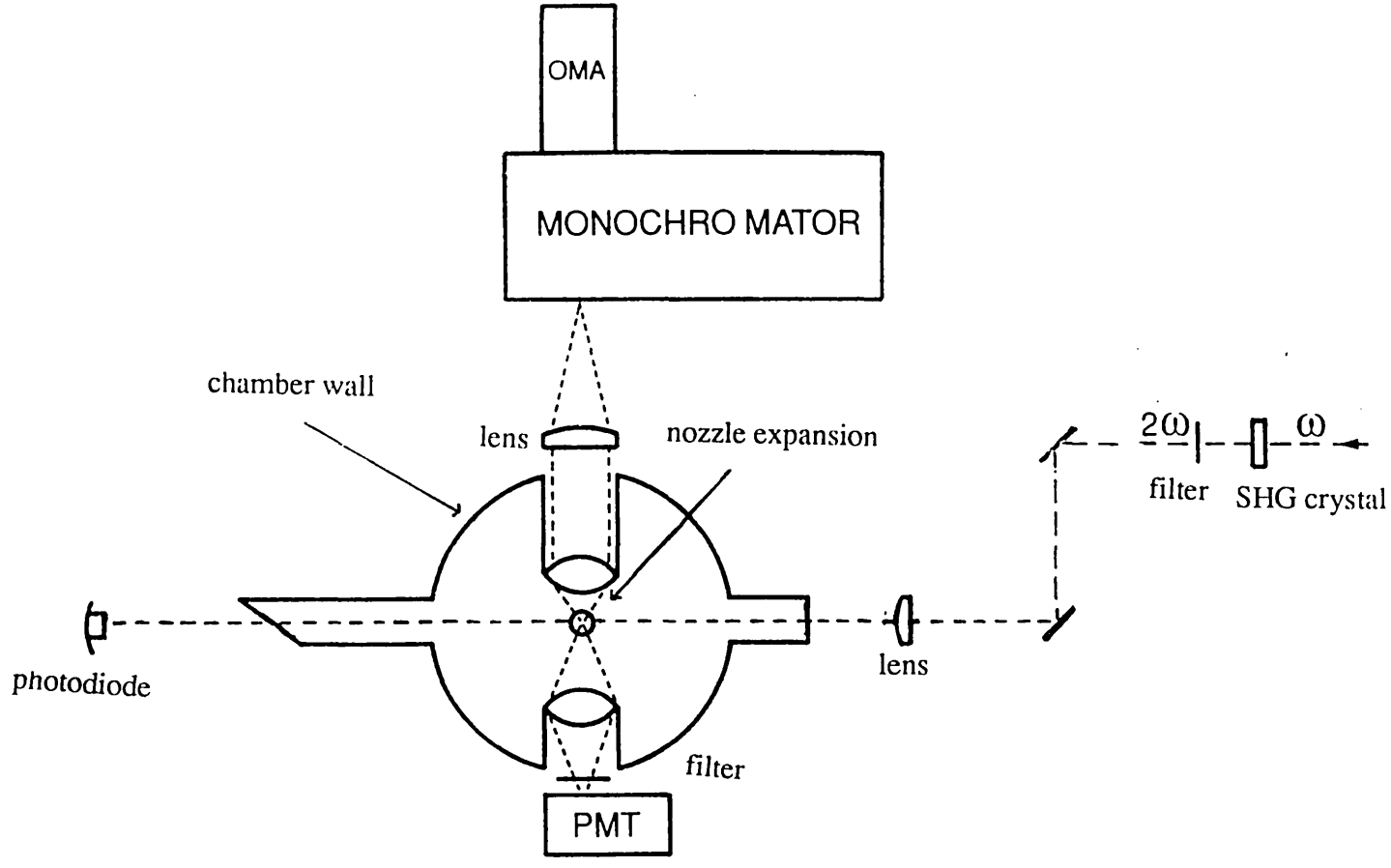

Figure 2.8 Schematic diagram of experimental layout used for dispersed fluorescence measurements

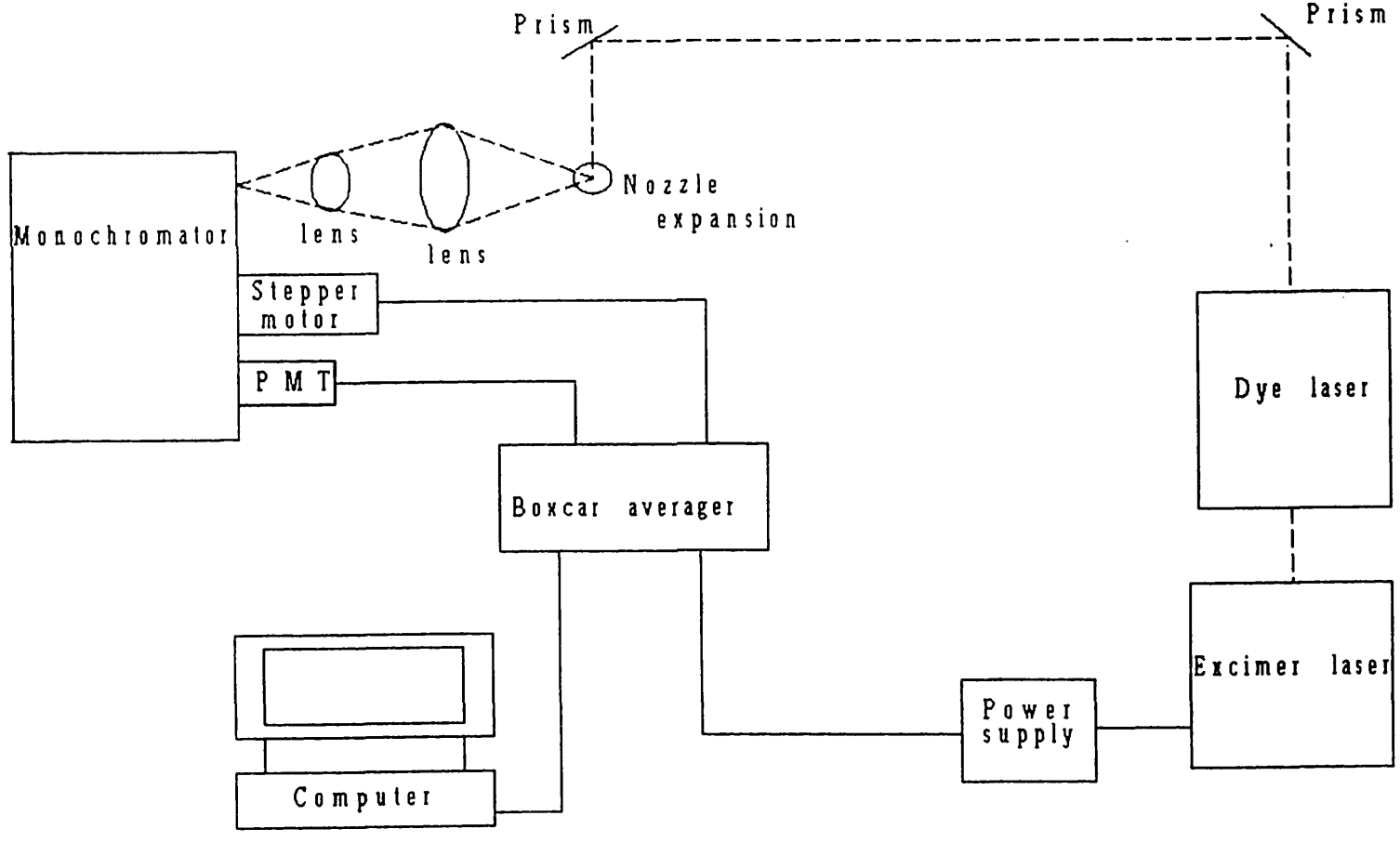

wavelength of the molecule, and the light emitted was dispersed through a monochromator.

A schematic representation of the apparatus used in most experiments is given in figure 2.8. In all cases the unattenuated output of the laser was used to obtain maximum signal.The laser beam was aligned to cross the expansion, at a point 4mm downstream of the nozzle, in the same way as for recording excitation spectra, however it was found that maximum signal was obtained with the laser beam defocussed slightly where it crossed the expansion. Fluorescence was collected mutually perpendicular to the laser and molecular beam using a quartz lens (5cm diameter, 5cm focal length) and after leaving the chamber was focussed onto the slit of a monochromator using a second quartz lens (diameter 5cm, focal length 5cm) as depicted in figure 2.

The monochromator used was a Hilger monospek 1000 fitted with a 2400 lines per mm holographic grating with reciprocal dispersion of 8A per mm. This was driven by a stepper motor (Sanyo Denki 103-770-2) giving accurate 1.8^{o} turns to the grating drive, equivalent to a step of 0.0625A, ~ 0.54 cm^{-1} in the 340nm wavelength region when using the 2400 lines per mm grating. The stepper motor was controlled using a home made controller and stepping of the grating was synchronised with the boxcar signal averaging system. The dispersed fluorescence was then detected using a side on photomultiplier tube (Hamamatsu R928), the output of which was fed into a boxcar averaging unit. Adequate signal to noise ratios were obtained by integrating the signal over 30 or 100 laser shots at each step of the monochromator. The

dispersed emission spectra were corrected for any fluctuations in laser intensity and sample concentration with time by monitoring the total fluorescence simultaneously, however in practice little or no correction was required for typical scans(approx. 2 hours). The ultimate resolution for dispersed fluorescence spectra was limited to $5cm^{-1}$ FWHM[6]. For experiments on DMABN the laser beam was focussed at a point 7-10mm downstream from the nozzle as described for excitation spectra. The resultant light was collected mutually perpendicular to both beams as depicted in figure2.7 using a 50mm focal length f/1 CaF_2 lens, and focussed using a 125mm focal length f/1 lens onto the slit of a 250mm spectrograph which was fitted with either 147.5 lines/mm grating blazed at 500nm (used in 2nd order) or 590 lines/mm grating blazed at 300nm(used in 1st order). The spectra were recorded with a 700 channel (PAR 1420) optical multichannel analyser, which was interfaced to a microcomputer. The resolution of measured spectra was limited by the 4 channel (100 micron) effective resolution of the OMA.Since by the use of an OMA, the time required to record a complete emission spectra was approximately 1-2minutes, it was not considered necessary to correct for changes in laser intensity or sample density.

2.3.4 Calibration

The accuracy of the laser wavelength as given by the intracavity grating was determined periodically by a method which utilises the opto - galvanic effect. The laser beam was

passed through an iron - neon hollow cathode lamp (Cathodeon 3 QNY /Fe) which had a high D.C. voltage across it and was connected to the boxcar averager. When the wavelength of the laser corresponded to an optical transition of a species present in the lamp discharge, a change in the voltage across this discharge was recorded[16-18]. The absolute wavelengths of these transitions as measured by the dye laser grating were found to be within 0.04nm of those reported in the literature[18]. Better agreement was found for the frequency shift (relative wavelength). For excitation spectra reported here the relative shift was found to be reproducible to within $0.4cm^{-1}$, and for dispersed fluorescence $1.0cm^{-1}$ for well resolved bands.

For most dispersed fluorescence measurements, the wavelength calibration of the monochromator was made relative to the wavelength of the dye laser. The spectrograph and optical multichannel analyser were calibrated by monitoring the discharge from an iron neon cathode tube.

2.4 Further Experimental Details

DMABN, DMAEB and N - ethylcarbazole were obtained from Aldrich Ltd and DMAMB was obtained from Lancaster Synthesis Ltd. All samples were used without further purification. Cyanophenylcarbazole was synthesized especially for use in this work by an established synthetic route, and purity was tested by NMR, IR and TLC techniques. The solvents used were either Aldrich spectroscopic grade or BDH hipersolv grade and were used without further purification.

2.5 References

1 A.Kantrowitz and T.Grey,
Rev. Sci. Instrum. 22 (1951), 328.

2 D.H.Levy, L.Wharton and R.E.Smalley,
Chemical and Biochemical Applications of Lasers
(Academic press New York 1977) 2 (1977) 1.

3 D.H.Levy,
Nature 250 (1984) 68.

4 A.Amirav, U.Even and J.Jortner,
J. Chem. Phys. 51 (1980) 31.

5 R.E.Smalley, L.Wharton and D.H.Levy,
Acc. Chem. Res. 10 (1977) 139.

6 A.R.Auty,
University of London (1986) PhD Thesis.

7 A.C.Jones,
Private Communication

8 A.G.Taylor,
University of London (1989) PhD Thesis.

9 R.E.Smalley, L.Wharton and D.H.Levy,
J. Chem. Phys. 63 (1975) 4977.

10 D.H.Levy,
Ann. Rev. Phys. Chem. 31 (1980) 197.

11 H.Ashkenhas and F.S.Sherman,
"Rarefied Gas Dynamics", 4th symposium, ed. J.H.DeLeeuw,
Academic Press N.Y. 2 (1965) 84.

12 J.B.Anderson and J.B.Fenn,
Phys. Fluids 8 (1965) 780.

13 E.P.Muntz,
"Rarefied Gas Dynamics", 4th symposium, ed. J.H.DeLeeuw,
Academic Press N.Y. 2 (1965) 147.

14 H.Petek, K.Yoshihara, Y.Fujiwara, Z.Lin, J.H.Penn and
J.H.Frederick,
J.Phys.Chem. accepted.

15 H.Petek, K.Yoshihara, Y.Fujiwara and J.G.Frey,
J.Opt.Soc.Am.B,(Aug 1990).

16 R.B.Green, R.A.Keller, C.G.Luther, P.K.Schenck and
J.C.Travis,
Appl. Phys.Letters 29 (1976) 727.

17 R.A.Keller, R.Engleman and B.A.Palmer,
Applied Optics 19 (1980) 836.

18 H.Crosswhite,
Journal of Research of the National Bureau of Standards
79A (1975) 17

CHAPTER THREE - A STUDY OF 4-N,N DIMETHYLAMINOBENZONITRILE AND RELATED MOLECULES

3.1 Introduction

This chapter is concerned with an investigation of the fluorescence behaviour of the molecule 4-N,N-dimethylamino-benzonitrile (DMABN) and the related molecules 4-N,N-dimethylaminoethylbenzoate (DMAEB) and 4-N,N-dimethylamino methylbenzoate (DMAMB). An outline of previous work on these and related molecules is provided in section 3.2. The results obtained for the isolated DMAEB, DMAMB and DMABN molecules will be presented in section 3.3, and a brief study of the solvated DMABN molecule complexed with various solvents will be reported in section 3.4. Finally the implications of these results will be discussed in section 3.5.

3.2 The Anomalous Fluorescence Behaviour of DMABN

The unusual fluorescence behaviour exhibited by DMABN was first reported by Lippert et al[1] ~25 years ago. In non polar solutions DMABN was found to exhibit normal emission related to that observed for related benzene derivatives, and maximising at approximately 350nm. However in a polar environment a red shifted fluorescence band was observed in addition to the normal fluorescence which was solvent dependent, maximising in the region 420-500nm. An example of this is given in figure 3.1[2]. These fluorescence bands were assigned to emission from the two close lying ^1L_a and ^1L_b

Figure 3.1 Absorption A and fluorescence F of DMABN in n-hexane at room temperature and dual fluorescence and fluorescence polarisation P in ethanol at 140K

[reproduced from ref. 2]

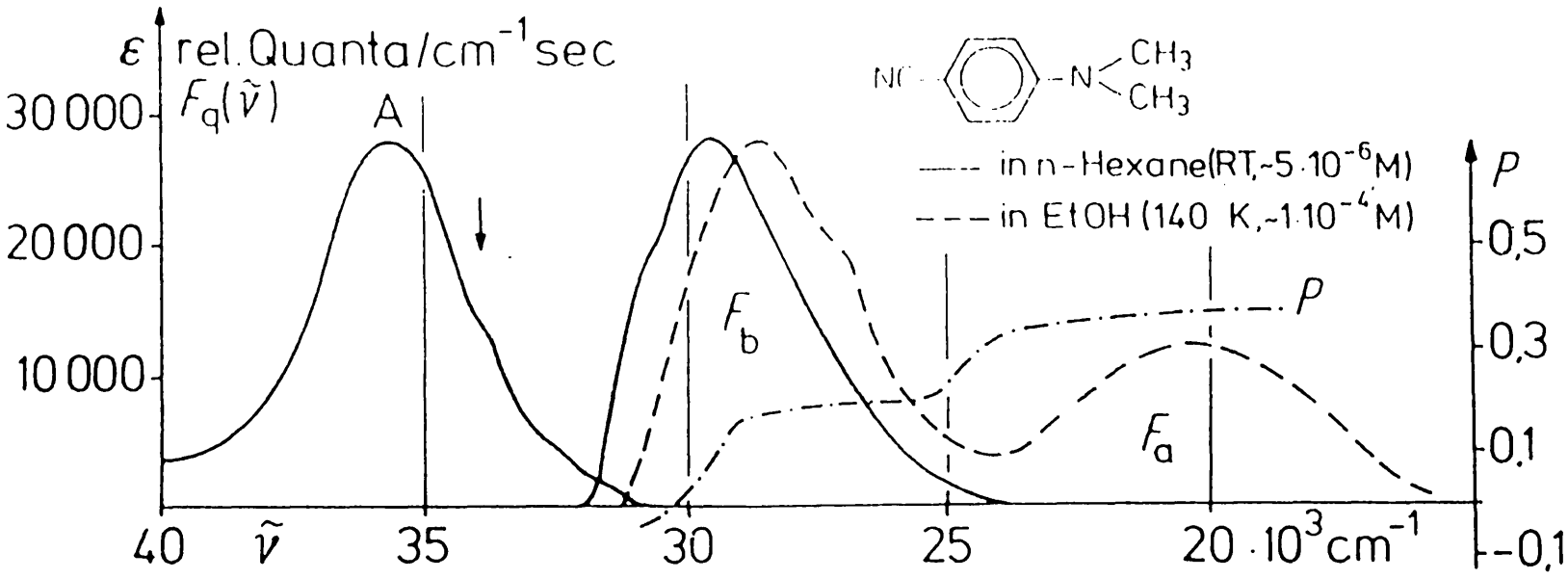

type states(using the established Platt notation, derived from the perimeter free electron orbital model[3]). The short wavelength emission was assigned to the b-band (b^* fluorescence) arising from the less polar ^1L_b type state, whose polarisation lies along the short axis of the molecule. The anomalous red shifted band was assigned as the a-band (a^* fluorescence) arising from the more polar ^1L_a type state, whose polarisation lies along the long axis of the molecule. Lippert proposed[1] that in polar solvents the two close lying states undergo level reversal brought about by solute - solvent level reorganisation (figure 3.2). The solvent molecules around the excited DMABN molecule reorientate themselves and relax to a lower energy equilibrium configuration prior to emission. In non polar solvents the ^1L_b type state remains lower in energy than the ^1L_a type state and hence only the b-band is observed. In polar solvents the ^1L_a type state is lowered due to the interaction of the dipole moments of the excited DMABN and solvent molecules[4] hence a^* fluorescence is observed.

This model was later discounted by Rotkiewicz et al[5] who found from fluorescence polarisation studies that in glycerol the two emission transition moments have the same polarisation, along the long axis of the molecule, thus discounting Lippert's proposal of emitting ^1L_a and ^1L_b type states with perpendicular transition moments. For the same experiment in ethanol[2] the fluorescence polarisation of the two bands was found to be different, that of the b-band being characteristic for a ^1L_b type state with a transition moment

Figure 3.2 Diagram of level - reversal brought about by solute - solvent reorganisation

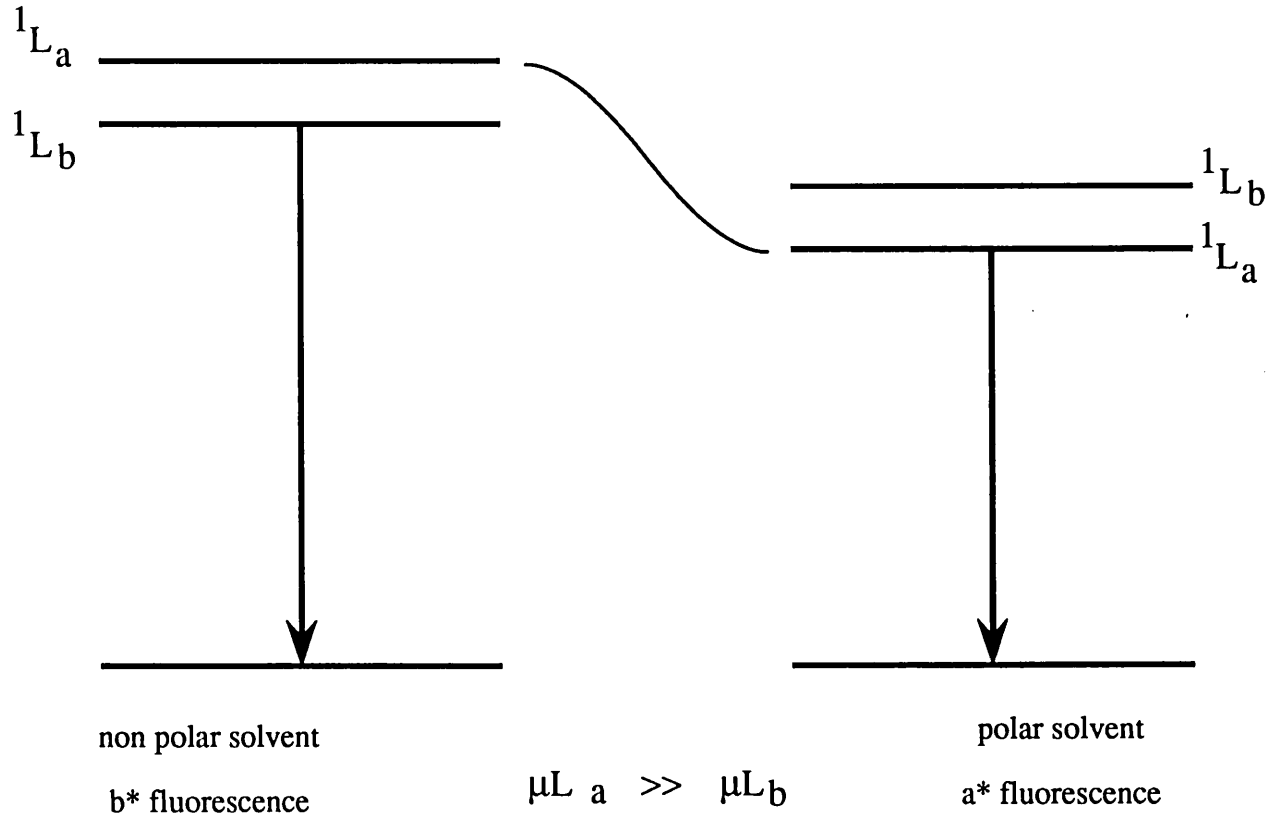

perpendicular to the molecular long axis. Thus the b-band arises from different states in glycerol and ethanol, the reasons for which will be discussed in section 3.2.1.
Much interest has been generated in trying to explain the anomalous fluorescence and many hypotheses have been put forward[6-10] to explain the behaviour of DMABN in the solution phase. Two of these proposals have attracted most support, firstly that put forward by Visser et al[9,11-13] in which exciplex formation is claimed to be responsible for the long wavelength emission, and secondly that proposed by Grabowski et al[10] namely the formation of a twisted intramolecular charge transfer (TICT) state.

Exciplex formation requires the association of a polar solvent molecule with a molecule of DMABN, involving specific solvent-solute interactions. The exciplex theory was also supported by Cazeau - Dubroca et al[14,15], who ascribe the long wavelength fluorescence to excitation of groundstate complexes of DMABN with ubiquitous traces of water. These complexes are said to be hydrogen bonded at the amino group, which is said to be twisted out of the molecular plane in the ground state. Evidence against this assignment was presented in several papers[16,17]. The evidence to contradict the exciplex model was provided by Suppan[18], who found that generally the solvation of DMABN was due to non specific (polar solvent - polar solute) interactions.

Currently the most experimentally confirmed mechanism which describes the anomalous behaviour of DMABN in polar solvents

is that of emission from a so called TICT state[10], which will be outlined in the following section. It is worth noting that this scheme holds true for the solution phase, and that the role of the solvent in this process is of great importance. In section 3.2.2 recent studies carried out to investigate microscopic solvent effects on TICT state formation will be discussed.

3.2.1 The TICT State Hypothesis

The TICT state hypothesis was first put forward by Grabowski et al[10,19] for the molecule DMABN. They proposed that the a^* state was formed via a dynamic relaxation of DMABN with internal twisting of the dimethylamino group, coupled with an electron transfer from the amino nitrogen to the π_z^* orbital[19,20] extending over the entire benzonitrile group (see figure 3.3). A more general model which holds for DMABN and other electron donor - acceptor molecules can be given, which involves the donor and acceptor parts of the molecule, which are linked by a single bond, reacting upon excitation to form a highly polar state with mutually perpendicular conformation of the D^+ and A^- sub units (figure 3.4[21]). Generally for DMABN this transition involves (i) intramolecular rotation, (ii) crossing of the excited states and non adiabatic coupling, (iii) further charge transfer approaching full electronic charge, and (iv) relaxation of the polar solvent molecules around this increased dipole. Quantum chemical calculations[22,23] show the amount of charge transferred to be of the order of 0.8 of an electronic

Figure 3.3 Schematic representation of TICT state formation in DMABN

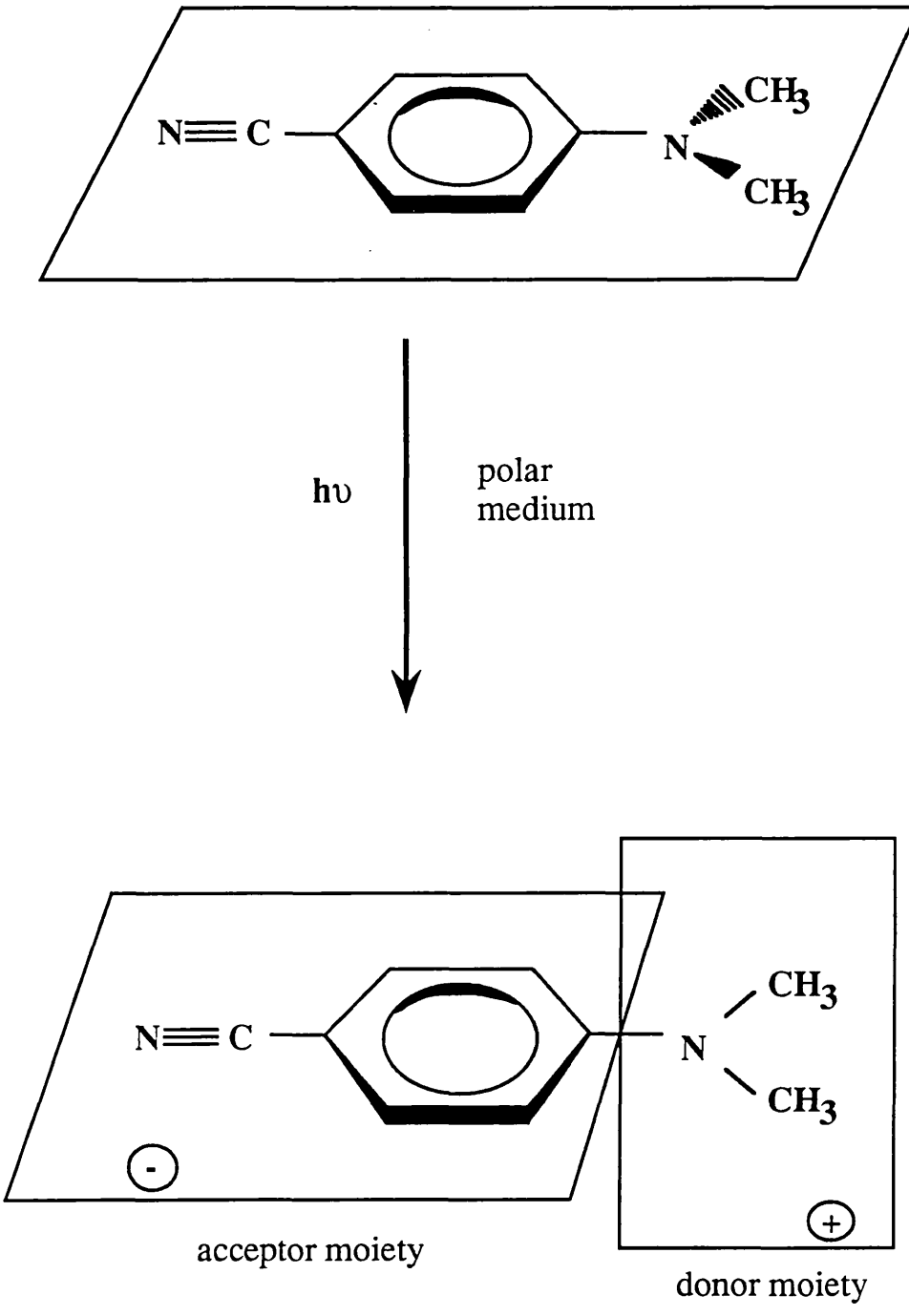

Figure 3.4 Schematic representation of the change in geometrical arrangement of the donor group (D) and acceptor group (A) on going from the b* state to the TICT state

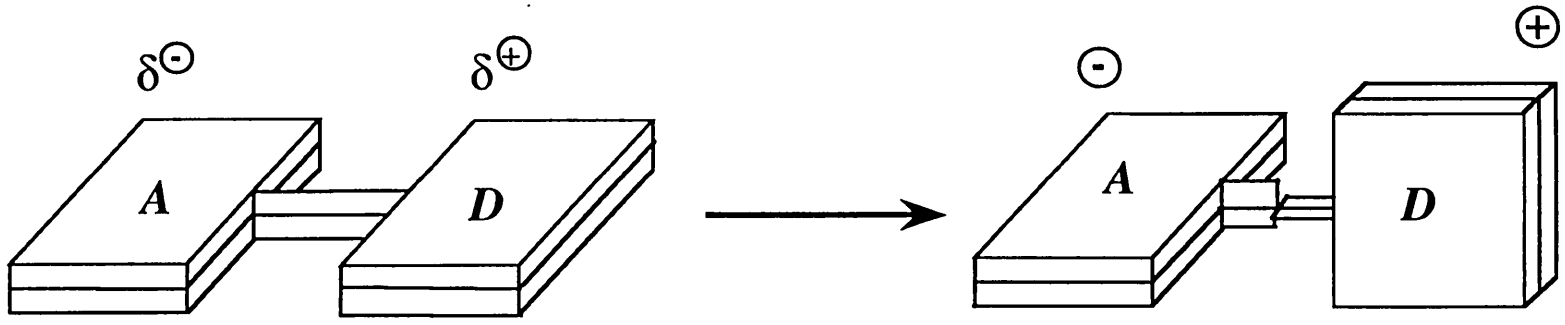

charge. The charge separation is detectable experimentally by measuring the dipole moment of the TICT state by means of the influence of an electrical field on the emission, electro-optical emission measurements,and for the TICT state of DMABN the dipole moment was determined to be ~12D[24,25].

As previously mentioned, the b-band arises from different species in glycerol and ethanol, and this can be explained in terms of solvent induced level reversal. In ethanol the b-band is characteristic of a ^1L_b-type state which fits the above model, however for glycerol the b-band originates from the ^1L_a state which is lower in energy than the ^1L_b in this solvent. A similar example of solvent induced level reversal in the nearly planar molecule has been found for the naphthalene analogue of DMABN [26-28]. Thus the simple excited state reversal scheme proposed by Lippert[1] appears to hold for DMABN in most cases, but is merely a manifestation of the underlying rules which govern dual fluorescence of this type.

In addition to solvent induced level reversal of the excited states, it is also possible for this type of molecule to exhibit a substituent induced level reversal. Using the example of DMABN, on going from the cyano to alkoxycarbonyl derivative, as illustrated in figure 3.5, the ^1L_b-type state is shifted to higher energy and the ^1L_a-type to lower energy,therefore the b-band fluorescence changes its nature. Another effect of this level reversal, either solvent or substituent induced, is that TICT state formation is facilitated, since both the ^1L_a-type and TICT states are of

Figure 3.5 Schematic representation of substituent induced excited state level reversal.

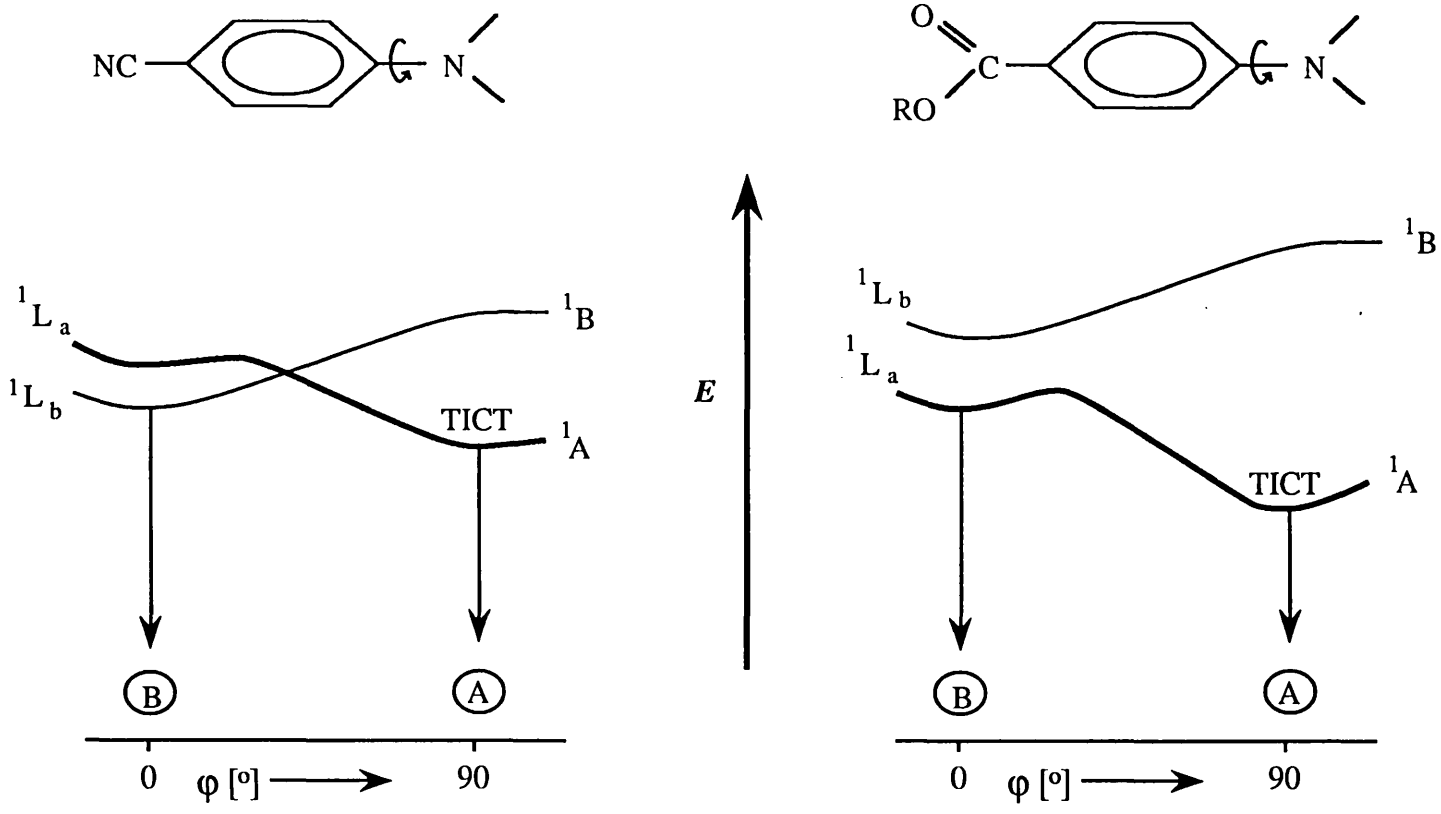

the same symmetry species (A in C_2 point group, which is valid for idealised non pyramidal amino groups at any twist angle φ), and therefore correlate without crossing. The general case for para substituted dialkylanilines is illustrated in figure 3.6[21] which gives a representation of the potential hypersurfaces along the reaction coordinate towards the TICT state. For the cyano derivatives the crossing of the two states causes a conical intersection at the critical twist angle φ_{cr} which necessitates either the coupling to a non-totally symmetric vibration q_n, or solvent relaxation; for the alkoxycarbonyl derivatives this crossing of levels is not necessary and therefore the reaction can proceed smoothly downhill, however a small activation energy is believed to be required.

The kinetics of TICT state formation can be summarised by the following scheme:

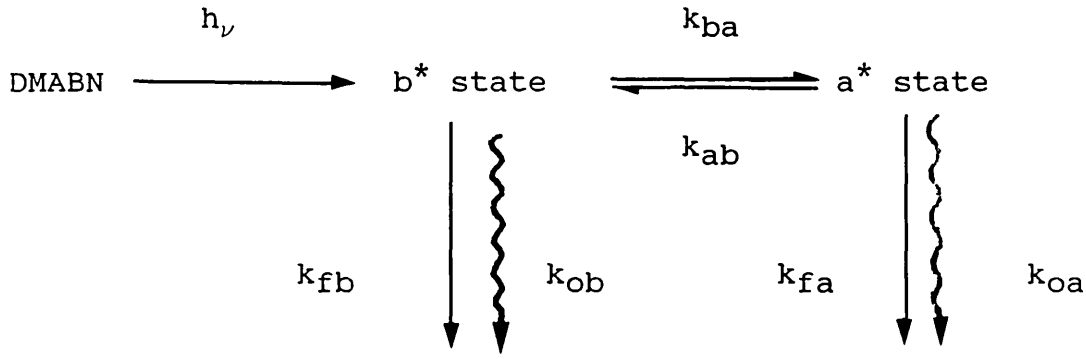

where:

k_{ba} = rate constant of forward reaction

k_{ab} = rate constant of backward reaction

Figure 3.6 Schematic representation of the potential hypersurfaces along the reaction coordinate toward the TICT state in para-substituted dialkylanilines,
a) the cyano derivatives b) the alkoxycarbonyl derivatives

[reproduced from ref. 21]

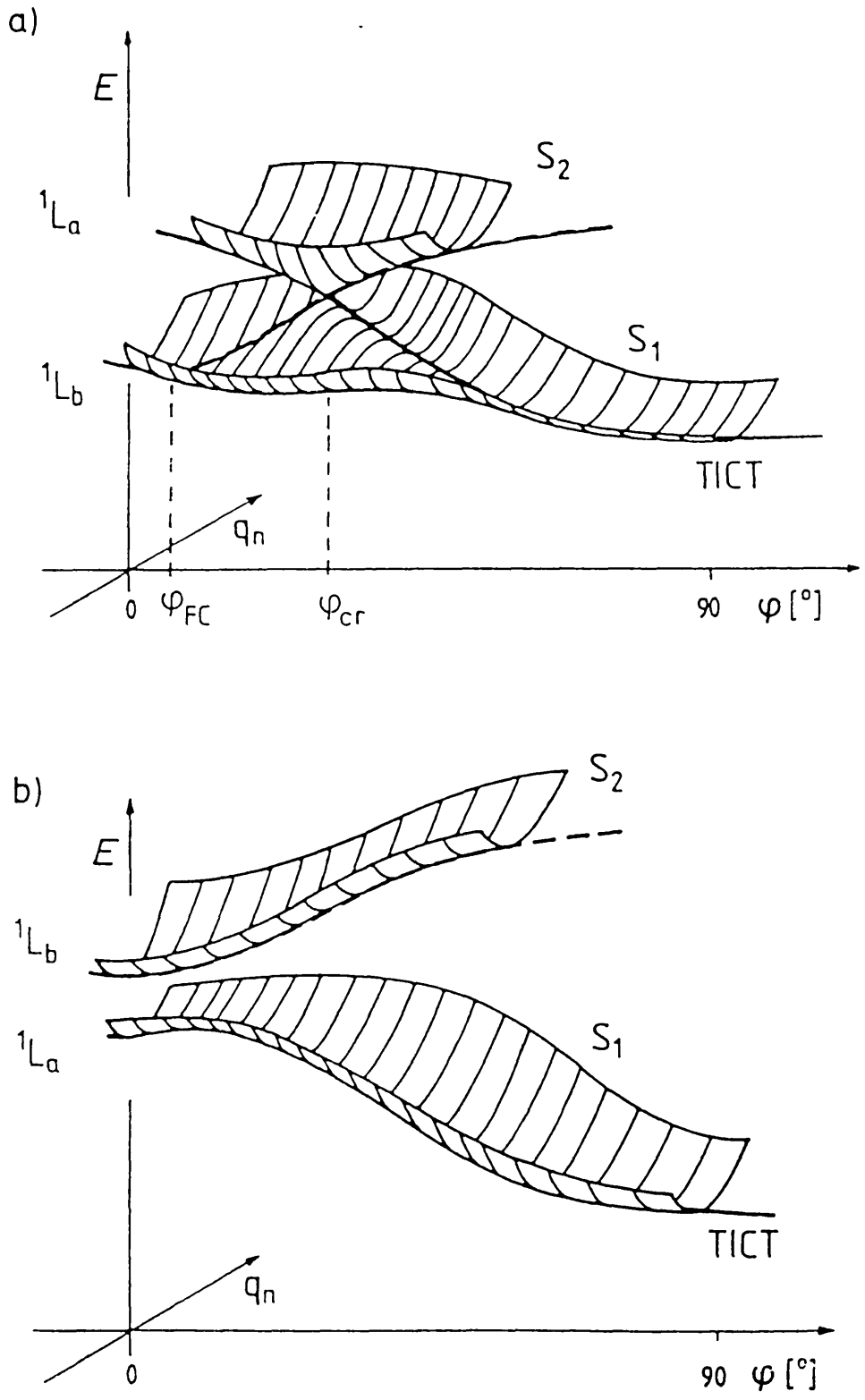

k_f = radiative decay rate to ground state

k_o = non radiative decay rate to ground state

k_{ba}, k_{ab} and k_{fa} are temperature dependent rate constants. This precursor - product relationship is supported by numerous nanosecond and picosecond studies[12,29-36], which show that when k_{ab} is negligible (irreversible reaction) the a* fluorescence builds up with a rise time that is related to the decay time of the b* emission. The rate constant kba is determined by both solvent(polarity,viscosity) and solute (eg ground state twist angle, molecular shape and flexibility, state correlation and conical intersection) parameters.

Much work has been carried out in the solution phase to provide evidence for the twist hypothesis[10,22,37,38], most of which has been concerned with investigating the fluorescence behaviour of model compounds for DMABN where the dimethylamino group is held rigidly in the planar or perpendicular position, or where the planar arrangement of the dimethylamino group was increasingly hindered by ortho substituents on the benzene ring. For the molecules I,II and III in figure 3.7 [37,39,40], which are held rigidly planar, exhibit only b band fluorescence, however for the fully perpendicular benzoquinuclidine IV only the a-band was observed[38]. This clearly illustrates the necessity of twisting for the occurrence of a* fluorescence. The dynamics of intramolecular twisting was also studied[41] as a function of the size of the rotating moiety. At room temperature, where thermodynamic equilibrium between the a* and b* state is established within the lifetime of the excited state, the

Figure 3.7 Some derivatives of DMABN

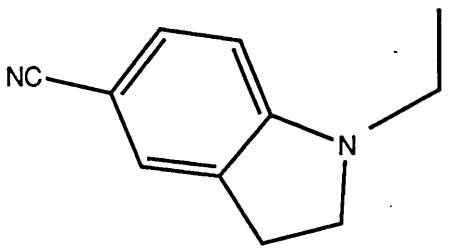

I

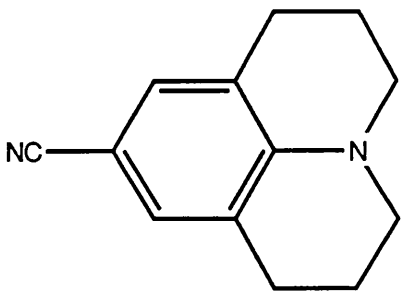

II

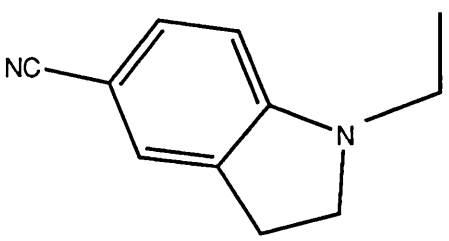

III

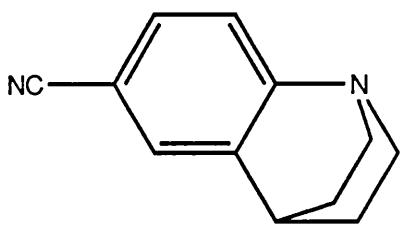

IV

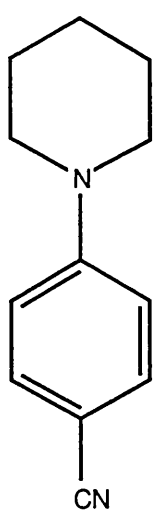

V

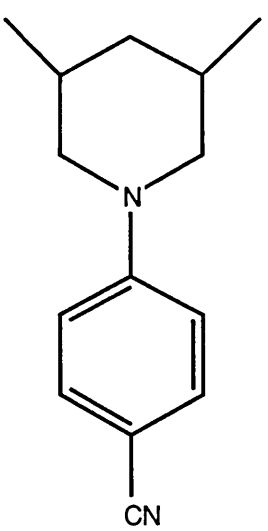

VI

fluorescence of both V and VI was identical, however at lower temperatures, the relative intensity of the a* fluorescence for VI decreased considerably, indicating slower TICT state formation in VI than V.

Okada et al[42] reported S_n <- S_1 picosecond transient absorption studies on DMABN and the related molecule 2,3,5,6-tetramethyl-4-N,N-dimethylaminobenzonitrile (HMABN). The authors found that the S_n <- S_1 absorption spectrum of DMABN in acetonitrile was essentially the same as that for HMABN, in which the amino group is twisted out of plane in the ground state. They also found that spectra of DMABN in medium polarity solvents (e.g. dioxane) compare well with the superposition of the absorption spectra recorded in non polar solvents (eg cyclohexane) and polar solvents (e.g. acetonitrile). They concluded that the electronic structure of the TICT state may be represented by a full charge transfer from the amino group to the benzonitrile group, and that reorientated relaxation of the polar solvent molecules induces twisting in the excited state leading to formation of the TICT species. Similar conclusions were reached by Ruilliere et al[17] from picosecond absorption studies of carbonyl derivatives of dimethylaniline and both groups were in agreement with the TICT mechanism proposed by Grabowski[10].

In summary the rate of TICT state formation was shown to be controlled by a combination of factors such as molecular flexibility, symmetry of rotating moieties, volume of solvent molecules displaced during rotation, and the mean ground state twist angle[31,40,41,43].

The role of the solvent in TICT state formation has also attracted much interest[21 and references therein]. Most studies to date have been carried out in solution, where the 'TICT' molecule is surrounded by large numbers of more or less polar and polarisable solvent molecules, but where specific solute-solvent interactions may occur. As previously mentioned, some mechanisms invoking this type of specific interaction to explain the dual fluorescence of DMABN in polar solvents have been proposed and subsequently discounted. There is some evidence however that one such mechanism (which received much support from Visser et al[9,11-13] as an alternative to the TICT hypothesis), whilst not replacing the TICT mechanism, may supplement it, namely that of exciplex formation.

An exciplex is a complex of definite stoichiometry that is associated in an electronically excited state but dissociated in the ground electronic state. The stoichiometry of these exciplexes may in some cases differ from 1:1, but is well defined involving specific solvent - solute interactions, as opposed to a solvated excited molecule which interacts with an ill defined solvent shell.

Exciplex formation in the case of DMABN involves the association of a polar solvent molecule with a molecule of DMABN in its excited state. Evidence to support of the hypothesis exciplex formation was provided by Wang and Eisenthal[44], who reported time resolved fluorescence measurements of DMABN in various butan-1-ol solutions. They reported the presence of both a fast (30ps rise) and slow decay component upon dilution of the butan-1-ol solution with

non polar solvent. The fast component, which dominates at high butanol concentrations and the dynamics of which were independent of the dilution, was attributed to originate from excitation of DMABN-butanol complexes formed in the ground state, and due mainly to twisting motion along the C-N$(CH_3)_2$ bond in the excited complex. The dipole moment of DMABN in the ground state is large(7D[10]), and therefore the formation of this type of ground state complex is not unexpected. This short lived component was also observed by Meech and Phillips[30] for DMABN in ethanol. The slow process, which showed a linear dependence on butanol concentration, was attributed as arising from excitation of uncomplexed DMABN molecules, or those with the wrong orientation of butanol molecules for facile exciplex formation. These two studies[30,44] have shown that the formation kinetics of the a* state in solution are complicated and inadequately described by simple kinetic schemes based on either the TICT or exciplex model alone. A kinetic scheme illustrating the parent daughter relationship between the b* and a* states is given in figure 3.8. The stoichiometry of the ground state complex appeared not to be critical for TICT state formation. Wang and Eisenthal[44] concluded that specific short range interactions with the polar solvent molecule were the major cause of stabilisation of the TICT state. Bonding between the exciplex components was attributed[9] to the overlap of the lone pair orbitals of the solvent molecule and the amino group. The complex is further stabilised by long range polarisation interactions with solvent molecules.

Figure 3.8 Kinetic scheme showing the relationship between b* and a* states of DMABN in lower alcohols.[44]

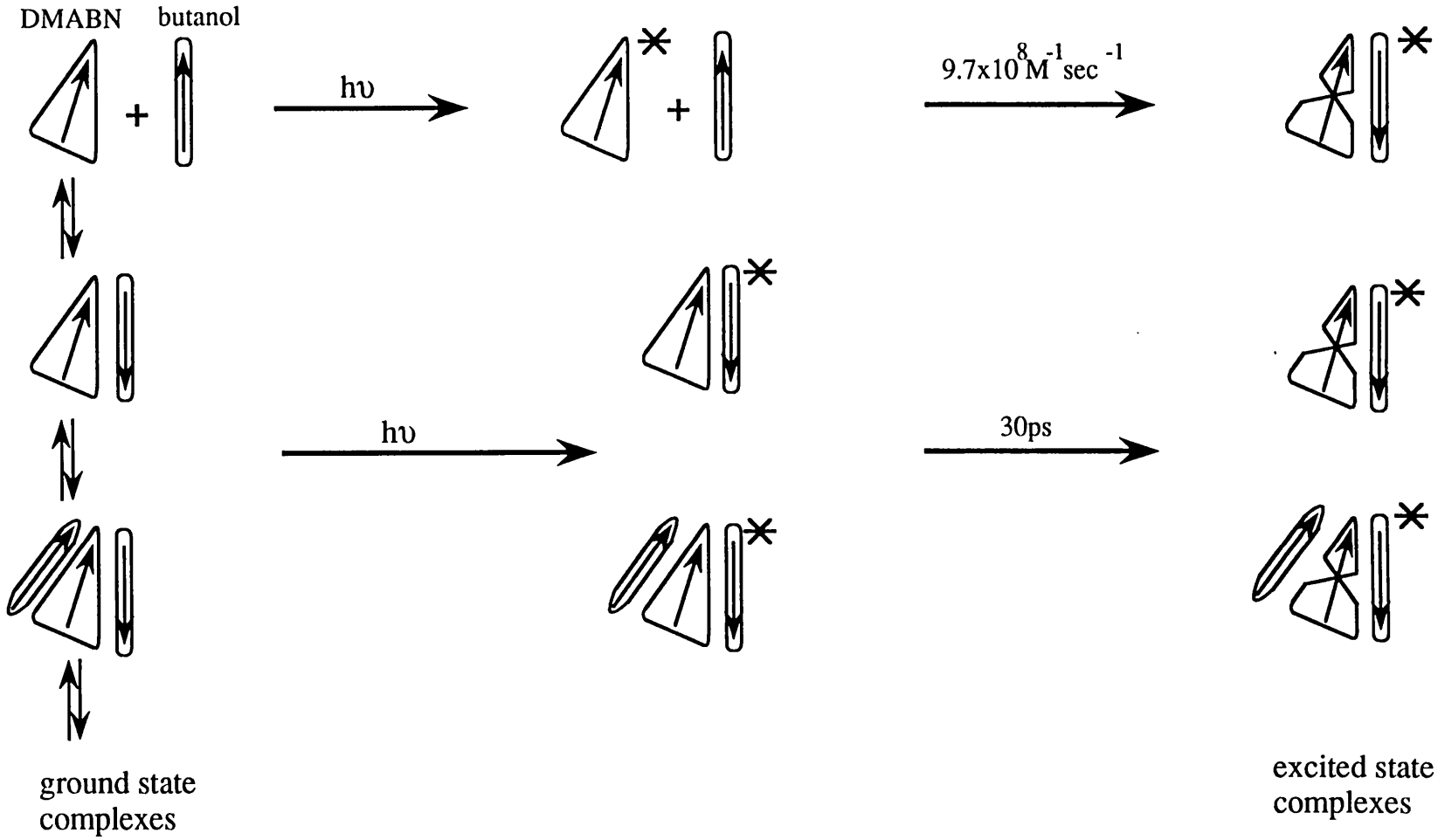

This mechanism is thought to be the case for lower alcohols but not the general case for TICT emission[21], principally because emission from a TICT state has been observed for derivatives of DMABN in aliphatic hydrocarbons, and also because some molecules exhibit TICT fluorescence in the gas phase, for example a series of N-phenyl pyrrole derivatives[21,45]. The 'red shift' of emission from the TICT state is found to correlate well with the bulk solvent polarity properties for nearly all known molecules that exhibit TICT fluorescence, even though these species differ greatly in structure and electronic properties[1,46].
At present, despite many investigations on the subject it is still unclear by what mechanism the solvent molecules stabilise the intramolecular charge transfer. That is whether long range polarisation interactions or local, more specific, solute-solvent interactions are of greater importance.

3.2.2 Recent work

In recent years interest has been generated in investigating molecules in the gas phase which are known to form TICT states in the solution phase. Laser induced fluorescence studies and two colour time of flight mass spectroscopy in combination with a free jet expansion can yield detailed information about any structural changes that occur in the excited state of these molecules. By the formation of van der Waal's (vdW) complexes in the expansion it is possible to overcome problems encountered in the solution phase, and

study microsolvation effects on these 'isolated' solvated molecules.

As mentioned in chapter 1, a van der Waal's complex can be formed between a polyatomic molecule such as DMABN and simple ligands, and the excited state features of this complex can be studied in a supersonic jet. The evidence for formation of ground state complexes in lower alcohol solutions[30,44], suggests the possibility that a* fluorescence could be observed from these complexes under supersonic expansion conditions. This technique has previously been applied to the observation of intermolecular charge transfer fluorescence, for example the formation of anthracene exciplexes with dimethylaniline[47]. A general indication that a charge transfer type interaction has taken place is the observation of broad red shifted fluorescence[48]. Excited state intramolecular proton transfer(ESIPT), which is characterised by a broad red shifted fluorescence, was observed for the jet cooled molecules 2,5-bis(2-benzoxazilyl)hydroquinone[49] and 2,5-bis(2-benzothiazoly) hydroquinone [50,51].

A few results concerning studies of TICT state forming molecules in a supersonic jet have been recently reported, the first of these being 9,9'-bianthryl[52]. In the ground state, the two anthracene moieties of 9,9'bianthryl are considered to be orthogonal, but the torsional angle must be relaxed from 90^{o} in the excited state to allow electron transfer from one moiety to the other[53]. The LIF excitation spectrum of 'bare'9,9'bianthryl showed only emission from the locally excited state(b* fluorescence), but microsolvation by

acetone molecules[54] gave rise to fluorescence from the charge transfer(CT) state. The ratio of CT emission to LE emission increased with increasing degree of solvation .It is not entirely clear whether CT emission arises from 1:1 complexes or higher stoichiometry complexes.

Kobayashi et al[55] reported the structureless LIF spectrum of supercooled unsolvated 4-dimethylamino-3,5-dimethyl-benzonitrile (TMABN), which had been previously shown to exhibit CT fluorescence in the gas phase[56]. Due to the presence of methyl groups in the ortho positions on the benzene ring, the nitrogen lone pair in the dimethylamino-group is twisted in the ground state. The emission was found to be composed of two kinds of fluorescence, one from the CT state and the other from a twisted higher excited S_2 state.

Herbich et al[57] recently reported the LIF excitation and fluorescence spectra of jet cooled 4-(dimethylamino) benzonitriles and 4-(dialkylamino) pyrimidines (I-V in figure 3.9) and their complexes with small polar molecules. The bare monomer molecules (except TMABN) do not exhibit any distinct long wavelength fluorescence that can be assigned to a TICT state. Microsolvation of the ground state twisted molecules(III,IV and V) with methanol and acetonitrile gave rise to the red shifted emission which the authors attributed to emission from the TICT state.

There have been several studies of jet cooled DMABN, both of the unsolvated molecule and of small van der Waals

Figure 3.9 Some alkylamino benzonitriles and pyrimidines studied in a supersonic jet [57].

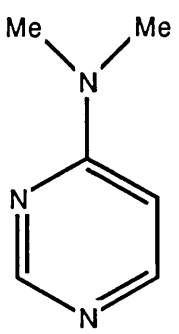

I

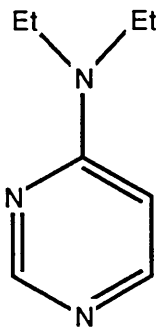

II

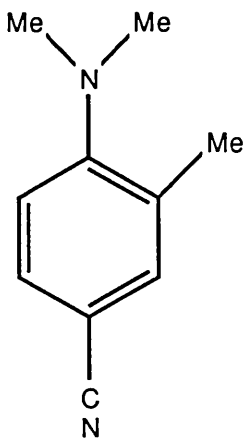

III

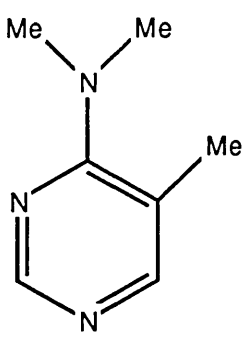

IV

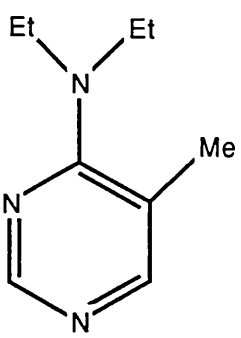

V

clusters[58-63], in addition investigations have been carried out in a supercritical fluid[64]. Assignments of the observed spectra will be discussed later in the chapter.

Kobayashi et al[58] reported the absence of any a* emission in LIF studies of the jet cooled 'bare' DMABN molecule and of vdW complexes of DMABN with water and with trifluoromethane. The 0-0 bands in the excitation spectra of the complexes showed blue shifts in contrast to the vdW complexes with rare gas atoms. These facts were interpreted in terms of the structure of the vdW complexes and the authors stressed the importance of the location of the solvent molecule in order for the complex to form a CT state.

Gibson et al[59] reported excitation and dispersed fluorescence spectra as well as fluorescence lifetimes of jet cooled DMABN and its vdW complex with methanol. Neither the unsolvated or mono-solvated complex exhibited the anomalous a* fluorescence seen in polar solution. Multiple solvation resulted in a dramatic reduction in the fluorescence quantum yield, which was interpreted in terms of formation of an a* state that is non-emissive under jet cooled conditions. In a further paper Gibson et al[60] made a comparison of complexes of DMABN and 4-aminobenzonitrile with argon, alkyl cyanides, methanol, and water. Like those of DMABN, the complexes of 4-ABN,with the exception of 4ABN-argon, were found to exhibit hypsochromic spectral shifts relative to the bare molecule; complexes involving interaction with either the cyano- or amino- group were observed. Interaction of more than one

protic solvent molecule with the dimethylamino group of DMABN was found to result in efficient fluorescence quenching which was attributed to formation of a non emissive exciplex.

Peng et al[61] presented a fluorescence study of DMABN both in a thermalised vapour and in a supersonic jet. From the jet studies, excited and ground state vibrational spectra of the isolated molecule are resolved, and the spectroscopy of the stoichiometric complexes with water, methanol, ammonia and acetonitrile are reported. It is concluded that 1:1 complexes are not sufficient for the local perturbation to cause charge separation. At higher temperatures in the jet, red shifted emission attributed to DMABN self complexes was reported, however no data were presented. Under high pressure and temperature vapour conditions, another fluorescence band with a greater red shift was observed which was assigned as the charge transfer state of DMABN in self- complexes, however this was not observed under jet cooled conditions.

Bernstein et al[62] reported two colour time of flight mass spectra of jet cooled 3- and 4- dimethylaminobenzonitrile bare molecules and complexes with methane, water, acetone dichloromethane and acetonitrile. Both 3- and 4-DMABN were said to display significant changes in geometry, associated with rotation-inversion coordinates of the dimethylamino group, upon excitation from the ground electronic state S_0 to the first excited singlet state S_1. The mono-solvated complexes of 3- and 4-DMABN all showed two general types of behaviour:(1) Cluster spectra have both red and blue shifts

from their respective bare molecule origins which are relatively small(in general less than 200cm^{-1}). These cluster spectra are nearly identical with the bare molecule spectra, the solvation process seeming to have little effect on the DMABN molecule, especially the -N(CH_3)$_2$ moiety, for these clusters.(2) The cluster spectra have large shifts(500-1000cm^{-1}) to low energy compared with the bare molecule spectra,these spectra are composed of both sharp and broad features with little resemblance to the bare molecule spectra. Results of calculations lead the authors to suggest that clusters of differing geometry may be present. These data are interpreted in terms of solution behaviour of DMABN, and the relationship between the TICT model and these results is explored.

In a subsequent publication[63] the same group presented one colour time of flight mass resolved excitation spectra of jet cooled DMABN and some of its chemical analogues, dimethylaniline(DMA), 3-dimethylaminobenzonitrile(3-DMABN), N,N-dimethyl-4-(trifluoromethyl)aniline (4-CF_3-DMA), and 4-(d_6-dimethylamino)benzonitrile(4-d_6-DMABN). Near the origin of the S_1 - S_0 transition the low frequency transitions were assigned to motions of the dimethylamino- group, with the inversion motion and the dimethylamino group torsion about the C_{ipso} - N bond (the twist coordinate) in S_1 giving rise to the most prominent features. The potential parameters for the twist coordinate were found to be similar for all the molecules, as was the inversion motion. A Franck-Condon intensity analysis for the dimethylamino twist suggested that the dimethylamino group is displaced in the excited state by

~30° with respect to its planar orientation in the ground state. In both solution and 1:1 complexes of DMABN with polar aprotic solvents, a low lying CT state was identified in addition to the usual $\pi\pi^*$ excited state of the bare molecule. The relation between the bare molecule twisting displacement upon excitation and the low lying CT state is discussed.

Kajimoto et al[64] presented evidence for TICT state formation in a supercritical fluid of DMABN in CF_3H. A supersonic jet generally provides information of the solvent effect on a solute at very low temperatures and for a small number of solvating molecules. In order to study the effect of solvation by a moderate number of molecules at room temperature, the use of a supercritical fluid at varying densities is an attractive approach, since one can easily control the environment of the solute by changing the number of surrounding solvent molecules. For DMABN both the Stokes shift and the ratio between the CT and S_1 emissions increased with increasing density of the polar fluid. These features were rationalised by considering the aggregation of the solvent molecule around the solute. In order to estimate the degree of aggregation in the ground state, the shift of the absorption spectra and the solubility of DMABN was measured as a function of the fluid density. The intermolecular potential was first evaluated from the solubility data, and then the change of solvation number with increasing density was derived from the spectral shift by applying a simple model calculation.

The above studies showed that forming small vdW complexes of DMABN with various polar solvents does not yield any evidence of TICT emission, and also none is evident for the isolated molecule. Comparison with the behaviour of TMABN seems to confirm that the charge transfer can be promoted by the degree of deviation from planarity.

As previously discussed the alkoxycarbonyl derivatives of DMABN could be expected to form a TICT state more readily due to the substituent induced level reversal of the two close lying excited states.
August et al[65] recorded LIF excitation spectra for a series of DMABN derivatives, the para substituted nitrile or ester derivatives of dialkylamino benzene compounds (I-VIII in figure 3.10). LIF excitation spectra of the ester derivatives showed an underlying 'quasi continuum', and the authors reported observation of red shifted emission associated with this; however no emission spectra were presented. These results were claimed as evidence both for torsional motion and TICT state formation in the unsolvated DMAEB and DMAMB molecules.

In this chapter a further investigation of the LIF spectroscopy of the unsolvated DMAEB, DMAMB and DMABN is presented. The effect of forming larger clusters of DMABN with solvent molecules on the TICT state formation is investigated as a continuation of previous solvation studies carried out by this and other groups.

Figure 3.10 Aminobenzonitrile, dialkylamino- and cyclic amino- benzoic acid nitriles and esters.

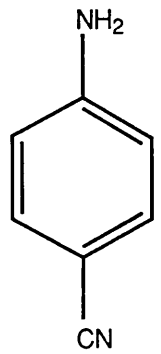

I

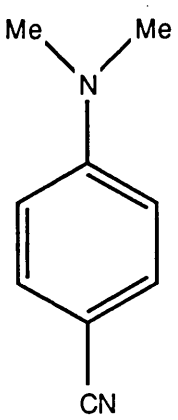

II

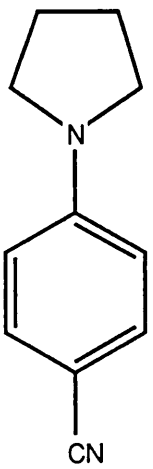

III

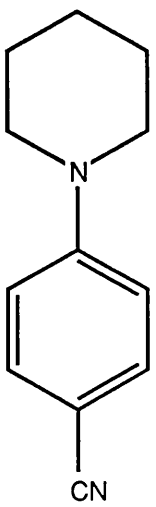

IV

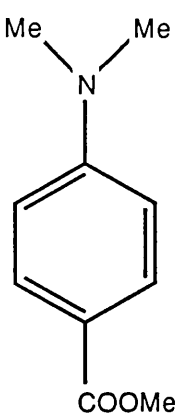

V

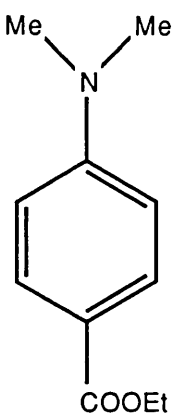

VI

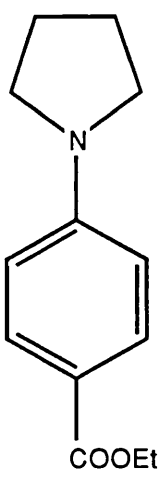

VII

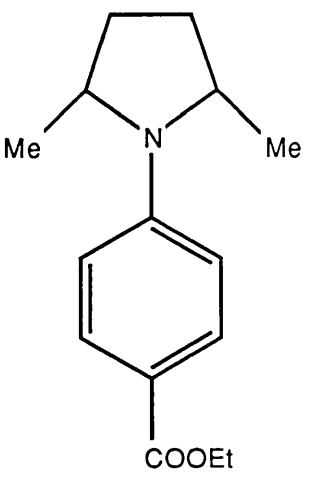

VIII

3.3 Results: Unsolvated Molecules

3.3.1 4-N,N-dimethylaminoethylbenzoate (DMAEB)

The laser induced fluorescence excitation spectrum of jet cooled DMAEB in helium expansion is given in figure 3.11. The electronic origin region of the spectrum is made up of a large number of low frequency transitions. On going to higher energies only weak, partially resolvable structure is observed. There are no resolvable vibronic features at ~800 cm^{-1} higher energy than the origin region. The spectrum was recorded at high sample oven temperatures, and an underlying quasi-continuum is evident, which extends over most of the spectral range, however on recording the same excitation at lower sample oven temperatures this component is not evident. It is important to mention here that increasing the sample oven temperature has the effect of increasing the number density of sample molecules in the expansion prior to excitation, but has no real effect on the 'temperature' of the expansion.

Figure 3.12 shows the origin region of the excitation spectrum of DMAEB recorded at higher resolution. The first prominent feature in this spectrum occurs at 33096cm^{-1} and is assigned as the 0(0,0) transition (electronic origin transition). The observed pattern of low frequency transitions, dominated by a 65cm^{-1} transition, is believed to be characteristic of the dimethylamino group, which will be discussed later in this chapter. The frequencies of these transitions are given in table 3.1. The spectrum shows a

Figure 3.11 LIF excitation spectrum of 4–N,N– dimethylaminoethylbenzoate (DMAEB).

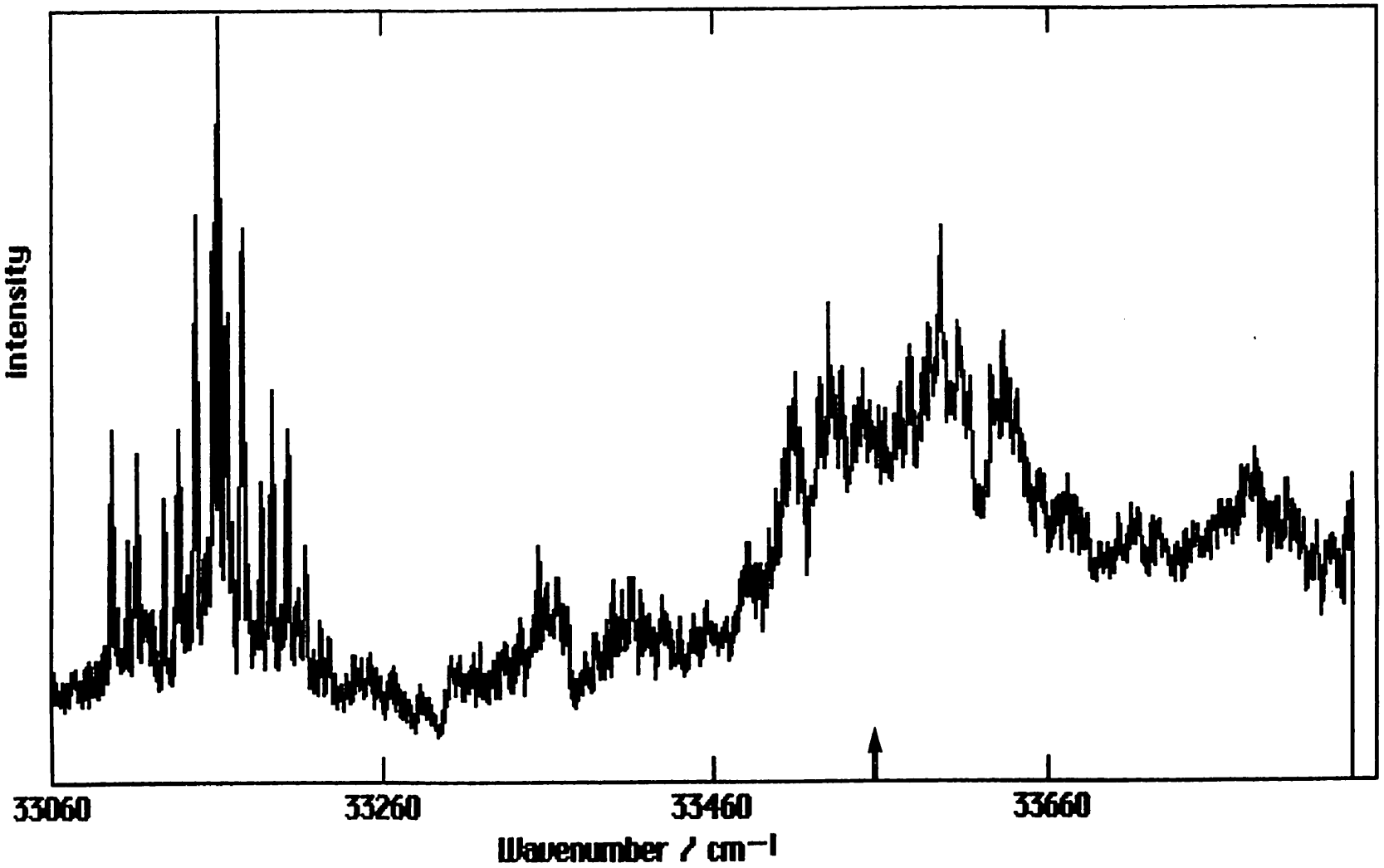

Figure 3.12 Origin region of LIF excitation spectrum of DMAEB.

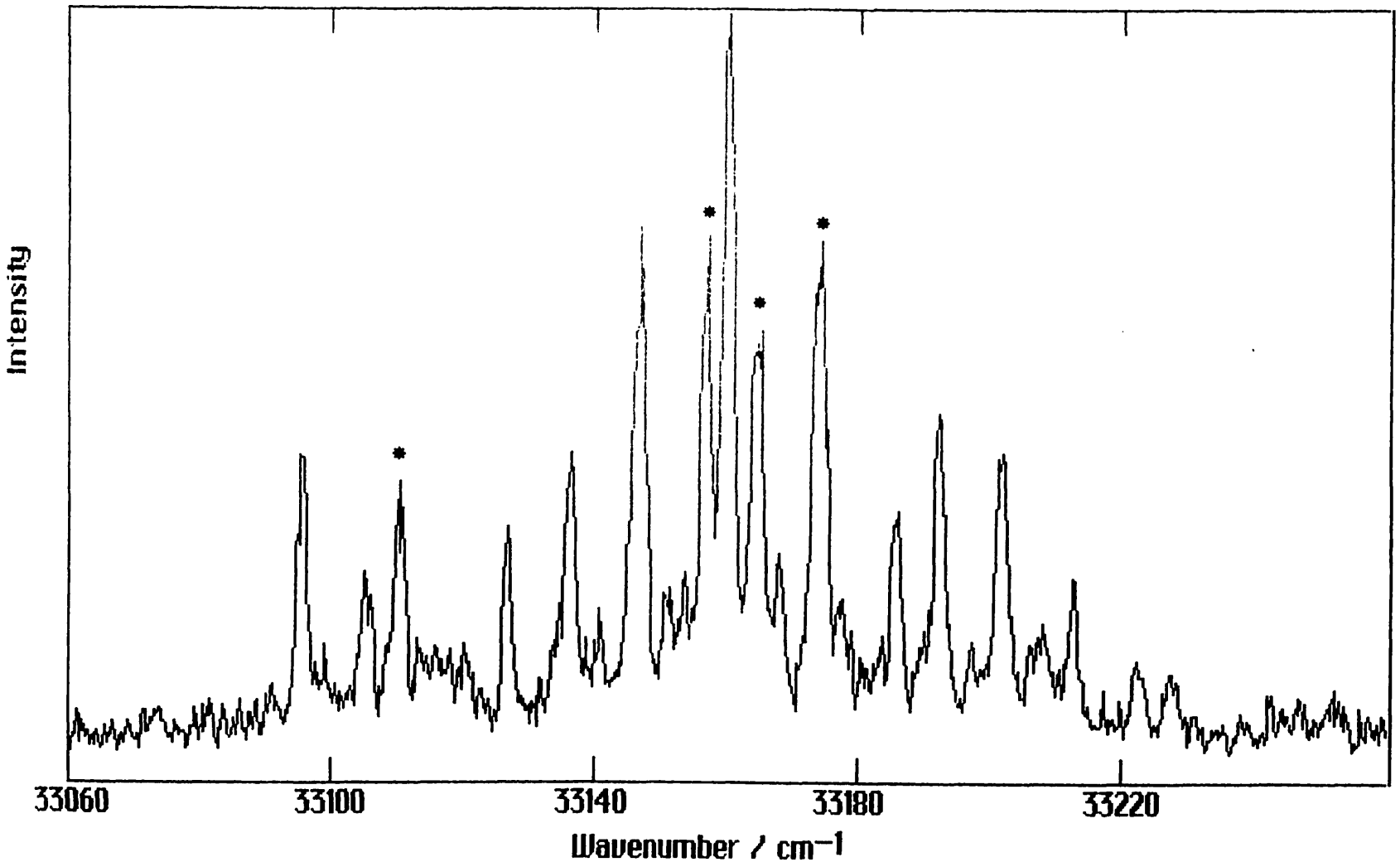

great similarity to that obtained for the methyl ester, however there are several features that do not appear in the DMAMB spectrum, and these are indicated by an asterisk (*).

The dispersed fluorescence spectrum of DMAEB recorded after exciting the most intense low frequency vibrational transition at 301.565nm is given as figure 3.13. The first transition observed is the resonance band, the contribution to this band by scattered laser light is ~35% of the overall intensity. The spectrum contains some resolvable low frequency structure although it was not possible to use sufficiently narrow monochromator slits to resolve single vibronic transitions. At a slit width resolution of ~50cm^{-1} fwhm, the spectrum becomes featureless beyond ~900cm^{-1}.

Figure 3.14 shows the dispersed fluorescence spectrum of DMAEB after excitation of the same intense transition as in figure 3.13 (301.565nm). This spectrum was recorded at a lower resolution, and no features were resolvable at the resolution used. Unresolved fluorescence is observed which has a maximum at ~320nm and extends out to 370nm. This is assigned as emission from the DMAEB S_1 (b^*) state. At this excitation wavelength and under these expansion conditions there is no evidence for emission at wavelengths greater than 370nm.

The fluorescence spectrum obtained by exciting the broad and relatively intense feature ~450cm^{-1} higher in energy than the origin at an oven temperature of 120°C is shown in figure 3.15a. The point of excitation is indicated by an arrow in figure 3.11. In addition to unresolved redistributed fluorescence from the S_1 (b^*) state, maximising at ~320nm, a

Figure 3.13 Dispersed fluorescence spectrum of DMAEB exciting intense band = 301.565nm

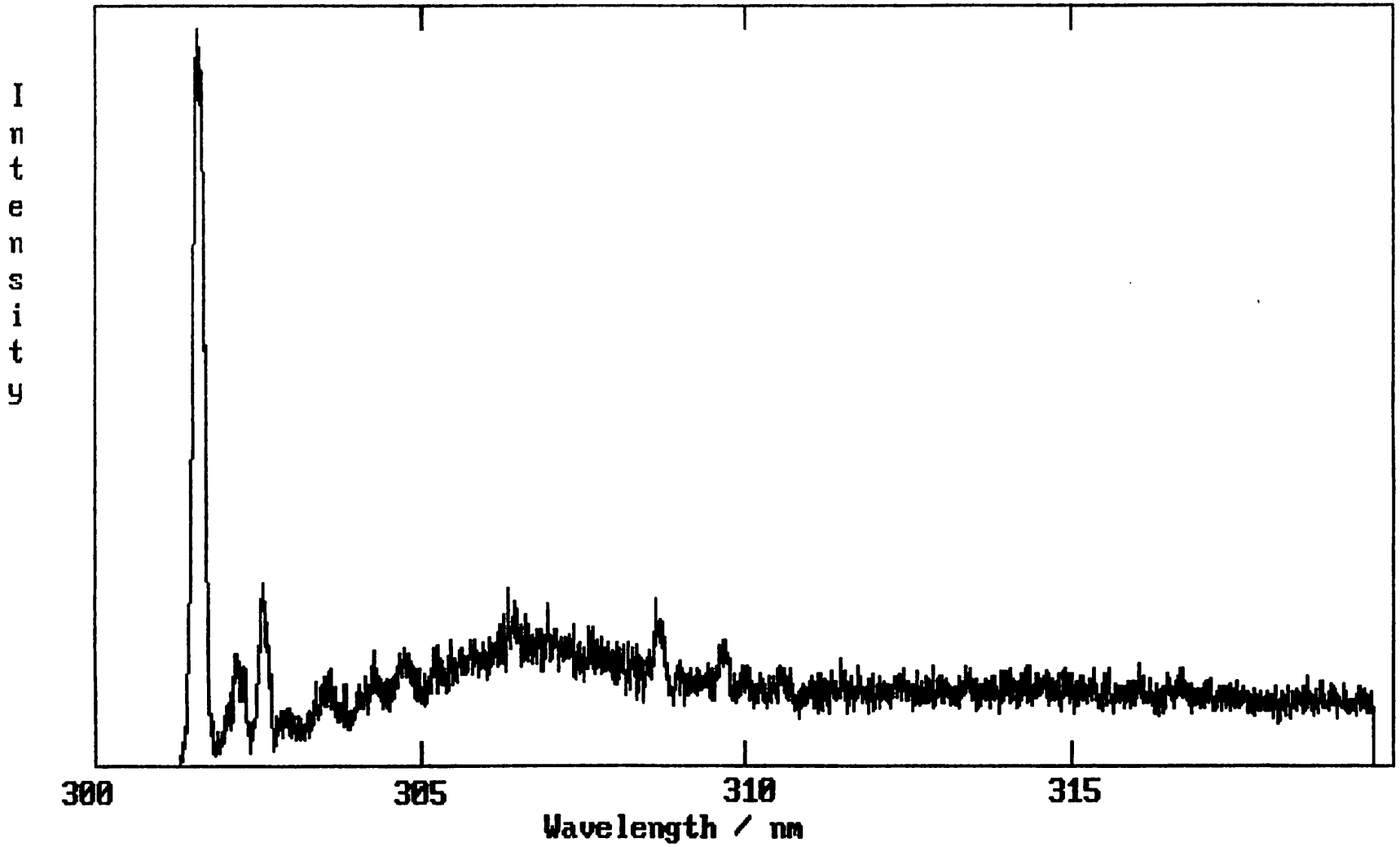

Figure 3.14 Low resolution dispersed emission spectrum of DMAEB exciting intense feature at 301.565nm

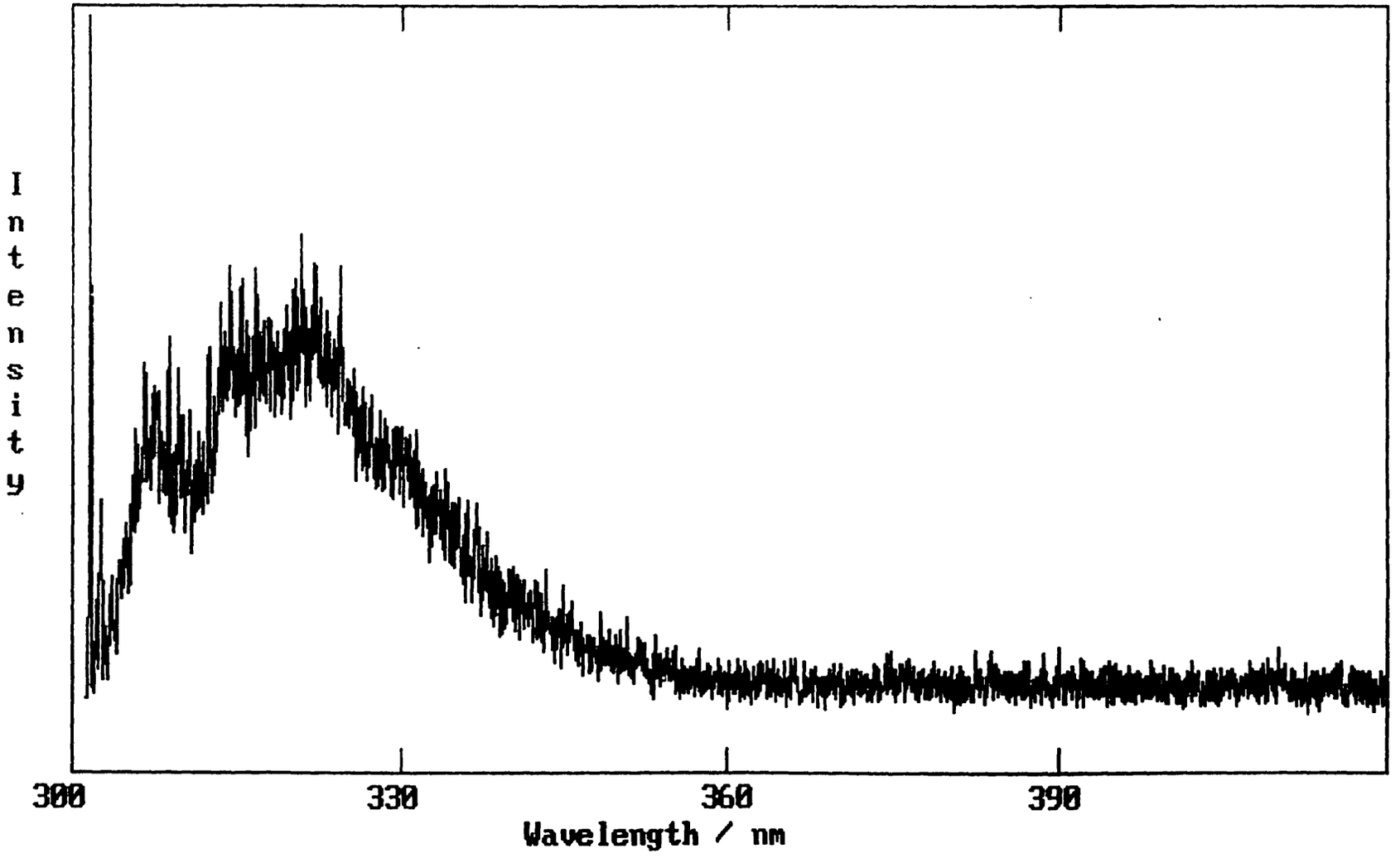

Figure 3.15 Dispersed emission spectra of jet cooled DMAEB after excitation at 298nm recorded at various sample oven temperatures a) 120°C b) 140°C c) 160°C.

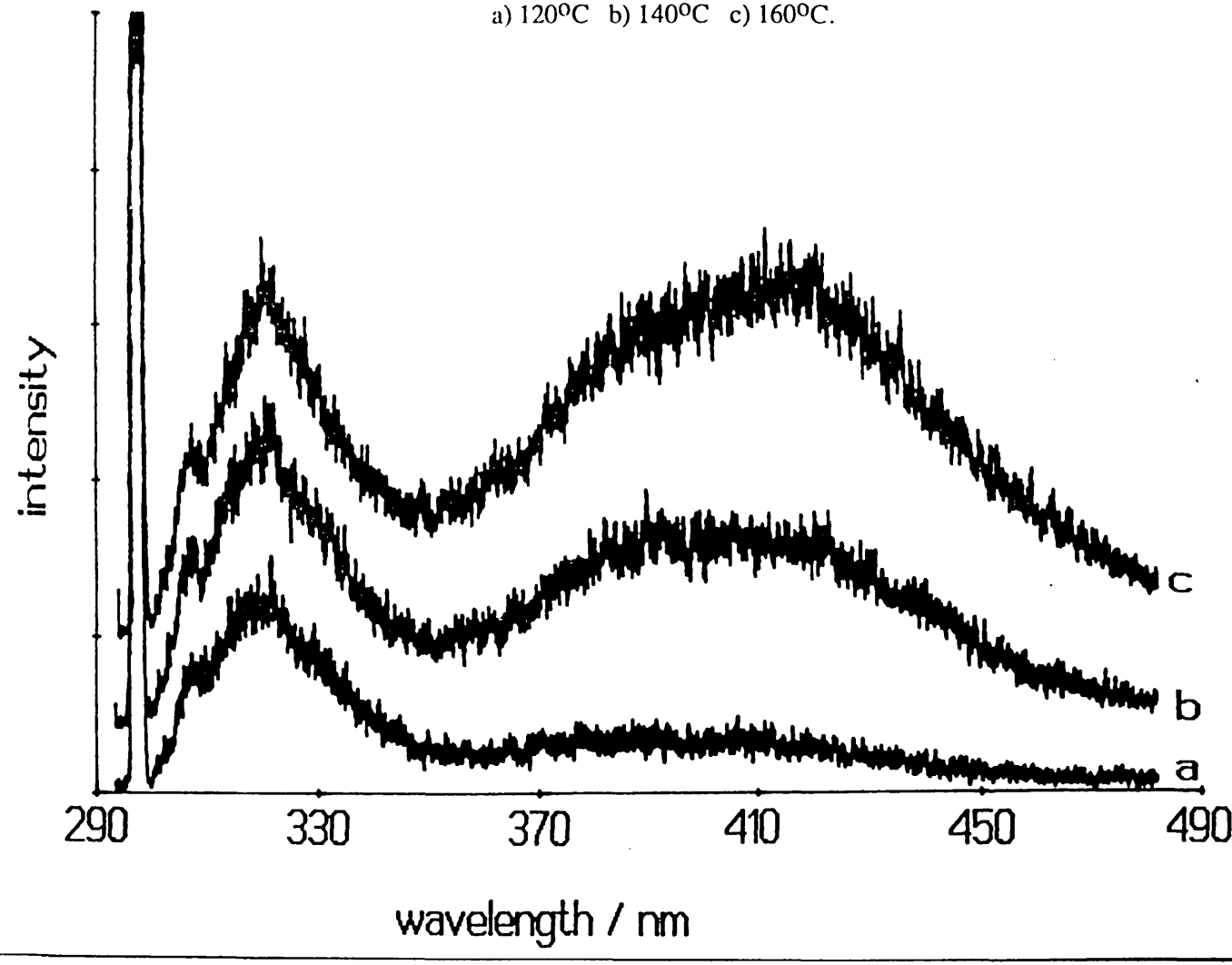

second, broad, red shifted band extending from ~340nm to 500nm ($-D\nu$ ~ 4000-14000cm^{-1}) is apparent. As illustrated in figures 3.15 b and c, increasing the oven temperature (and thus the partial pressure of DMAEB in the expansion) results in a considerable increase in the intensity of the red shifted fluorescence relative to the short wavelength fluorescence. It was not possible to obtain a quantitative relationship to describe the relative intensities of the two bands, but the variation of the intensity of the red shifted fluorescence with the intensity of the short wavelength fluorescence can be approximated to a quadratic.

Excitation spectra recorded through the monochromator at detection wavelengths of 315nm and 415nm are shown in figures 3.16a and b respectively. These spectra were recorded at greatly elevated oven temperature (160 °C) to maximise the amount of both short and long wavelength emission. Figure 3.16a reveals resolvable vibronic features superimposed upon a clearly evident continuous fluorescence component. Figure 3.16b shows the excitation spectrum associated with the red shifted emission band only. It reveals only structureless quasi-continuum with no resolvable excitation features. The laser light was blocked off during the spectrum to illustrate that this was in fact a real component and not merely an instrumental artefact for example a drifting baseline. The onset of the quasi-continuum was estimated to occur some 600cm^{-1} to the red of the DMAEB S_1 origin. These spectra reveal that the red shifted emission arises from excitation of the quasi-continuum, and the short wavelength emission from excitation of the S_1 vibronic features. The quasi-

Figure 3.16 LIF excitation spectra of jet cooled DMAEB recorded monitoring fluorescence at a) 315nm b) 415nm.

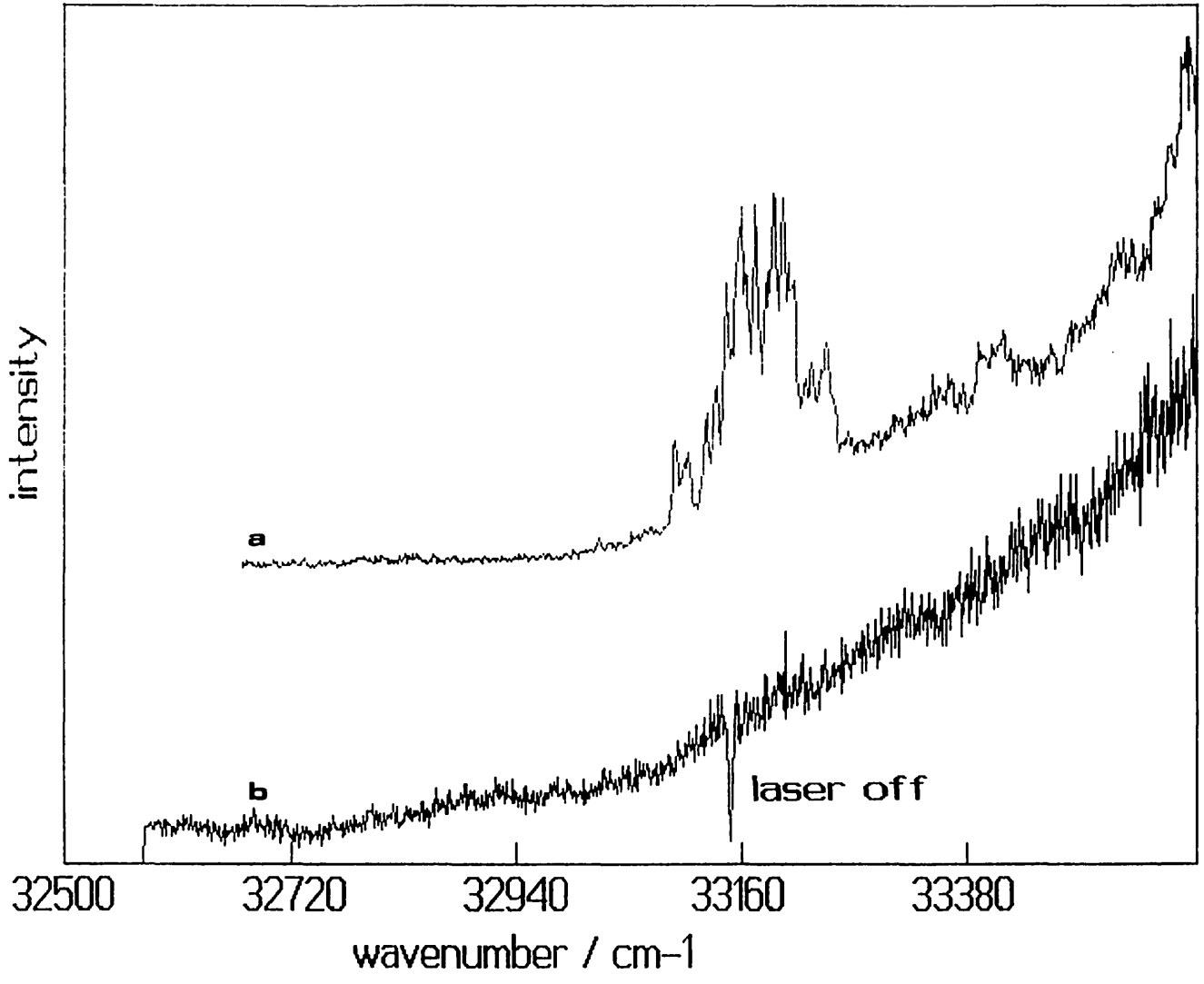

continuum is evident in figure 3.16a due to detection of part of the broad red shifted emission which overlaps with the short wavelength emission at 315nm.

3.3.2 4-N,N-dimethylaminomethylbenzoate (DMAMB)

The LIF excitation spectrum of jet cooled DMAMB is shown in figure 3.17. This is in good agreement with that reported by August et al[65] and as expected there is great similarity between this and the excitation spectrum of DMAEB. There are a number of resolvable vibronic transitions in the origin region of the spectrum. As observed for the ethyl ester there is an underlying quasi-continuum evident and on going to higher energies the spectrum becomes congested and there is little resolvable structure. Partially resolved features can be observed extending some $1200cm^{-1}$ above the origin in contrast to the case of the ethyl ester.

The origin region of the excitation spectrum is shown as figure 3.18 and as for DMAEB there is a characteristic pattern of low frequency vibrational modes, dominated by a $65cm^{-1}$ transition. This pattern bears a strong similarity to those observed for both the ethyl ester and for DMABN. The frequencies of these transitions are given in table 3.1. All of the low frequency modes observed for DMAMB have counterparts in the ethyl ester excitation spectrum. These are characteristic of the dimethylamino group and will be discussed in terms of all three molecules later.

Figure 3.19 shows a high resolution spectrum of the intense $65cm^{-1}$ transition in the excitation spectrum. The resolution

Figure 3.17 LIF excitation spectrum of jet cooled 4-N,N-dimethylaminomethylbenzoate

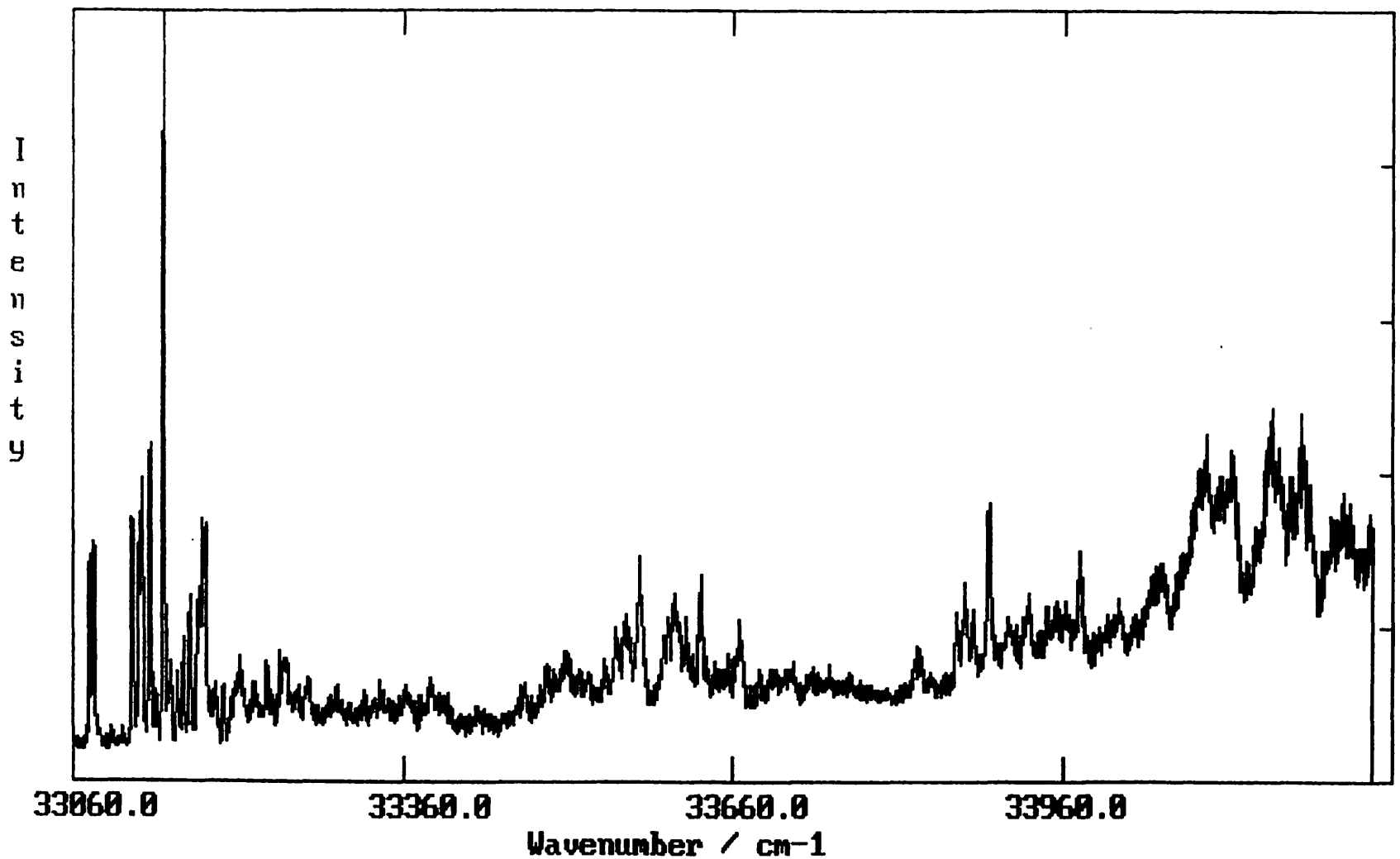

Figure 3.18 Origin region of LIF excitation spectrum of jet cooled DMAEB.

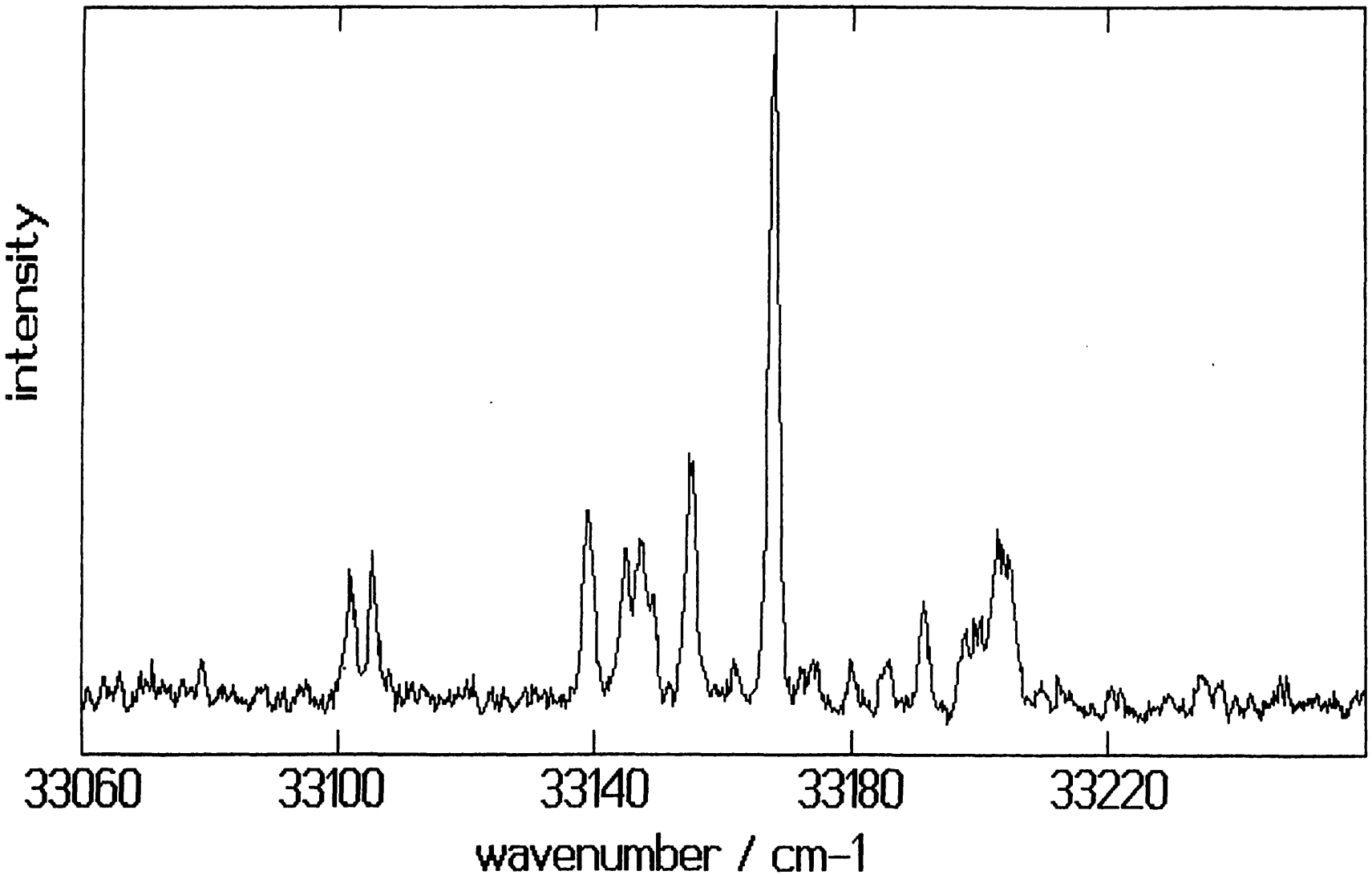

Table 3.1 Relative shifts of the prominent low frequency modes from the origin transition in the excitation spectra of DMABN, DMAMB and DMAEB.

	DMABN	DMAMB	DMAEB
	relative shift / cm^{-1}		
i	0	0	0
ii	-	4	10
iii	-	-	15
iv	37	38	31
v	43	46	41
vi	-	53	51
vii	-	-	60
viii	61	65	65
ix	-	-	69
x	-	-	78
xi	-	89	90
xii	-	95	96
xiii	100	98	106
xiv	118	101	116

Figure 3.19 High resolution excitation spectrum of DMABN intense band.

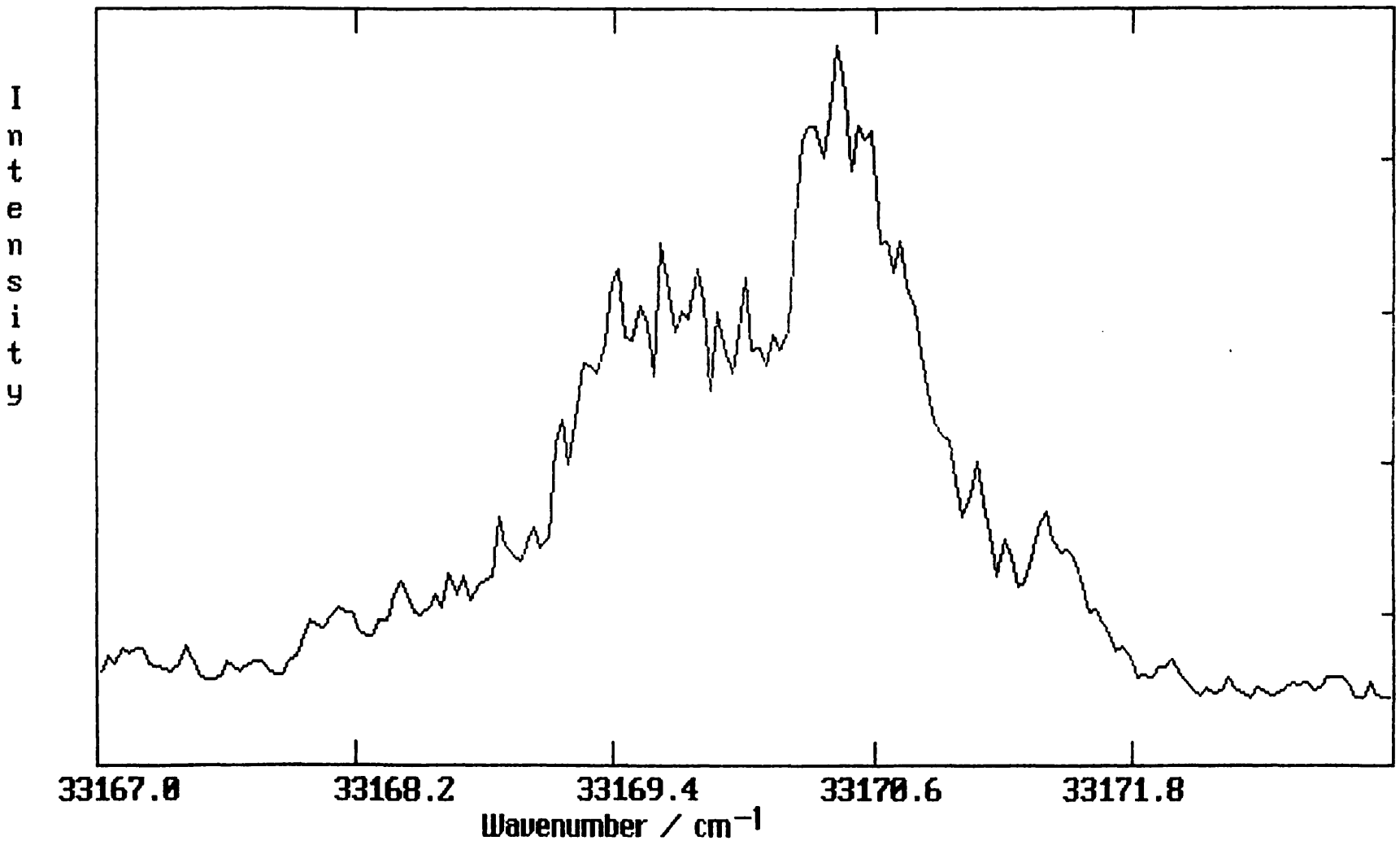

is limited by the dye laser grating and it was not possible to resolve the rotational envelope any further. This band contour is typical of those obtained for the origin region transitions of both the methyl and ethyl esters, and exhibits a typical double headed 'b' type rotational contour.

The dispersed fluorescence spectrum of DMAMB recorded after excitation of the intense feature at 33167cm^{-1} is shown in figure 3.20. As for the ethyl ester there is low frequency structure evident in the spectrum but due to the low fluorescence intensity it was impossible to reduce the monochromator slit width sufficiently to resolve individual vibronic features. Vibronic structure was observable some 1500cm^{-1} to the red of the origin, further than for the ethyl as it has a lower density of optically active low frequency modes.

Upon excitation at higher energy, 291.000nm (~1260cm^{-1} to the red of the origin), a low resolution dispersed fluorescence spectrum of DMAMB was obtained at an oven temperature of 125°C(see figure 3.21). Only redistributed S_1 fluorescence was observed, which has a maximum at ~320nm and extends out to ~360nm. There was no evidence for any red shifted emission.

The emission spectrum recorded after excitation at 291.000nm at a much higher oven temperature,180°C, is given in figure 3.22. This shows in addition to the normal S_1 emission (maximising at ~320nm) a 'shoulder' which is in fact a second red shifted fluorescence band. It was not feasible to elevate the temperature any further to try to increase the intensity of this band.

Figure 3.20 Dispersed fluorescence spectrum of DMAMB exciting intense band = 301.507nm

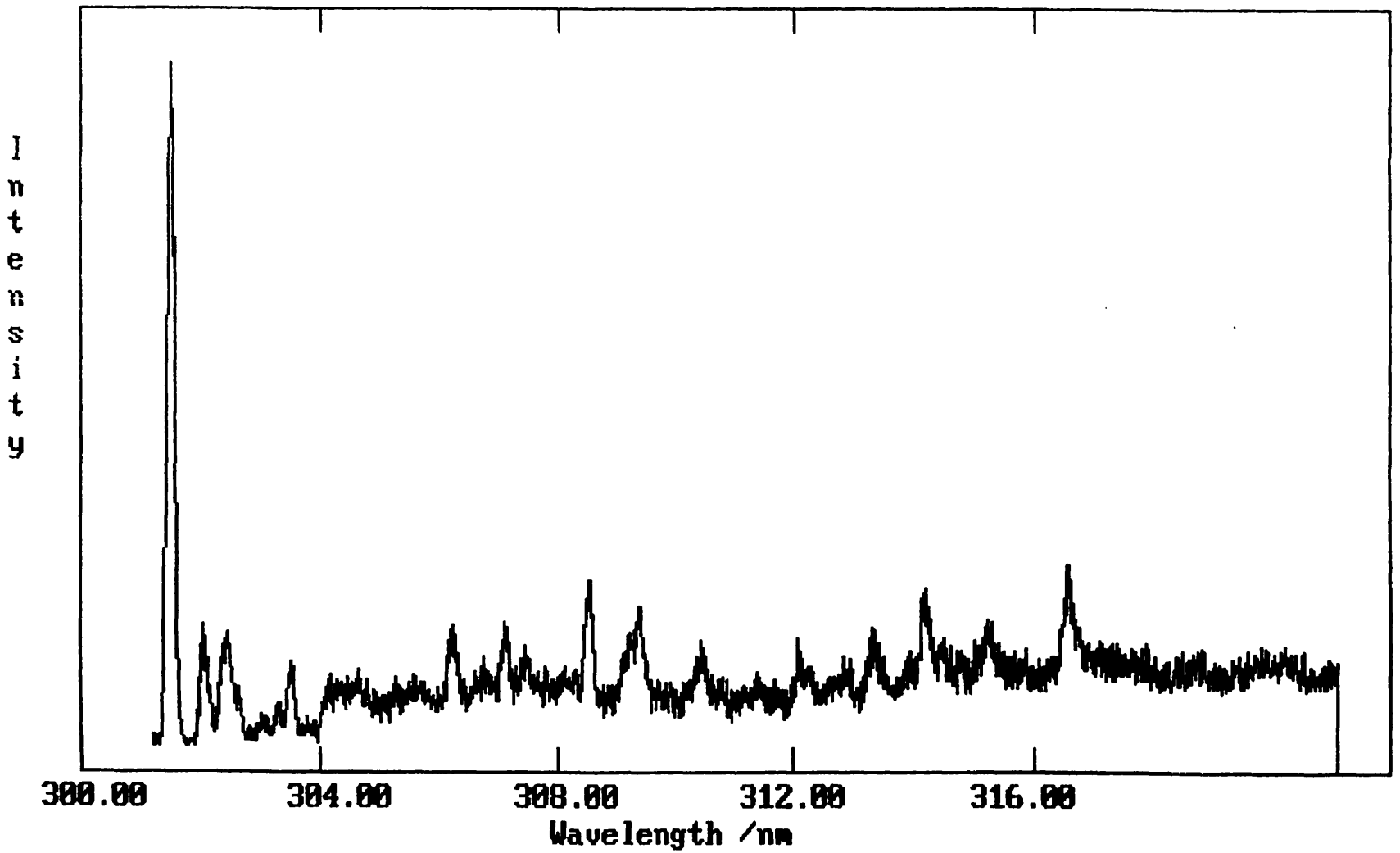

Figure 3.21 Dispersed fluorecence spectrum of jet cooled DMAMB after exciting at 291nm recorded at low oven temperature 120^{0}C

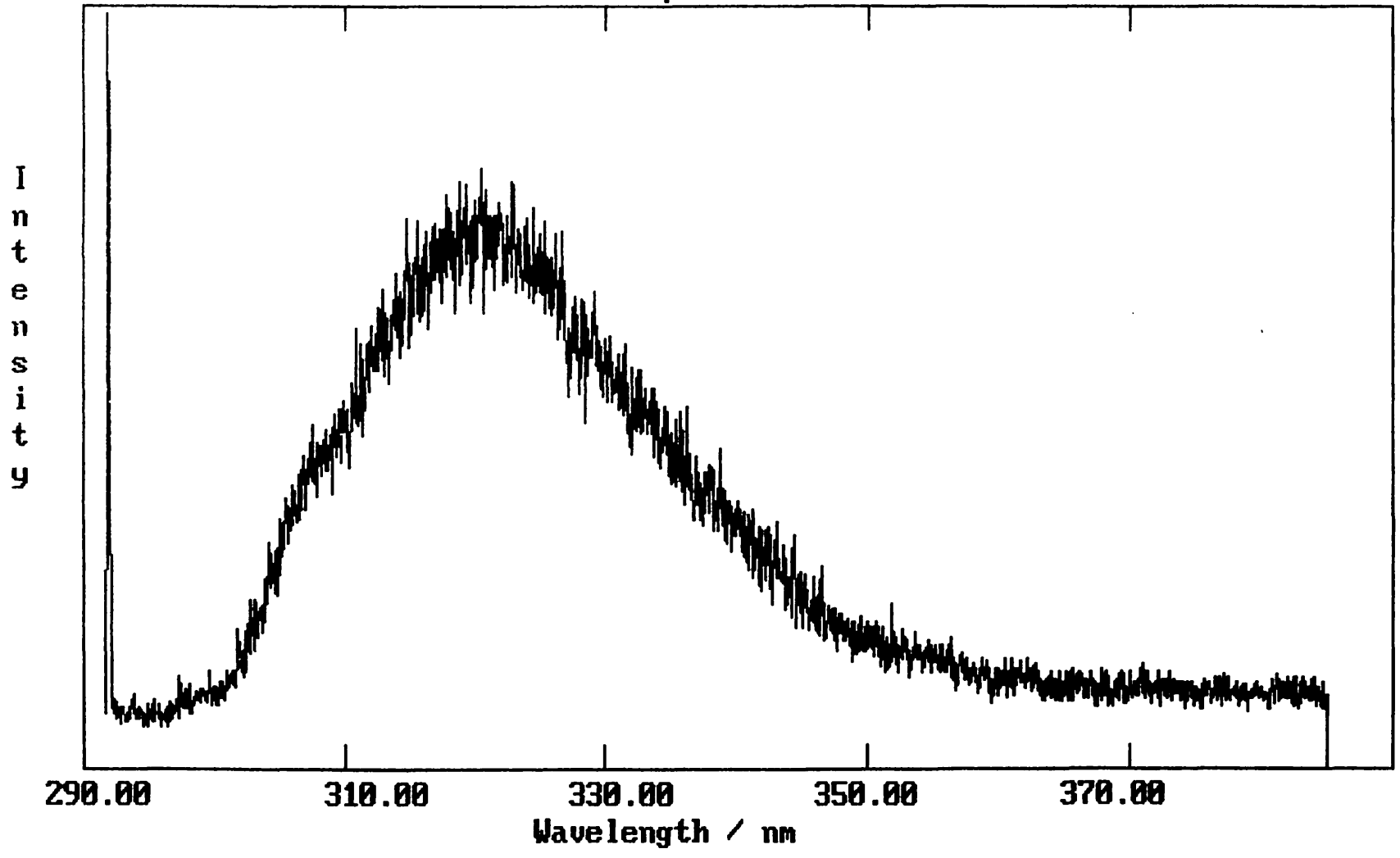

Figure 3.22 Dispersed fluorescence spectrum of DMAMB exciting at high energy 291nm at high temperature 180°C

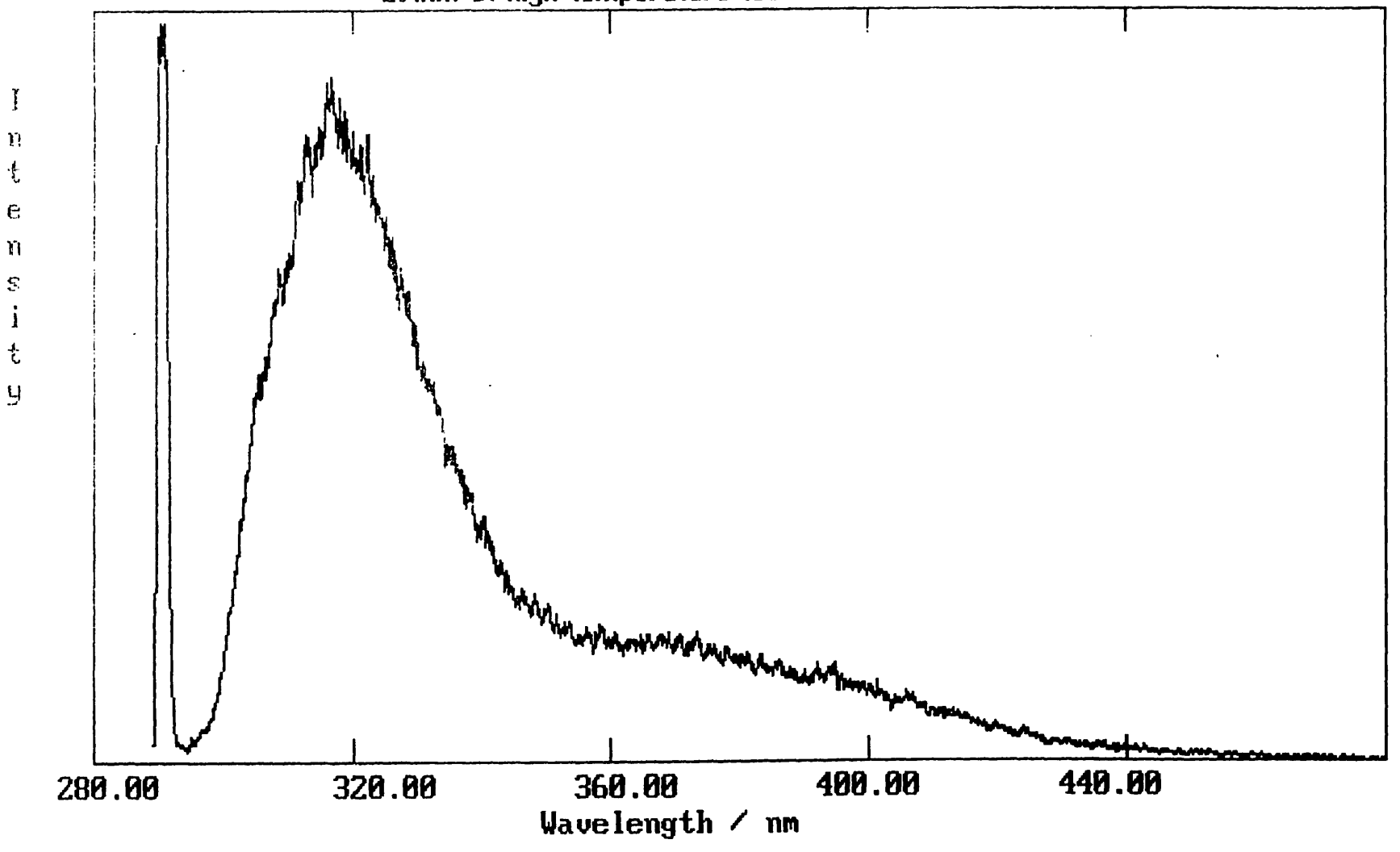

3.3.3 4-N,N-dimethylaminobenzonitrile (DMABN)

Figure 3.23a and b shows the LIF excitation spectrum of DMABN recorded at nozzle temperatures of 65°C and 110°C respectively. Both are in good agreement with those reported by previous authors[58,59]. The characteristic pattern of low frequency modes, which is shown at higher resolution in figure 3.24 recurs three times in the spectrum. It appears to consist primarily of six bands , the frequencies of which are given in table 3.1. The lowest energy transition occurs at 32333cm^{-1}. As can be seen from figure 3.24 all of the transitions exhibit typical 'b' type rotational contours. At higher oven temperature the spectrum can be seen to be broadened and the intensity of the transitions decrease relative to the background and an increase in the background can be seen, particularly in the higher energy region of the spectrum.

Dispersed emission spectra recorded after excitation at 308.47nm are given in figure 3.25. The excitation source gives broad excitation (~60cm^{-1} fwhm) so all features within this region were excited. The spectra all show an unresolved fluorescence band maximising at ~330nm with some partially resolved transitions superimposed upon this. This band is assigned as b* emission from the locally excited S_1 state. On increasing the temperature of the nozzle and hence the partial pressure of the sample in the expansion, a broad red shifted emission appears maximising at 390nm and extending out as far as 450nm, which increases relative to the short

Figure 3.23 LIF excitation spectra of DMABN at increasing sample oven temperatures : a) 65°C b) 110°C

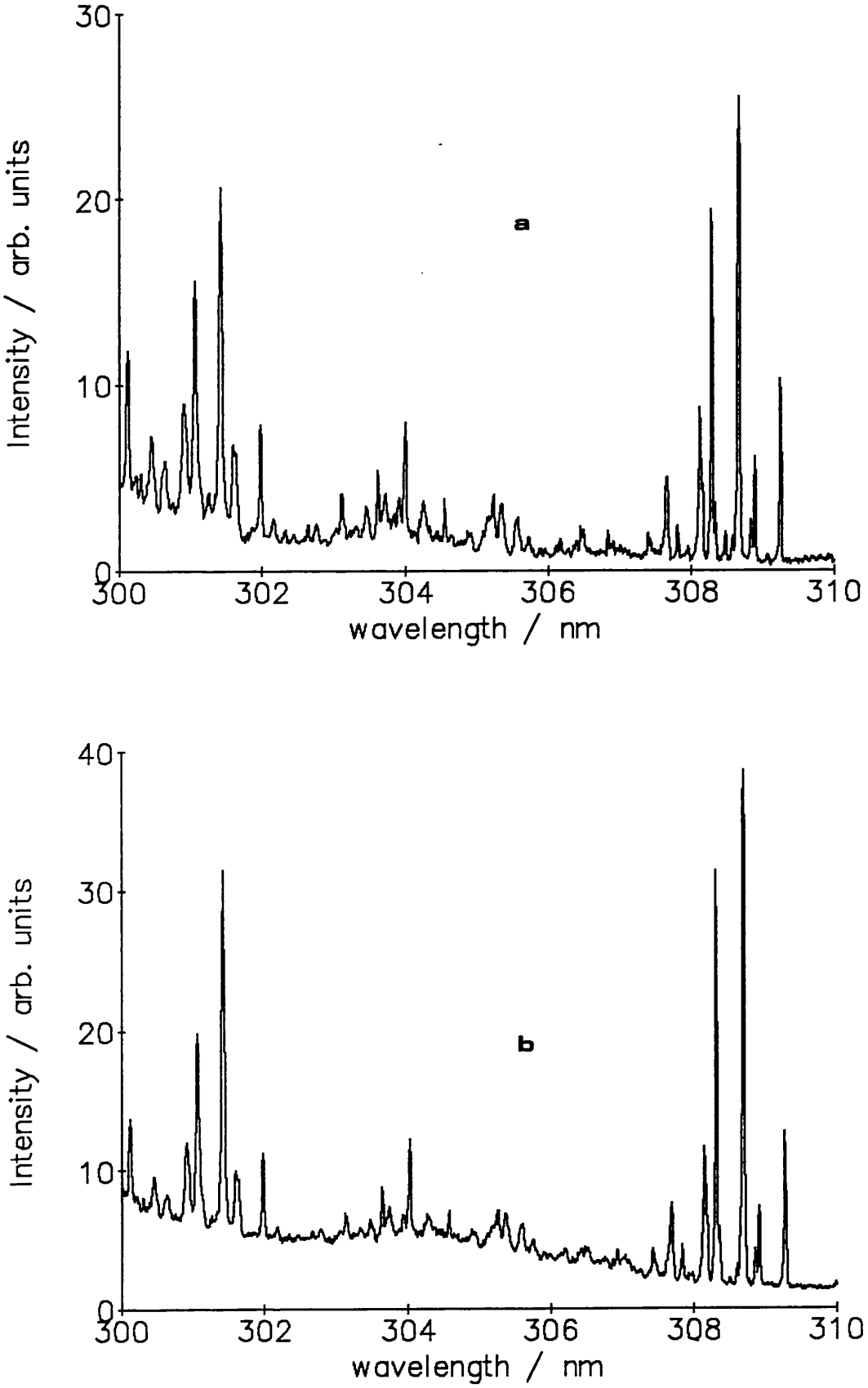

Figure 3.24 L.I.F. excitation spectrum of the origin region of DMABN

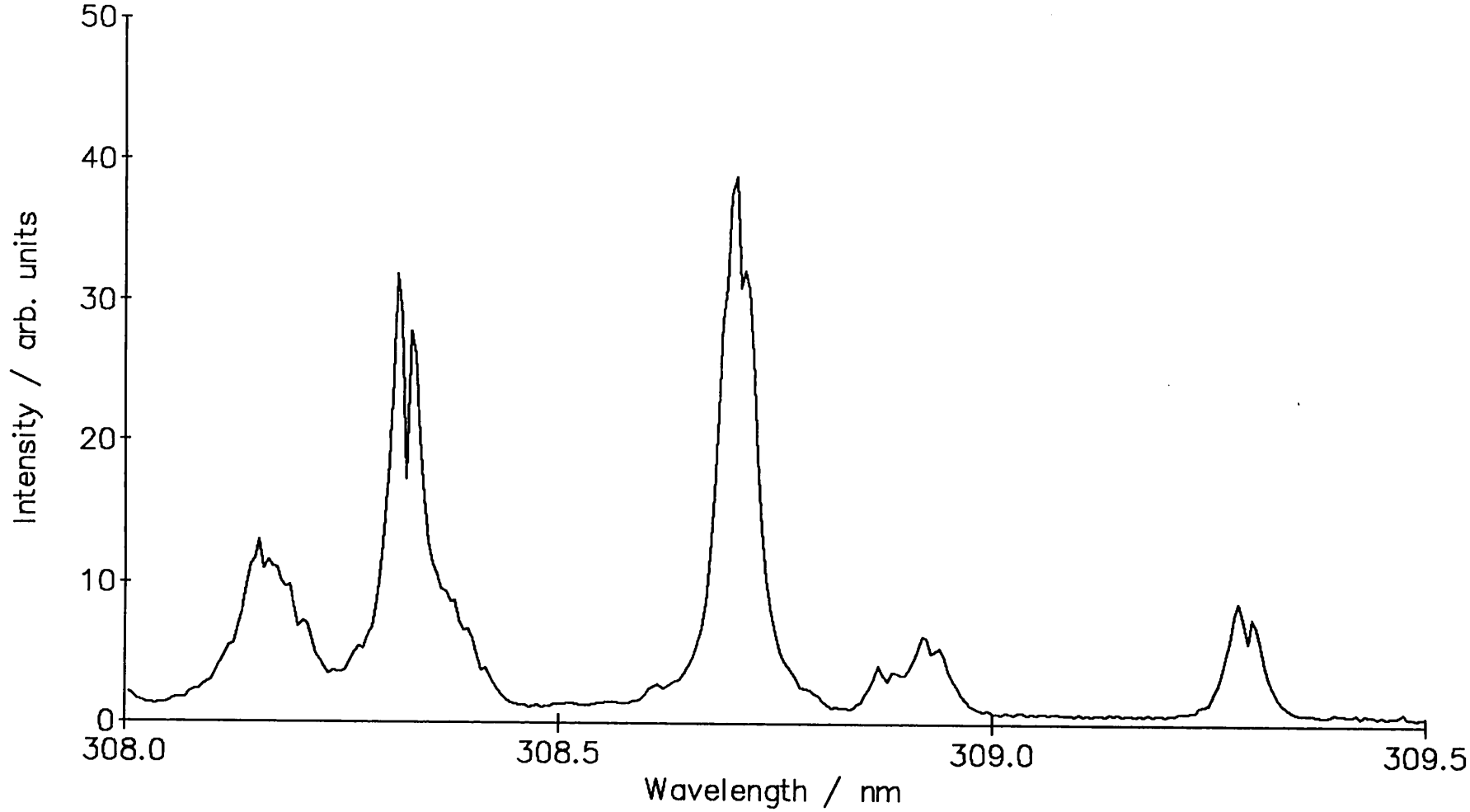

Figure 3.25 Dependence of the emission spectrum of DMABN on sample oven temperature

a) 65°C b) 80°C c) 95°C d) 110°C

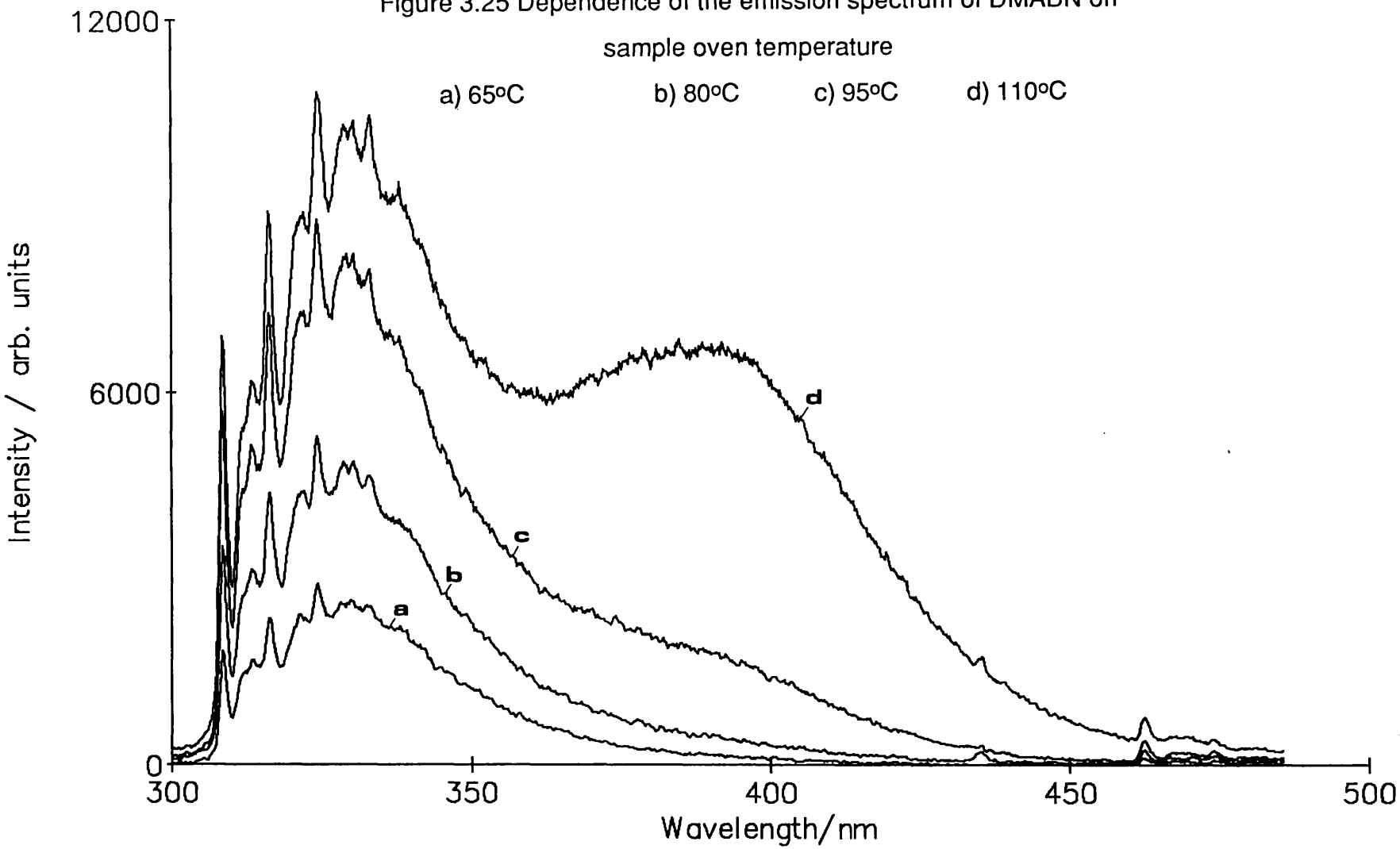

wavelength at increasing partial pressures. This emission is similar to that observed for both ester derivatives.

Figure 3.26a shows the LIF excitation spectrum recorded monitoring fluorescence between 330 and 380nm. The spectrum shows a number of low frequency vibrational modes. On monitoring fluorescence between 340 and 480nm (see figure 3.26b) which allows most of the red shifted emission to be detected, the continuous spectrum becomes evident. This reveals that the short wavelength fluorescence emanates from excitation of the vibronic levels of the locally excited S_1 state, and the red shifted emission arises from excitation of the continuous spectral component.

3.4 Results: The Solvated DMABN Molecule.

LIF excitation spectra of DMABN complexed with the different solvents were all found to be broad and structureless, the excitation wavelength used for recording fluorescence spectra was 308.45nm and these were recorded at moderate resolution, and wavelength accuracy is therefore ± 1nm.

3.4.1 DMABN / Cyclohexane

The dispersed fluorescence spectra of DMABN complexed with cyclohexane recorded at different sample oven temperatures, and hence DMABN partial pressures, are shown in figure 3.27a. The total pressure of carrier gas (including solvent) was $0.2 kgcm^{-2}$. At low nozzle temperatures (low partial pressure of DMABN) a single unresolved fluorescence band is observed

Figure 3.26 L.I.F. excitation spectra of DMABN

a) monitoring emission from both fluorescence bands

b) monitoring mostly red shifted emission

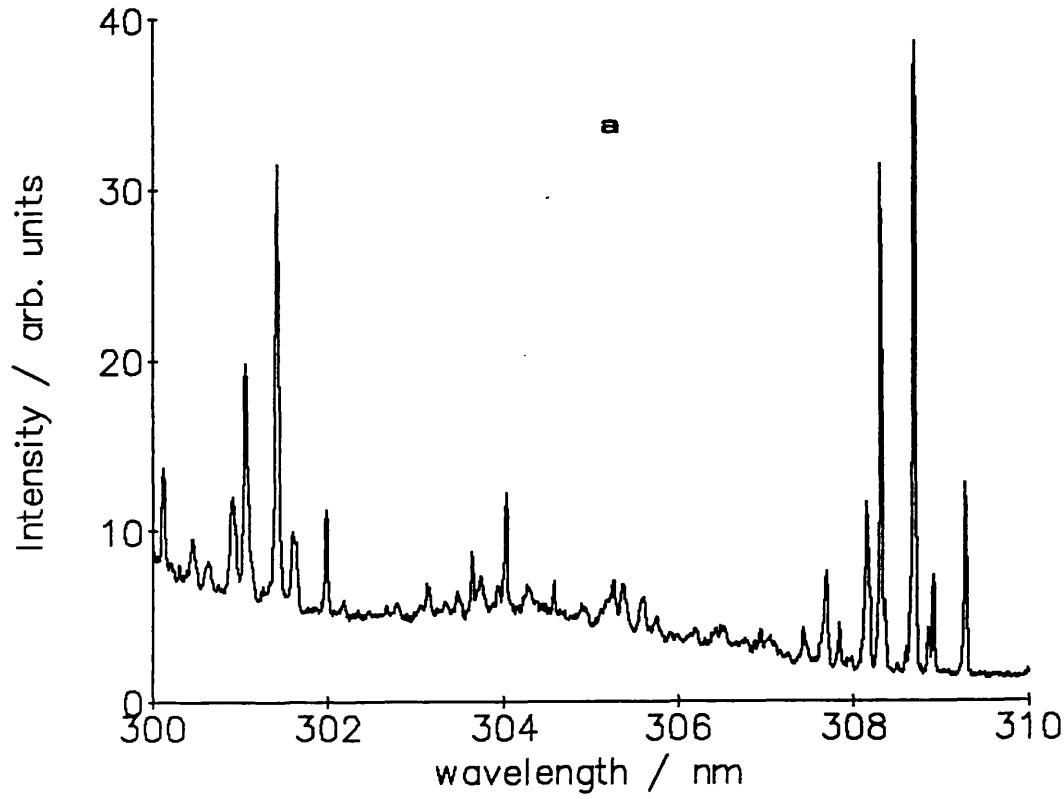

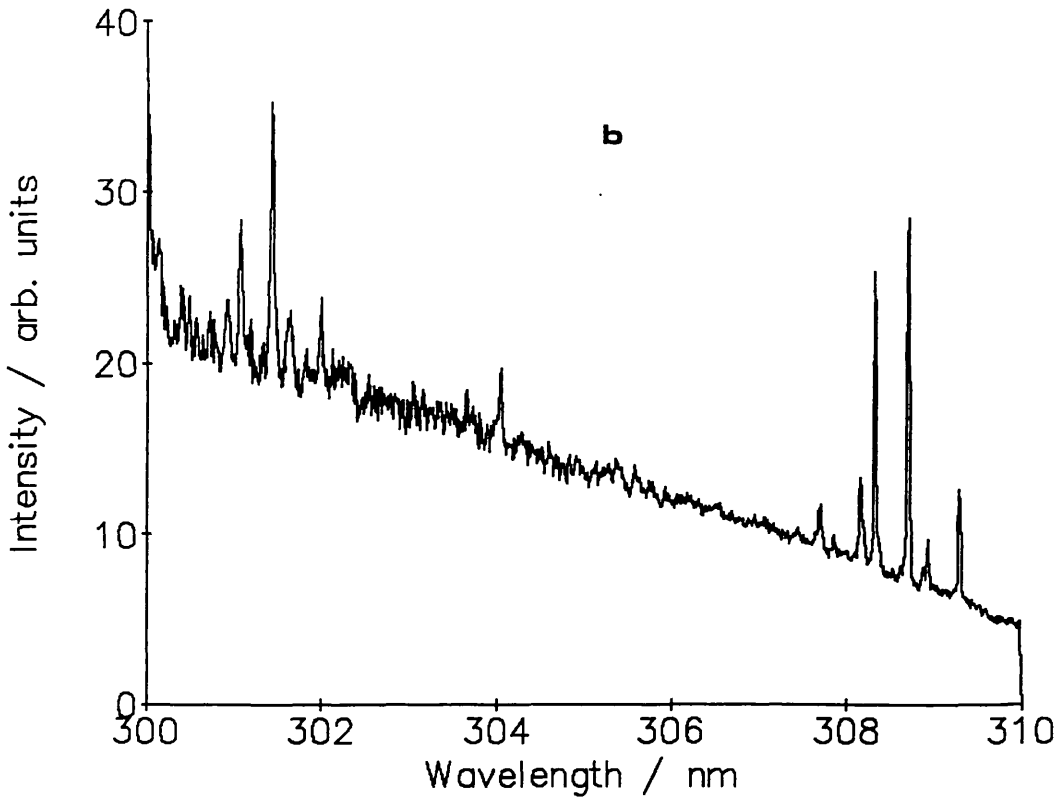

Figure 3.27 Dispersed emission spectra of jet cooled DMABN / cyclohexane clusters.

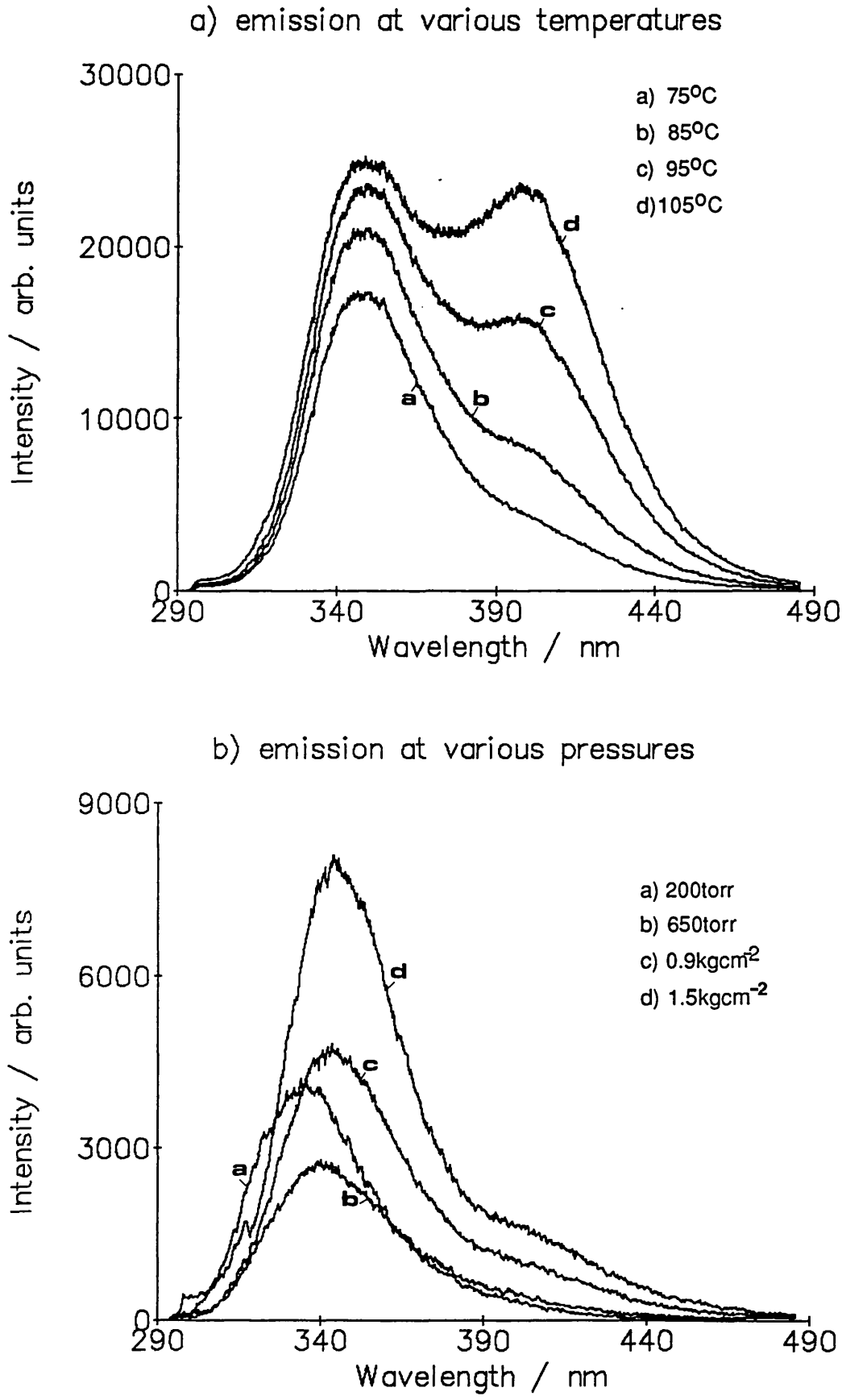

maximising at ~ 348.5nm, shifted some 18.5nm to the red of the unsolvated molecule. On increasing the nozzle temperature the overall intensity of emission increases, and a second broad, red shifted emission band appears, maximising at 399nm and extending out to 480nm.

In figure 3.27b the fluorescence spectra of DMABN / cyclohexane recorded at various carrier gas backing pressures are presented. The spectra were all recorded at 85°C. At very low backing pressures a single fluorescence band was observed maximising at 335nm, on increasing the backing pressure there is an initial decrease in the intensity of emission, upon further increase in pressure the intensity grows back, but the single emission band is shifted to lower energy, maximising at 344nm. There is no evidence of a small shoulder on the red edge of the emission band at all but the lowest pressure. It is important to mention here that the pressures quoted are total pressures of helium plus solvent.

3.4.2 DMABN / Methanol

Dispersed fluorescence spectra of DMABN complexed with methanol at various sample oven temperatures are presented as figure 3.28. All spectra were recorded at a backing pressure of 0.75kgcm^{-2}. At low oven temperature, unresolved redistributed fluorescence band is observed, maximising at 352nm. On increasing the nozzle/oven temperature, a second broad red shifted emission band appears, maximising at 430nm which dominates the spectrum at very high temperatures.

Figure 3.28 DMABN / methanol
Emission at various temperatures

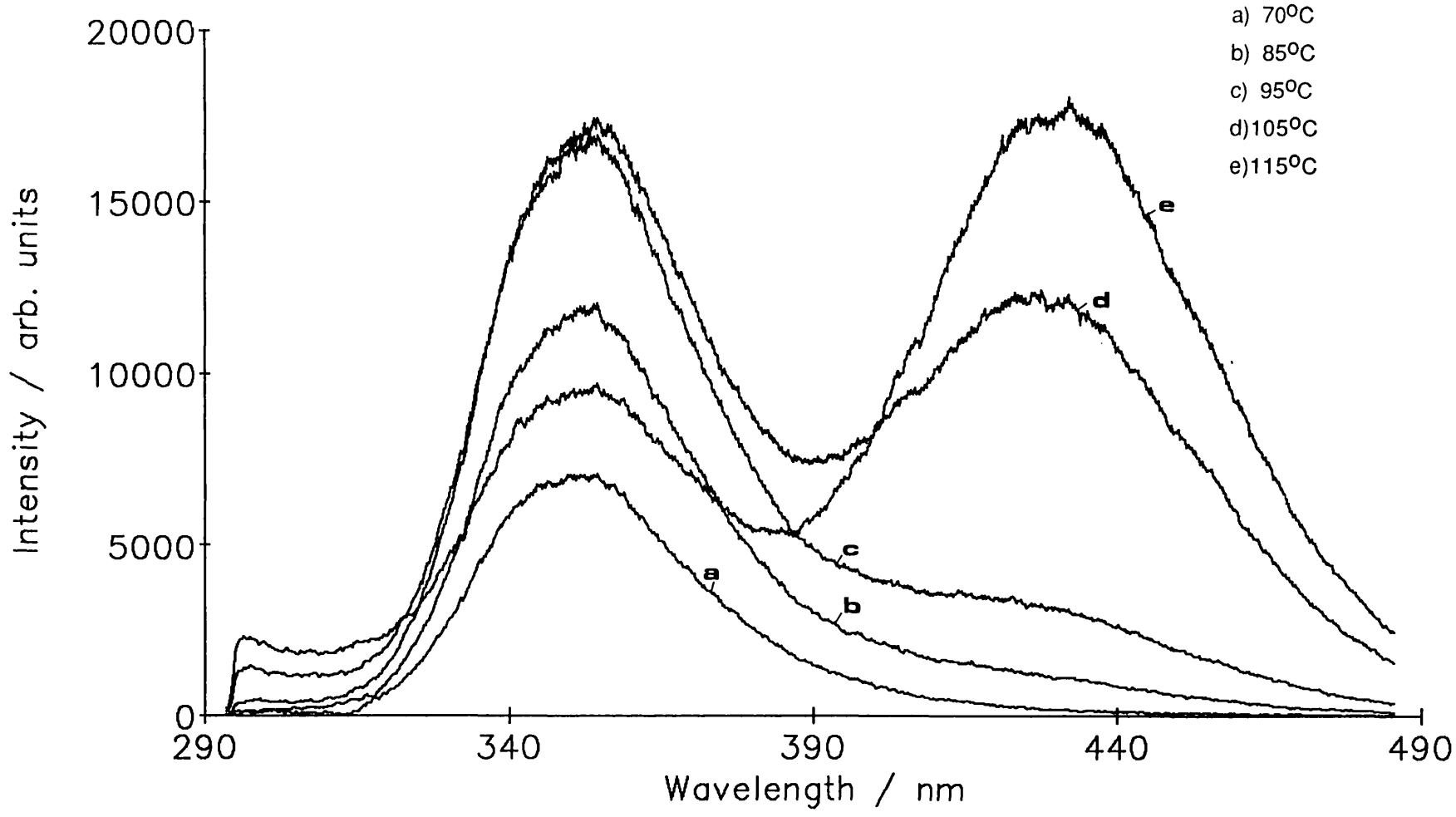

In figure 3.29a the dispersed fluorescence spectra of DMABN / methanol recorded at various carrier gas backing pressures are presented. The spectra were all recorded at 75°C. At very low backing pressures a single fluorescence band was observed maximising at 335nm, on increasing the backing pressure the overall intensity of emission initially decreases, and then increases with a single fluorescence band maximising at 352nm.

A similar study of pressure dependence is presented in figure 3.29b, but recorded at elevated nozzle temperature,122°C. At very low backing pressures a single fluorescence band was observed maximising at 335nm, on increasing the backing pressure there is an initial decrease in the intensity of emission, and a second emission band becomes apparent, maximising at ~430nm. Upon further increase in pressure the intensity grows back, but only a single emission band is observed, shifted to lower energy than that observed at very low pressure, maximising at 352nm.

3.4.3 DMABN / Acetone

The dispersed fluorescence spectra of DMABN complexed with acetone recorded at different sample oven temperatures are shown in figure 3.30a. The total pressure of carrier gas (including solvent) was 650torr. At low oven temperatures (low partial pressure of DMABN) two emission bands are observed, maximising at 348nm and 408nm, the shorter wavelength band having slightly greater intensity. On increasing the oven temperature the overall intensity of

Figure 3.29 Pressure dependence on dispersed emission spectra of jet cooled DMABN / methanol clusters.

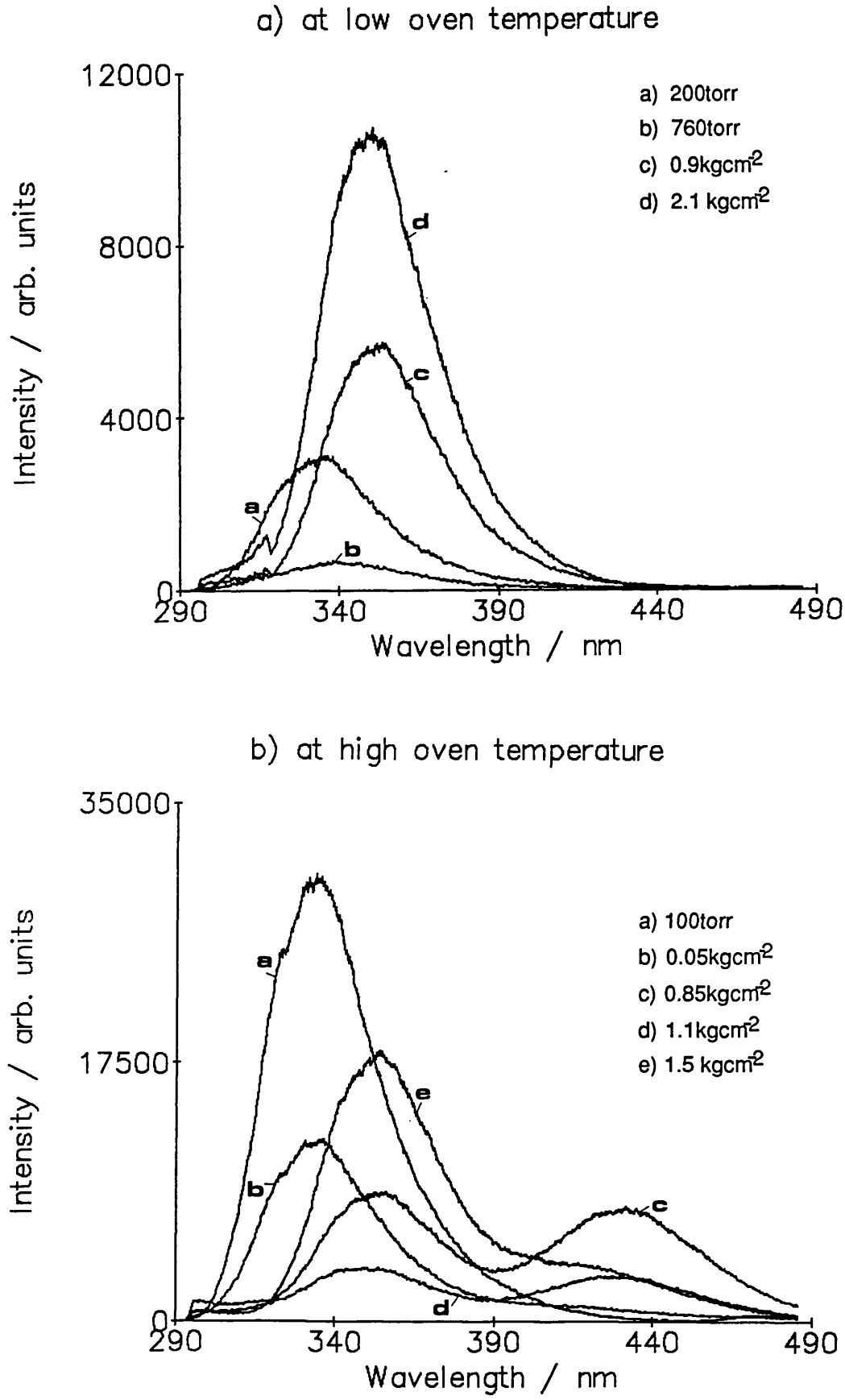

Figure 3.30 Dispersed emission spectra of jet cooled DMABN / acetone clusters.

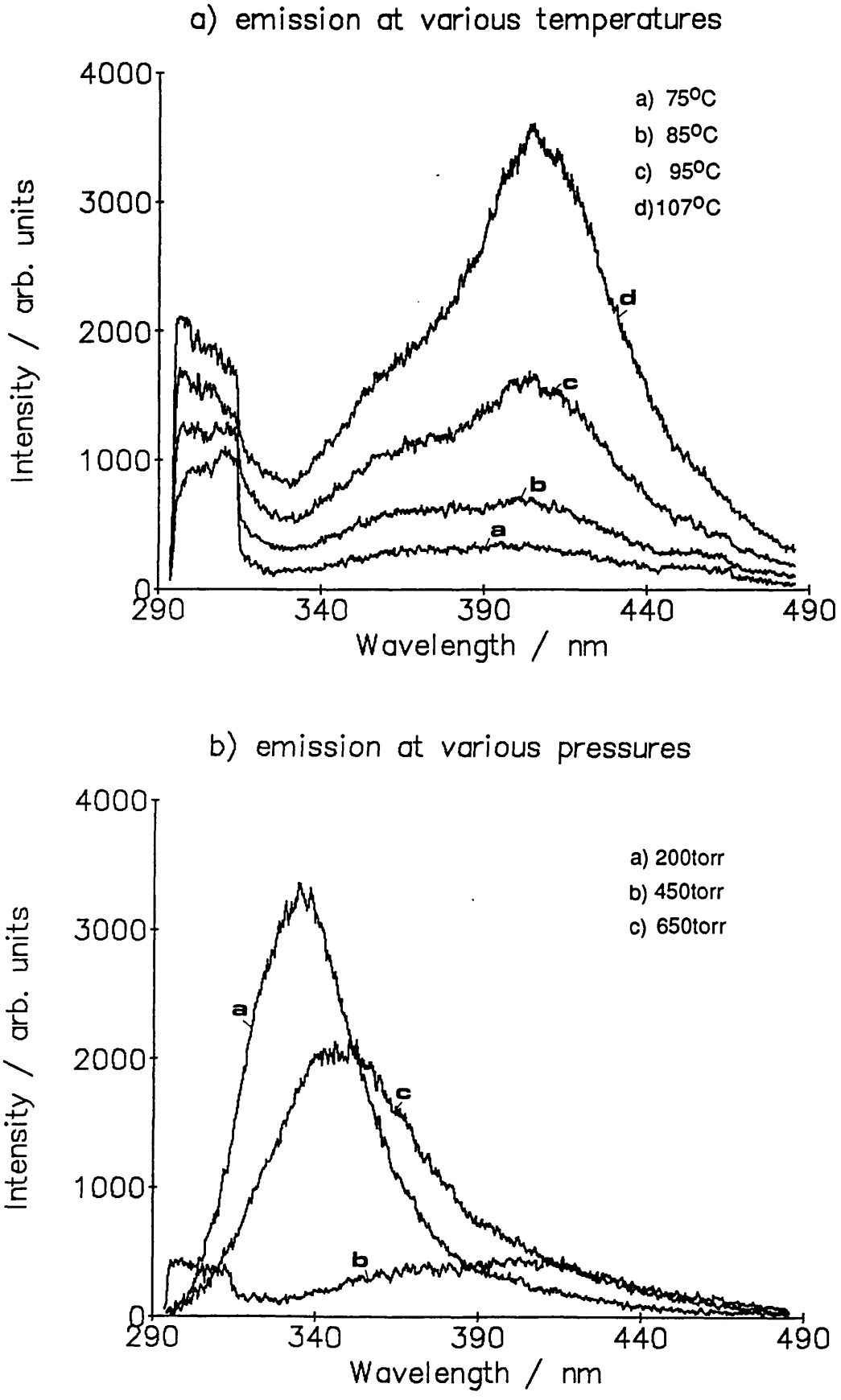

emission increases, and the second emission band, maximising at 408nm, increases in intensity relative to the short wavelength band and eventually dominates the spectrum.
In figure 3.30b the dispersed fluorescence spectra of DMABN / acetone recorded at various carrier gas backing pressures are presented. The spectra were all recorded at 75°C. At very low backing pressures a single fluorescence band was observed maximising at 335nm, on increasing the backing pressure a small amount a single emission band is again observed, however with the emission maximum shifted to 348nm. At higher pressures the signal intensity decreases, the fluorecence appears to be quenched in some way as the fluorescence intensity for all spectra is very low.

3.4.4 DMABN / Acetonitrile

The dispersed fluorescence spectra of DMABN complexed with acetonitrile recorded at different sample oven temperatures are shown in figure 3.31a. The total pressure of carrier gas (including solvent) was $0.1 kgcm^{-2}$. At low temperatures (low concentration of DMABN) a single unresolved fluorescence band is observed maximising at 354nm, shifted some 24nm from that of the unsolvated molecule. On increasing the temperature a second broad, red shifted emission band appears, maximising at 414nm and extending out to ~490nm.
In figure 3.32a the dispersed fluorescence spectra of DMABN / acetonitrile recorded at various carrier gas backing pressures are presented. The spectra were all recorded at 75°C. At low backing pressures a single fluorescence band was

Figure 3.31 DMABN / acetonitrile
Emission at various temperatures

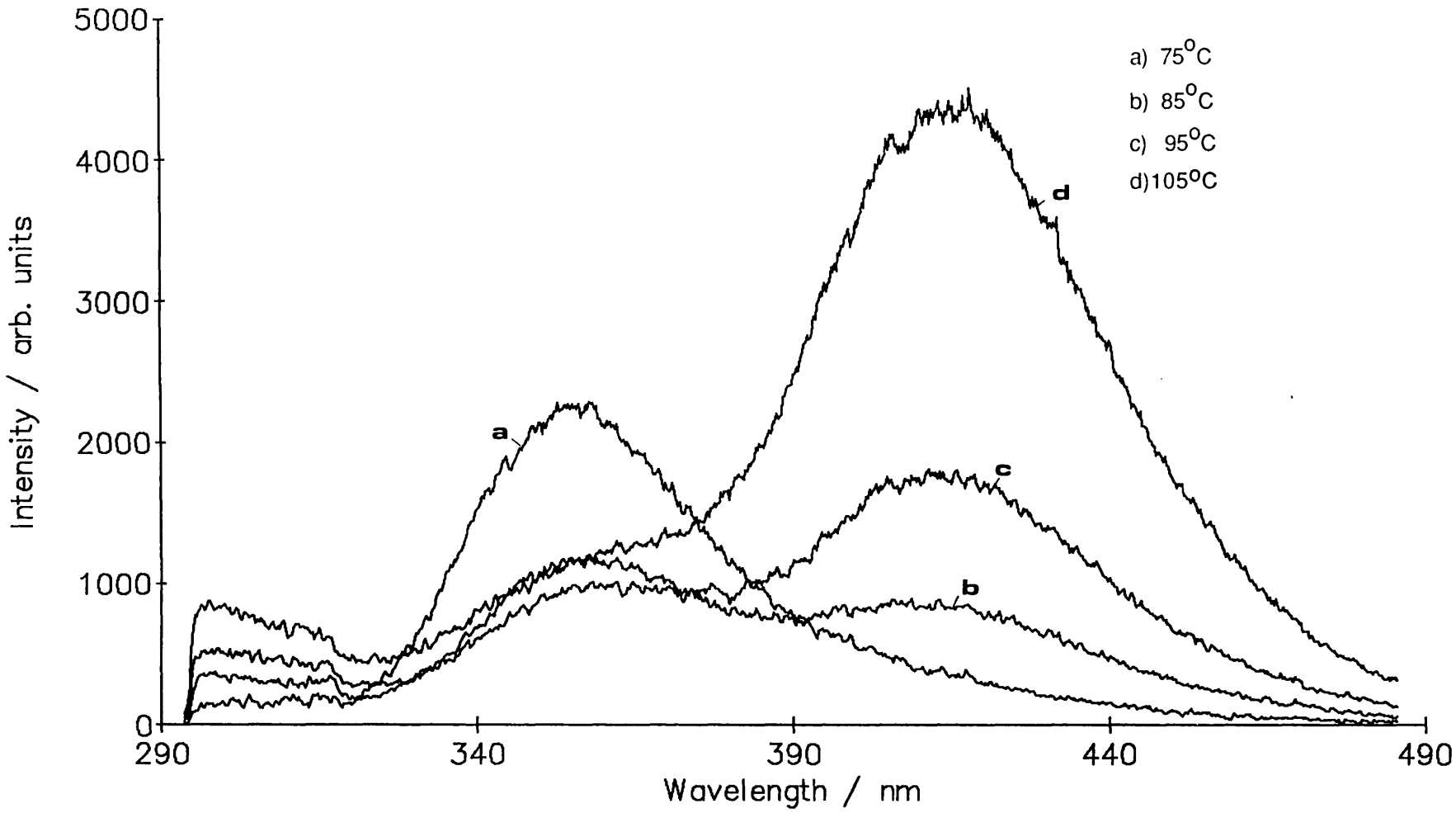

Figure 3.32 Pressure dependence on dispersed emission spectra of jet cooled DMABN / acetonitrile clusters.

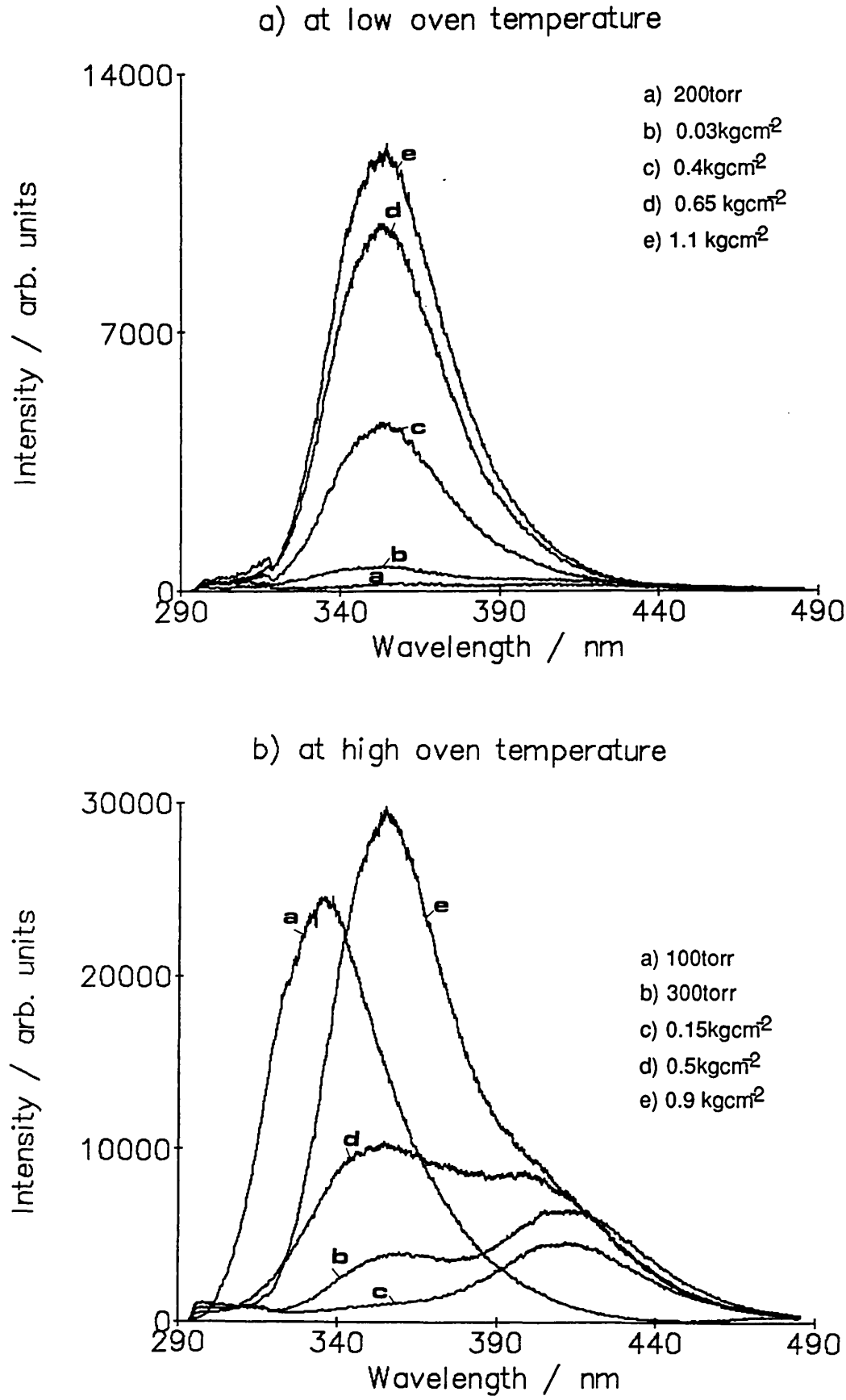

observed maximising at 354nm, on increasing the backing pressure the overall intensity of emission increases. There is no evidence of any red shifted fluorescence.

A similar study of pressure dependence is presented in figure 3.32b, but recorded at elevated temperature,105 °C. At very low backing pressures a single fluorescence band was observed maximising at 335nm, on increasing the backing pressure there is an initial decrease in the intensity of emission, and a second emission band becomes apparent, maximising at ~414nm. Upon further increase in pressure the intensity grows back, but only a single emission band is observed, shifted to lower energy of that observed at low pressure, maximising at 354nm.

3.4.5 DMABN / Chloroform

The dispersed fluorescence spectra of DMABN complexed with chloroform recorded at different sample oven temperatures are shown in figure 3.33a. The total pressure of carrier gas was 650 torr. At low oven temperatures an unresolved fluorescence bands was evident, maximising at 347nm, shifted some 17nm from that of the unsolvated molecule in addition to a second broad fluorescence band maximising at 413nm. On increasing the oven temperature the overall intensity of emission increases, and the two emission maxima shift back to higher energy, The emission maxima for the short and red shifted fluorescence bands shift to 343nm and 402nm respectively. The relative intensities of the two fluorescence bands do not vary linearly with sample oven temperature, and hence partial pressure of DMABN.

Figure 3.33 Dispersed emission spectra of jet cooled DMABN / chloroform clusters.

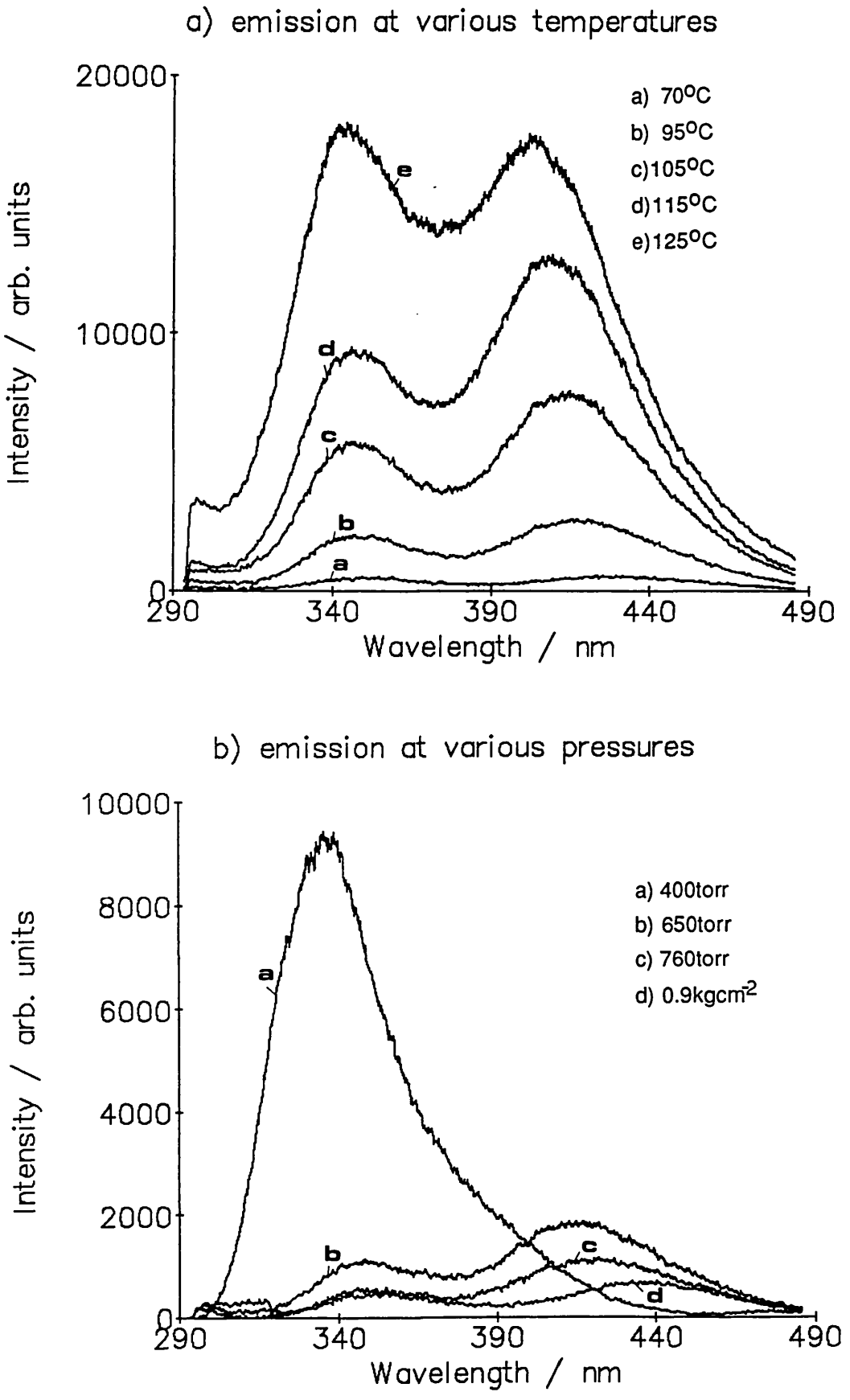

In figure 3.33b the dispersed fluorescence spectra of DMABN / chloroform recorded at various carrier gas backing pressures are presented. The spectra were all recorded at low nozzle temperature, 75°C. At low backing pressures a single emission band was observed maximising at ~334nm, on increasing the backing pressure there is a marked decrease in the intensity of emission, and two emission bands are observed, maximising at 347nm and 408nm respectively.

3.4.6 DMABN / dichloromethane

The dispersed fluorescence spectra of DMABN complexed with dichloromethane recorded at different sample oven temperatures are shown in figure 3.34a. The total pressure of carrier gas was 550torr. At low sample oven temperatures an unresolved fluorescence band is observed maximising at 351nm in addition to a broad emission band maximising at 438nm. On increasing the temperature the overall intensity of emission increases, and the red shifted band emission maximum is shifted to higher energy, eventually maximising at 398nm, the short wavelength emission maximum remains unchanged.

In figure 3.34b the dispersed fluorescence spectra of DMABN / dichloromethane recorded at various carrier gas backing pressures are presented. The spectra were all recorded at 85°C. At very low backing pressures a single fluorescence band was observed maximising at 351nm, on increasing the backing pressure there is a marked decrease in the intensity of emission and a second emission band is observed,

Figure 3.34 Dispersed emission spectra of jet cooled DMABN / dichloromethane clusters.

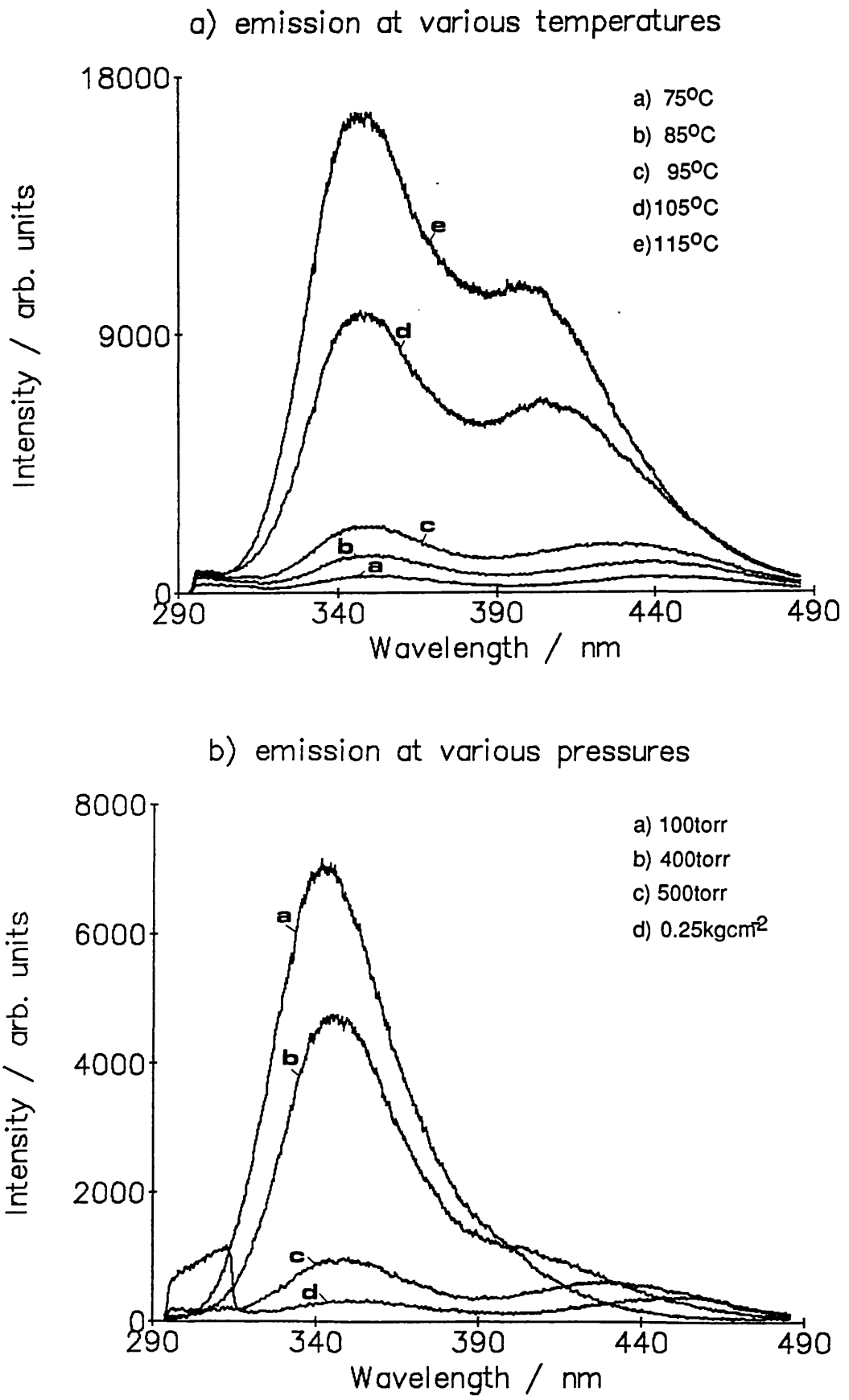

maximising at ~438nm, and this is further red shifted at increasing pressure.

3.4.7 DMABN / Carbon Tetrachloride

The dispersed fluorescence spectra of DMABN / carbon tetrachloride recorded at different sample oven temperatures are shown in figure 3.35a. The total pressure of carrier gas was 350torr. At low sample oven temperatures a single unresolved fluorescence band is observed maximising at nm. On increasing the temperature the overall intensity of emission increases, and a shoulder becomes apparent on the red edge of this band.

In figure 3.35b the emission spectra of DMABN / carbon tetrachloride recorded at various backing pressures are presented. The spectra were all recorded at 85 °C. At very low backing pressures a single fluorescence band was observed maximising at 335nm, on increasing the backing pressure there is a marked decrease in the intensity of this emission.

Figure 3.35 Dispersed emission spectra of jet cooled DMABN / carbon tetrachloride clusters.

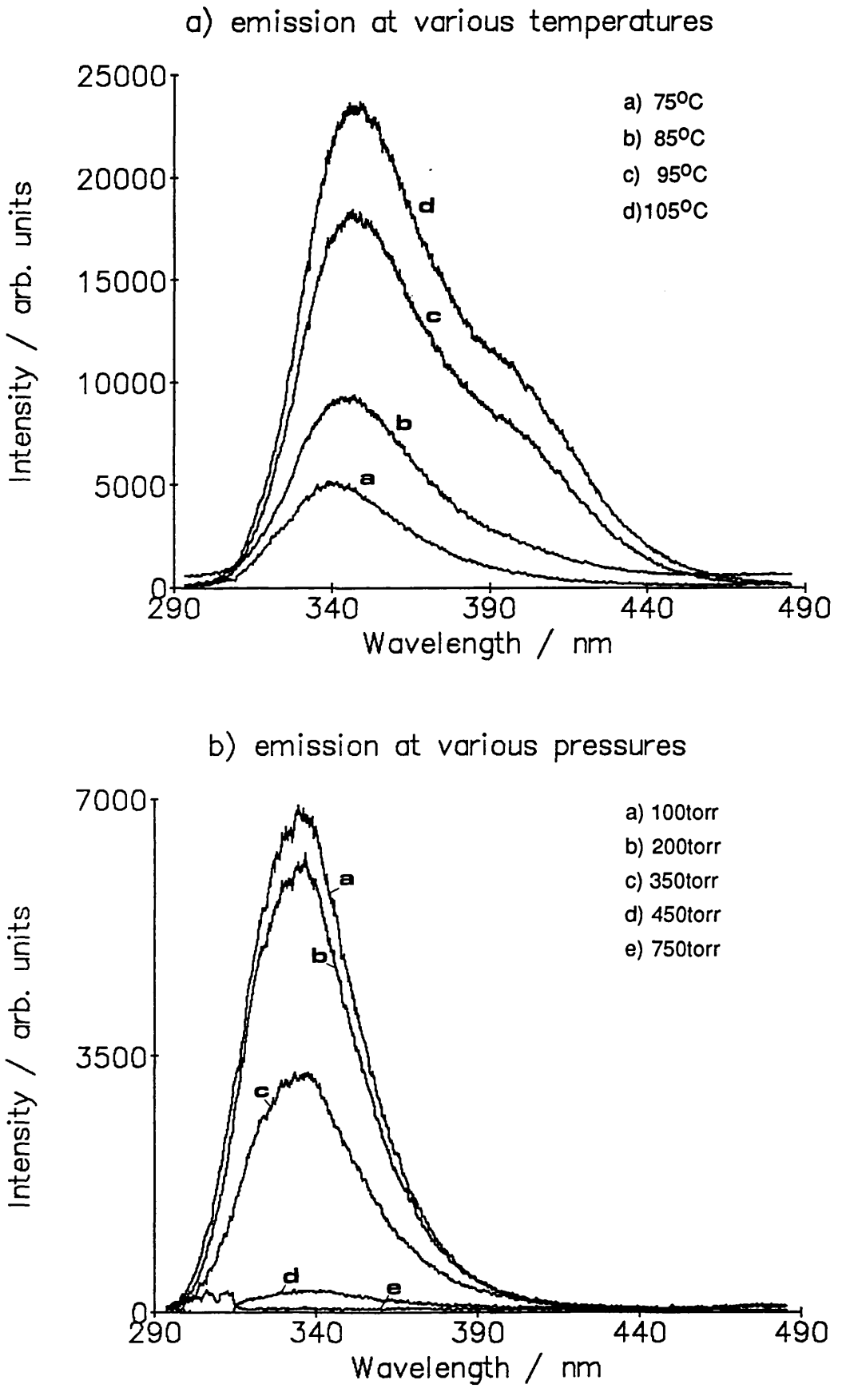

3.5 Discussion

3.5.1 The Unsolvated Molecules

A study of the unsolvated molecules is of great importance, as it is necessary to understand the fluorescence behaviour of the bare molecule before the effects of complexation are considered.

The spectroscopy of DMABN has been the subject of previous studies and the findings will be briefly mentioned.

The spectroscopy of DMABN is complicated due to the nature of the molecule, in particular the dimethylamino group. DMABN is reported to be of planar geometry in the ground state[10] and hence belongs to the C_{2v} point group (approximately, ignoring the hydrogens on the two methyl groups). INDO type calculations carried out by Lipinski et al[22] reveal that this planar structure is the most stable in the ground state and that the dipolar charge distribution of the ground state is largely associated with the benzonitrile moiety. The lowest energy transition is to the short axis polarised $^1B_2$ singlet state,and excitation into this state results in a reversal of the local benzonitrile dipole as a result of charge transfer from the dimethylamino group to the benzene ring (see figure 3.36). The observed low frequency torsional modes in the excitation spectrum suggest that the S_1 state may be twisted relative to the ground state by torsions of the dimethylamino group, though not to the full extent required for a* emission. In fact Bernstein et al[63] have presented evidence to show that the dimethylamino group in

Figure 3.36 Charge distribution in the ground and lowest excited electronic states for DMABN [22]

a) ground state ($^1A_1$)

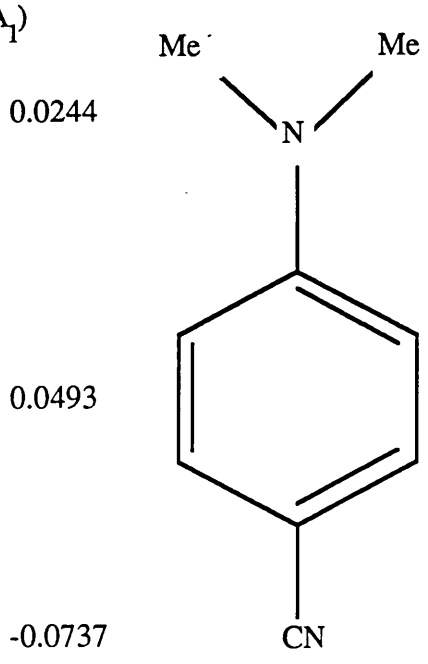

b) excited state ($^1B_2$)

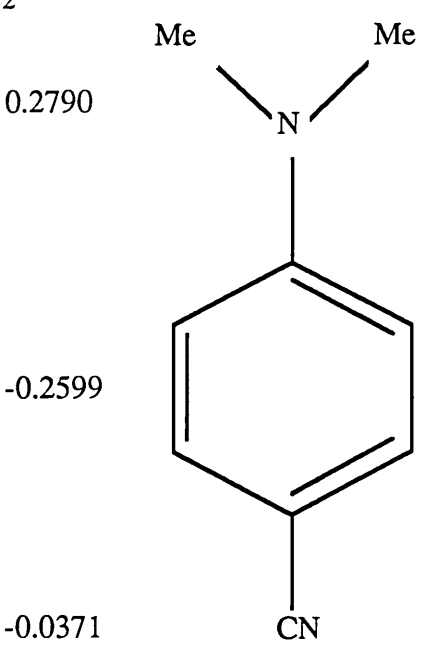

DMABN is ~30% twisted out of plane in the excited state. The observed low frequency modes can be attributed to the torsion of the amino group around the N-aryl bond, torsions of the CH_3 groups and the pyramidal inversion of the amino nitrogen.The oscillations of the amino group that must be considered to interpret the observed spectra are illustrated in figure 3.37. A comparison of the torsional frequencies of DMABN to those modes observed in the molecules DMAMB and DMAEB is shown in table 3.1. These torsional frequencies are comparable in magnitude to the frequencies found for torsions of the amino group in the far infrared spectrum of N,N-dimethylaniline (DMA) vapour; these were of the order of 66cm-1 and 117cm-1[66], and were assigned to the three torsions $N-(CH_3)_2$ and $C_6H_5-N(CH_3)_2$. Assignments of the low frequency modes observed for DMA and 4-N,N-dimethylaminobenzaldehyde (DMABA)[67] are shown in table 3.2. The inversion motion undergone by the amino group shows similarity to that seen for aniline[68] and for ammonia. The equilibrium configuration of NH_3 is pyramidal with HNH=106.7^o but, for large amplitude motion in the vibrational mode, the molecule may go through the planar configuration to the pyramidal configuration which is identical to the first except that it is inverted. The two pyramid configurations correspond to identical minima in the potential energy curve and the planar form to a maximum. The energy difference between these is the classical energy required to invert the pyramid, but in a quantum mechanical system it may be possible to go from one equilibrium configuration to another without surmounting this energy barrier. The phenomenon of

Figure 3.37 Some modes of vibration active in the ground and excited states of DMABN

A = Aryl-N torsion

B = N-CH_3 torsion

C = N inversion

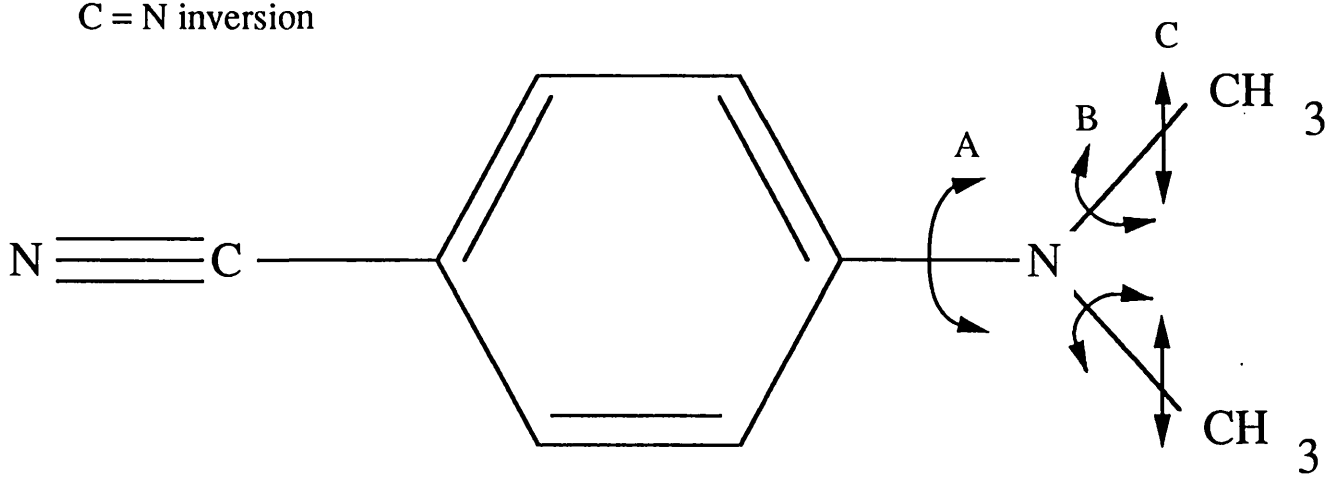

Table 3.2 Calculated ground state low-frequency normal modes of DMA and DMABA.

	DMA	DMABA	assignment
	frequency / cm^{-1}		
A	35-50	15-50	N(CH3)2-twist (and CH3 rotation)
B	65-80	65-75	N(CH3)2-pyramidal inversion
C	115-130	105-110	CH3-rotation
D	120-140	110-120	CH3-antirotation
E	240-250	170-185	?
F	260-275	210-230	strongly mixed mode containing pyramidal twist, CH3-rotation and ring deformation

quantum mechanical tunnelling allows a degree of penetration of the barrier. If the barrier is sufficiently low and/or narrow the amount of tunnelling increases and there is greater inversion probability. Aromatic amines such as aniline are known to have a lower barrier to inversion than aliphatic amines, and the effect of para-substitution with an electron acceptor is to lower this barrier further.

All of the observed transitions show typical double headed b-type rotational contours similar to those seen in aniline[69] and benzonitrile[70], and as such the transitions are all of the same symmetry species where the electronic transition is perpendicular to the principal moment of inertia of the molecule (which lies along the z axis of the molecule).

In DMA and DMABN the origin region is dominated by a transition at $61cm^{-1}$ which is believed to be due to torsion of the dimethylamino group about the N-aryl bond. For the unsolvated DMAMB molecule the LIF excitation spectrum is similarly dominated by a $65cm^{-1}$ transition and bears a strong similarity to the DMA and DMABN spectra, although two additional prominent features occur at 4 and $53cm^{-1}$. Although there are numerous low frequency transitions in the DMAEB spectrum, the majority can be identified with those in the DMAMB spectrum. However, four additional intense features are apparent, and these can be assigned in terms of molecular symmetry.

If these molecules are considered to be rigid (ie if the barriers to torsion and inversion are so significantly high that tunnelling can be neglected), their spectra can be interpreted in terms of point group symmetry (near symmetry).

The increasing complexity of the low-frequency spectral structure on going from DMABN to DMAMB to DMAEB can then be attributed to a corresponding decrease in point group symmetry as follows: If the dimethylamino group deviates little from planarity DMABN will have approximately C_{2v} symmetry; in DMAMB the symmetry will be reduced to C_s if the conformation of the ester group is assumed to be identical to that in methylbenzoate[71]; in the ethyl ester the symmetry is expected to be further reduced to C_1. If, however, tunnelling between different confomers does occur, the molecular symmetry (true symmetry)[72] of the system must be considered and the above point group symmetry arguments do not apply. If this is the case, the differences in low-frequency structure must be due to changes in the torsional and/or inversion potentials of the dimethylamino group or to the coupling of low frequency modes of the ester group to the electronic transition.

The major point of discussion in these experiments is the observation , for all three molecules, of a broad red shifted fluorescence band in the dispersed emission spectra recorded at elevated sample oven temperatures, which is associated with excitation of a continuous spectral component in the LIF excitation spectra. The nature of this red shifted emission is of great significance since DMABN and it's ester derivatives are known to form TICT states in polar solvents, which give rise to dual fluorescence including a broad red shifted fluorescence band. August et al[65] have previously observed a quasi continuum in the excitation spectrum of

DMAMB, which was attributed to the formation of a TICT state. TICT state formation requires excitation to the S_1 state (^1L_b-type for DMABN and ^1L_a-type in the case of the esters). The molecule then undergoes intramolecular charge transfer to a preferentially stabilised CT state. It is reasonable to assume that if this process was occurring the relative intensities of a* (TICT) and locally excited b* emission would remain constant on increasing the sample oven temperature and hence the number density of molecules in the expansion. Qualitatively, what is in fact observed for all three molecules is an increase in the red shifted emission relative to the short wavelength emission as a function of sample number density.

This behaviour is assigned in terms of excimeric emission following excitation of weakly bound ground state self-complexes, an assignment that is in contrast to that made by August et al[65], though the presence of self complexes in the expansion being supported by the findings of Peng et al[61]. Quantitative information on the size of the self - complexes present in the expansion cannot be obtained from the temperature dependence of the relative intensities of the red-shifted emission since the temperature dependence of the vapour pressure of the molecules is not known. In the presence of extensive clustering, the relative intensity of the monomer emission is not an accurate measure of the total concentration of the molecule in the expansion; at the sample temperatures used, the dimeric species is expected to be the predominant cluster species.

Hence the evidence presented here indicates that the red shifted emission and the broad underlying feature in excitation are due to molecular dimers in the expansion. A tentative prediction of the structure of these dimers is that of an excimer-like, overlapped sandwich structure, presumably with the monomer long axis lying antiparallel as shown in figure 3.38. This structure allows overlap of the opposing donor-acceptor moieties and the two molecules can therefore interact strongly.

Continuous spectra can be observed for species where the coupling between states is in the intermediate case[73,74]. Here the initially excited dimer state is strongly coupled to a nearby state, though the coupling strength is such that the typical lineshapes observed for statistical limit behaviour as characterised by ovalene S_2[75] are not observed. Continuous spectral features have been observed for the dimers of fluorene[76] and 9-ethylfluorene[77] and have been assigned in terms of an excited state dimer coupling to a nearby excimer state. In these cases the excitation spectra contained some structure, whereas for the molecules considered here the absorption appears continuous. This suggests that the electronic state of the aggregate is significantly different from the monomer, and that there is a considerable change in equilibrium intermolecular distances on going from the ground to excited state of the dimer.

Emission following excitation to high energies in a dimer could give rise to red shifted emission, but would in addition give a substantial contribution at shorter wavelengths, the ratio being invariant with sample

Figure 3.38 Prediction of most favourable dimer structure

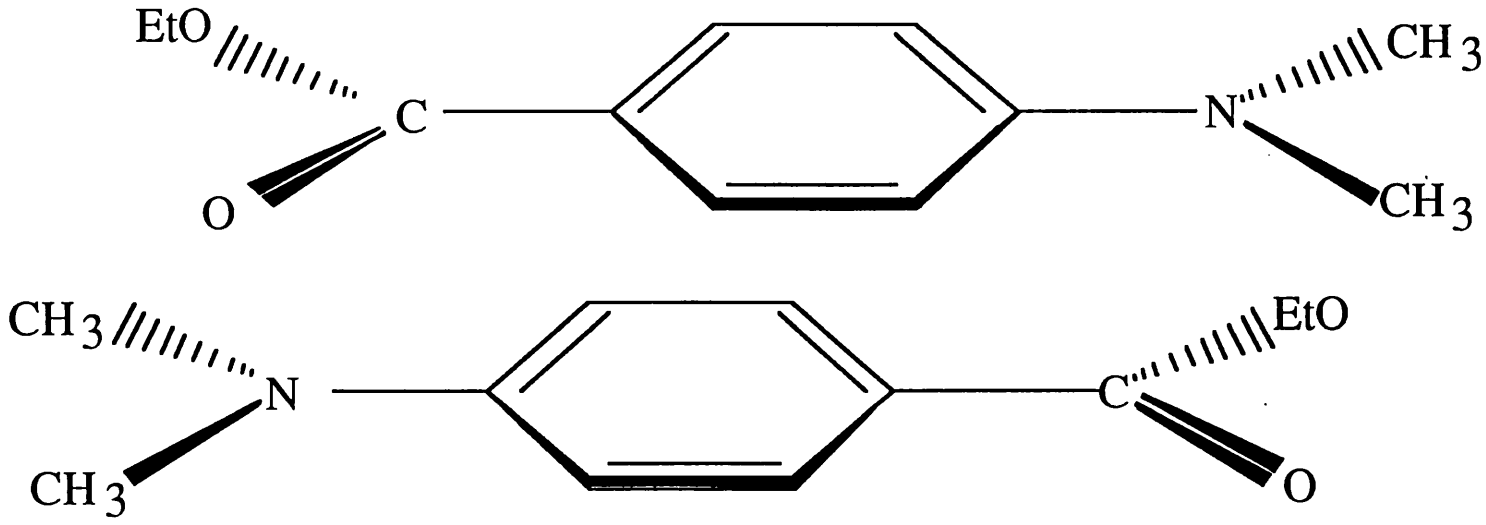

concentration. The extent of the red shift requires considerable relaxation which is unlikely to occur with a single electronic excited state. The alternative explanation is coupling of the initially excited state to another nearby state, as for example in the case of fluorene. The pronounced change in intensity ratio with sample concentration observed here requires this possibility to be considered.

In the case of DMABN and the ester derivatives the two chromophores can interact strongly in a head to tail arrangement such that the donor moiety of each overlaps with the opposite acceptor, and the initially excited state can couple strongly to the nearby background levels of an excimer state. Intermolecular charge transfer is expected to be important in stabilising the excimer state, it is well established[78] that dialkylamines can act as charge donors in jet cooled aromatic molecule exciplexes, therefore this behaviour seems likely.

Supporters of the TICT state hypothesis might argue that this second state is a TICT state and that the second molecule in the dimer, the partner to the excited chromophore, is acting as a highly polar solvent molecule and hence stabilising a TICT state in the chromophore. However, this argument would require a staggered sandwich structure for the dimer such that the dipole of the 'solvent' molecule is able to interact strongly with the excited molecule, and this interaction would have to be such that there was no steric hindrance to the twisting of the dimethylamino group in the chromophore, which seems unlikely. since the initial interaction in the ground state allowing alignment of the two donor-acceptor

pairs is likely to be the most strongly bound. Such behaviour would hinder rotation of the dimethylamino moiety and hence preclude TICT fluorescence. Whilst the present experiments cannot distinguish unambiguously between these two types of second state, the excimer explanation seems the most probable.

In conclusion , no direct evidence for TICT state formation was observed for the isolated unsolvated jet cooled monomer, even for the esters which are believed to form TICT states in polar solvents more readily due to the substituent induced level reversal discussed in section 3.2. The broad underlying feature in the excitation spectra is attributed to the presence of dimers and possibly larger aggregates in the expansion. The observation of red shifted emission is attributed to excitation of these aggregates which then undergo reorganisation to give excimeric emission.

3.5.2 The Solvated DMABN Molecule.

The key point to be considered here is the effect of solvation on the fluorescence properties of DMABN. Since DMABN is known to form TICT states in polar solvents, it was complexed with solvents of differing polarities, and trends in the fluorescence behaviour were noted. Initial studies carried out[58-60] have been concerned with low stoichiometry solvent-solute complexes. Here the effects of extensive clustering are investigated. A comparison of emission maxima for complexed and unsolvated DMABN is given in table 3.3. Table 3.4 gives the dipole moments[79] of the solvents used.

Table 3.3 Emission maxima of short and long wavelength emission bands of DMABN complexed with various solvents, and the shift of these bands from the unsolvated molecule.

	$se_{\lambda_{max}}$ /nm	$le_{\lambda_{max}}$ /nm	$se_{\Delta\lambda}$ /nm	$le_{\Delta\lambda}$ /nm
'Bare' Molecule	330	390		
Cyclohexane	348	399	18	9
Methanol	351	430	21	40
Acetone	349	409	19	19
Acetonitrile	354	414	24	24
Chloroform	347	413	17	23
Dichloromethane	351	438	21	48
Carbon tetrachloride	336	-	6	-

Table 3.4 Dipole moments and vapour pressures (at 25°C) of solvents used as complexing agents

	Dipole moment/D	Vapour pressure /torr
Cyclohexane	0.61	98
Methanol	1.7	125
Acetone	2.7	182
Acetonitrile	3.9	89
Chloroform	1.0	195
Dichloromethane	1.6	436
Carbon tetrachloride	0.0	115

In the context of the discussion of the unsolvated molecule in section 3.5.1, the spectra recorded for the various solvent clusters can be interpreted in terms of emission from a solvated monomer and from a solvated dimeric species.

It is important to mention before discussing the observations further that all experiments were recorded with the solvent reservoir at room temperature, and so the vapour pressure of solvent did not vary. The major effect of increasing the pressure is to increase the cooling of the expansion and hence both the probability of clustering of the solvent around DMABN and the formation of solvent self complexes. It is reasonable to assume that in these experiments higher pressures indicate a greater degree of solvation (ie larger cluster sizes). Comparison of cluster sizes for different solvents is not simple due to each solvent having a different vapour pressure and hence different number densities in the expansion. The relative vapour pressures are as follows[80]:

$MeCN < C_6H_{12} < CCl_4 < MeOH < Me_2CO < CHCl_3 < CH_2Cl_2$.

The absolute values of these are given in table 3.4. At high pressures the systems all exhibit bulk-solvent like properties since extensive complexation was taking place, there was a distribution of complexes of differing stoichiometry and it was not possible in the experiments performed here to determine this distribution. Temperature dependence studies were all performed at significant pressures and as such there was extensive complexation.

The emission observed for DMABN/cyclohexane maximises at ~348.5nm, this compares with ~350nm observed in the solution phase[44]. This emission band is therefore assigned as

arising from excitation of the solvated S_1 monomer state. On increasing the temperature a second band is observed, using the arguments in section 3.5.1, it is unlikely that this arises from a TICT state, as this mechanism would not result in an increase in the ratio of red shifted / short wavelength emission. A more probable explanation is that of emission from the solvated dimer, which would be expected to become more dominant on increasing the sample temperature. Cyclohexane, being a non polar solvent, would not be expected to stabilise the TICT state of DMABN, and emission attributed to fluorescence from a TICT state is not observed for DMABN in cyclohexane in the solution phase. The emission maximum for the red shifted emission band is shifted ~600cm^{-1} from that of the uncomplexed dimer, compared with a ~1600cm^{-1} for the corresponding monomer shift from the bare molecule. This implies that the monomer is solvent stabilised to a greater degree than the dimeric species. Possible intimate solvation of the monomer species is greater per DMABN molecule than for the dimer since there are two possible solvation sites for the monomer, above and below the plane of the molecule, whereas for the dimer there are also only two solvation sites, above and below the dimer, and hence the dimer should be stabilised to a lesser degree.

For DMABN complexed with methanol, the spectra recorded at different partial pressures of DMABN were recorded under conditions of moderate cluster formation. The maximum of the red shifted emission was found to be 430nm, in comparison to 457nm observed for emission from the TICT state in solution phase propan-1-ol experiments[81], if this band were due to

emission from a TICT state one would expect the emission maximum to be closer to that observed in solution phase. Again there is no reason to expect TICT state formation from the observed temperature dependence of the emission bands.

A pressure dependence study of methanol at low oven temperatures, where dimer formation is unfavourable, gave no evidence of a second red shifted fluorescence. The initial decrease in the quantum yield of fluorescence on complexation is as observed by Gibson et al[59], and is interpreted as the formation of non emissive low stoichiometry exciplexes involving specific solvent - solute interactions (hydrogen bonding). However at higher backing pressures a complete solvent shell is formed around the DMABN molecule and emission from the completely solvated DMABN monomer is observed. In the pressure dependence study at higher temperatures there is evidence for competition between dimer formation and clustering. At very low pressures only emission from the unsolvated monomer is observed. On increasing the pressure cooling occurs and formation of small non emissive clusters takes place as described above, accounting for the reduction in intensity. A red shifted fluorescence band is also observed due to formation of a dimeric species, possibly a solvated dimer, which competes with the above process.At very high pressures complete solvation of the monomer occurs and emission due to the solvated monomer is observed, with a small shoulder apparent on the red edge attributed to the dimer. Methanol is a polar protic solvent, and when DMABN is dissolved in it TICT state emission has been observed, as such a emission from a TICT state might be expected from a

DMABN/metanol cluster. A possible explanation why this is not the case under jet cooled conditions is that the molecule may have insufficient energy, due to the supersonic cooling, to overcome the small but finite barrier to TICT state formation (see fig 3.5).It is not possible to determine the cluster size in the expansion, but it may not be sufficient to induce solvent stabilisation of the TICT state since under these conditions microscopic solvent shell closure may not be complete. In addition twisting of the dimethylamino group would possibly require breaking of solvent-solute specific interactions , and solvent-solvent intermolecular bonds, such processes providing an energy barrier to TICT state formation. Similar behaviour is observed in the pressure dependence of DMABN complexed with acetonitrile, which is a more polar molecule than methanol. At low DMABN 'concentration' dimer formation is unfavourable, and only emission from the solvated monomer is observed. The absence of any shorter wavelength emission is attributed to some complexation having already taken place even at the lowest pressure recorded, giving rise to low stoichiometry non emissive complexes. On increasing the pressure of helium carrier gas cooling increases and further solvation of the monomer occurs, and emission from a more highly solvated species is observed. Another possible explanation of the increase in intensity is that a fixed excitation wavelength was used and on increasing the cluster size the absorption is broadened and becomes more 'in resonance' with the excitation wavelength. At higher sample oven temperature DMABN complexed with acetonitrile shows similar behaviour as when complexed

with methanol at high sample oven temperature. At high pressures there is extensive clustering and overlapping emission from the solvated monomer, the dimer and solvated dimer is observed.

The shift of the long wavelength band when DMABN is extensively complexed with acetonitrile is not as great as that observed for methanol, which indicates that the state from which this emission arises is preferentially stabilised in methanol clusters compared with acetonitrile clusters. This is in contrast to the observation[80] in solution phase for the TICT state, where the long wavelength emission is 452nm and 467nm for methanol and acetonitrile respectively. These observations in solution phase are readily explained in terms of solvent polarity and the expected stabilisation of the TICT state. The jet cooled clusters behave in a manner that is contrary to these expectations for TICT state emission and consequently assignment to emission from a solvated dimer is the more attractive proposition. A possible explanation of the greater stabilisation of the dimer state in methanol than in acetonitrile is the fact that methanol has the ability to undergo intermolecular hydrogen bonding within the solvent shell hence reducing the energy of the environment, as is seen in carbazole / water complexes[82]. DMABN can undergo specific interactions with methanol by means of hydrogen bonding, and DMABN has three possible sites for hydrogen bonding, as is the case for 4-aminobenzonitrile / water[60]. The dimeric species has six such sites. Acetonitrile, being aprotic, does not have this potential for specific solute - solvent interaction via hydrogen bonding.

Acetonitrile can however undergo specific dipole - dipole interactions with DMABN. The possibility of specific solvent - solute and solvent - solvent interactions is of great importance since the stabilisation of the solvated dimer would be expected to increase linearly with increasing solvent dipole moment if there were no specific interactions. The spectra obtained for acetone / helium expansions of DMABN are all low in intensity. At the pressure used to study the dependence of emission on DMABN partial pressure, extensive clustering is occurring. This is clearly illustrated by the large amount of scattered light at the excitation wavelength due to higher order clusters. The grow-in of the red shifted emission band attributed to the dimer is clearly apparent. At low acetone pressures unsolvated monomer fluorescence is observed. On increasing the pressure there is a decrease in intensity due to non emissive complexes or to energy transfer to acetone, and enhanced cooling gives rise to both competing processes of solvated monomer and dimer formation. At higher pressures monomer formation dominates.

Carbon tetrachloride is a volatile non polar solvent, with a dipole moment of 0 Debye, and is an ideal molecule for forming van der Waals clusters. In the oven temperature dependence study the very small shift in emission maximum from that of the bare molecule indicates that very little clustering is taking place at the backing pressure used. Increased pressure of DMABN in the expansion leads to the grow in of a shoulder due to enhanced competition for formation of dimers, but carbon tetrachloride seems unable to stabilise the dimeric species very effectively. Increasing

the pressure of carbon tetrachloride / helium leads to a dramatic reduction in fluorescence due to the formation of larger clusters with CCl_4. Chlorinated solvents are well established as being efficient at quenching fluorescence. Much of this quenching can be attributed to charge transfer effects ie formation of non emissive excited state complexes, or photochemistry, or the heavy atom effect[3,4].

In the case of dichloromethane extensive clustering is probably already occuring at the pressure used to measure the oven temperature dependence of the emission spectra. Emission from the solvated monomer is observed, but the intensity is low due to fluorescence quenching. This enables emission from the solvated dimer to be observed, although the partial pressure of dimer in the expansion is very low and would not be detected if 'normal' fluorescence from the monomer was observed, ie if there was no non radiative decay channel. The emission maxima of 351nm and 438nm for dichloromethane compare with 354nm and 425nm observed in the solution phase[81]. The other point of interest is that the emission maxima shift to shorter wavelength at higher temperatures. Increasing the partial pressure of DMABN in the expansion is likely to cause a reduction in the size of the clusters, therefore a shift of dimer fluorescence away from heavily solvated behaviour to less heavily solvated behaviour is observed. The overall intensity grows as a function of DMABN 'concentration' as expected. As with CCl_4 enhanced clustering leads to a dramatic decrease in fluorescence quantum yield, and the most likely explanation for this is enhanced ISC to the triplet state. Once again competing processes are

occurring, for smaller clusters a shoulder is appparent on the red edge of the solvated monomer emission band that has a maximum not dissimilar to that of the uncomplexed dimer, on increasing the pressure further clustering increases and the emission maximum of the dimer band shifts to that of the totally solvated dimer.

For the chloroform oven temperature dependence study the cooling conditions were not extreme, ie the pressure used was low, since greater cooling introduced too great a quenching of fluorescence. Initially emission from both monomer and dimer is observed, as explained for dichloromethane, and incresing the oven temperature causes enhanced dimeric emission. At higher oven temperatures however the amount of cooling possible reaches a maximum, ie is saturated, and monomer formation becomes the more favoured process. Enhanced clustering increases the cooling and leads to a dramatic reduction in the fluorescence due to the formation of less emissive complexes as for CCl_4. Also a red shift of the long wavelength emission band occurs as clustering becomes more extensive and solvent shell closure is completed.

In conclusion it has been shown that the molecules DMABN, DMAMB and DMAEB give rise to red shifted emission under conditions of high sample density in a solvent free supersonic expansion. The emission can be attributed to arising from an excimer state accessed by excitation of a pre formed dimer and subsequent relaxation. Although the aim of these experiments was to simulate conditions in which TICT behaviour might be observed, it was not considered necessary to invoke the TICT state hypothesis to explain the

observations. Similarly for mixed DMABN / solvent expansions red shifted emission was observed which could be explained in terms of the competing processes of monomer cooling, solvation, dimer formation and dimer solvation. Clearly the solvation mechanisms of such mixed expansions are highly complex and the conditions here represent an experimental situation between specific low stoichiometry complexes and true bulk phase behaviour. Due to the limitations of the experiment it is not possible to draw any firmer conclusions than those outlined above. Without the benefit of mass resolution, accurate picosecond dynamic studies and more sensitive control over DMABN / solvent expansion conditions TICT state formation cannot be categorically ruled out, however under the present conditions it seems unlikely.

3.6 References

1 E.Lippert, W.Luder and H.Boos,
"Advances in molecular spectroscopy" ed. A.Mangini,
Pergamon Press, Oxford (1962) 443.

2 W.Rettig, G.Wermuth and E.Lippert,
Ber. Bunsenges. Phys. Chem. 83 (1979) 692.

3 J.B.Birks,
"Photophysics of Aromatic Molecules,
Wiley-Interscience, New York (1970)

4 J.B.Birks,
"Organic Molecular Photophysics",
John Wiley and Sons 2 (1975).

5 K.Rotkiewicz, K.H.Grellmann and .R.Grabowski,
Chem. Phys. Letters 19 (1973) 315.

6 O.S.Khalil, R.H.Hofeldt and S.P.McGlynn,
Chem. Phys. Letters 17 (1982) 479.

7 O.S.Khalil,
Chem. Phys. Letters 35 (1975) 172.

8 H.Dodiuk and E.M.Kosower,
Chem. Phys. Letters 34 (1975) 253.

9 R.J.Visser, C.A.G.O.Varma, J.Konijnenberg and
P.Bergwerf,
J. Chem. Soc. faraday Trans. 2. 79 (1983) 347.

10 Z.R.Grabowski, K.Rotkiewicz, A.Siemiarczuk, D.J.Cowley
and W.Baumann,
Nouv. J. Chim. 3 (1979) 443.

11 R.J.Visser, P.C.M.Weissenborn, C.A.G.O.Varma, M.P.deHass
and J.M.Warman,
Chem. Phys. Letters 104 (1984) 38.

12 R.J.Visser, P.C.M.Weissenborn, J.Konijnenberg,
B.H.Huizer and C.A.G.O.Varma,
J. Photochem. 32 (1986) 217.

13 R.J.Visser, P.C.M.Weissenborn and C.A.G.O.Varma,
Chem. Phys. Letters 113 (1985) 330.

14 C.Cazeau-Dubroca, S.Ait-Lyazidi, P.Cambou, A.Peirigua,
Ph. Cazeau and M.Pesquer,
J. Phys. Chem. 93 (1989) 2347.

15 C.Cazeau-Dubroca, S.Ait-Lyazidi, G.Nouchi, A.Peirigua,
Ph. Cazeau and M.Pesquer,
Nouv. J. Chim. 10 (1986) 337.

16 D.Pilloud, P.Suppan, L.van Haelst,
Chem. Phys. Letters 137 (1987) 130.

17 C.Rulliere, Z.R.Grabowski, and J.Dobkowski,
Chem. Phys. Letters 137 (1987) 408.

18 P.Suppan,
Chem. Phys. Letters 128 (1986) 160.

19 K.Rotkiewicz, K.H.Grellmann and Z.R.Grabowski,
Chem. Phys. Letters 19 (1973) 315.

20 K.Rotkiewicz, Z.R.Grabowski, A.Krowczynski and
W.Kuhnle,
J. Lumin. 12/13 (1976) 877.

21 W.Rettig,
Angew. Chem. Int. Ed. Engl. 25 (1986) 971.

22 J.Lipinski, H.Chojnacki, Z.R. Grabowski and
K.Rotkiewicz,
Chem. Phys. Letters 70 (1980) 449.

23 W.Rettig and V.Bonacic-Koutecky,
Chem. Phys. Letters 62 (1979) 115.

24 H.Bischof, W.Baumann, N.Detzer and K.Rotkiewicz,
Chem. Phys. Letters 116 (1980) 180.

25 W.Baumann and H.Bischof,
J. Mol. Struct. 129 (1985) 125, and references therein.

26 A.A.Ayuk, W.Rettig and E.Lippert,
Ber. Bunsenges Phys. Chem. 85 (1981) 553.

27 E.Lippert, A.A.Ayuk, W.Rettig and G.Wermuth,
J. Photochem. 17 (1981) 237.

28 A.A.Ayuk,
J. Mol. Struct. 84 (1982) 169.

29 G.Wermuth,
Z. Naturforsch. 38a (1983) 641.

30 S.R.Meech and D.Phillips,
Chem. Phys. Letters 116 (1985) 262.

31 W.Rettig and G.Wermuth,
J. Photochem. 28 (1985) 351.

32 D.Huppert, S.D.Rand, P.M.Rentzepis, P.F.Barbara,
W.S.Struve and Z.R.Grabowski,
J. Chem. Phys. 75 (1981) 5714.

33 N.Nakashima, H.Inoue, N.Mataga, and Ch. Yamanaka,
Bull. Chem. Soc. Jpn. 46 (1973) 2288.

34 F.Heisel and J.A.Miehe,
J. Chem. Phys. 77 (1982) 2558.

35 F.Heisel and J.A.Miehe,
Chem. Phys. 98 (1985) 243.

36 F.Heisel and J.A.Miehe,
Chem.Phys 128 (1986) 323.

37 Z.R.Grabowski, K.Rotkiewicz and A.Siemiarczuk,
J. Lumin. 18/19 (1979) 420.

38 K.Rotkiewicz and W.Rubaszewska,
Chem. Phys Letters 70 (1984) 444.

39 G.Wermuth and W.Rettig,
J. Phys. Chem. 88 (1984) 2729.

40 W.Rettig and R.Gleiter,
J. Phys. Chem. 89 (1985) 4676.

41 W.Rettig,
J. Phys. Chem. 86 (1982) 1970.

42 T.Okada, N.Mataga and W.Baumann,
J. Phys. Chem. 91 (1987) 760.

43 G.Wermuth, W.Rettig and E.Lippert,
Ber. Bunsenges Phys. Chem. 85 (1981) 64.

44 Y.Wang and K.B.Eisenthal,
J. Chem. Phys. 77 (1982) 6076.

45 W.Rettig and E.Lippert,
J. Mol. Struct. 61 (1980) 17.

46 W.Rettig,
J. Mol. Struct. 84 (1982) 303.

47 M.Castella, A.Tramer and F.Piuzzi,
Chem. Phys. Letters 129 (1986) 112.

48 C.Haynam, D.Brumbauch and D.H.Levy,
J. Chem. Phys 79 (1983) 1581.

49 U. Brackmann, N.P.Ernsting, P.Ouw and K.Schmitz,
Chem. Phys. Letters 110 (1984) 383.

50 N.P.Ernsting,
J. Phys. Chem. 89 (1985) 4932.

51 N.P.Ernsting, A.ordzinski and B.Dick,
J. Phys Chem. 91 (1987) 1404.

52 K.Yamasaki, K.Arita, O.Kajimoto and K.Hara,
Chem. Phys. Letters 123 (1986) 277.

53 F.Schneider and E.Lippert,
Ber. Bunsenges Phys. Chem. 72 (1968) 1155.

54 O.Kajimoto, K.Yamasaki, K.Arita and K.Hara,
Chem. Phys. Letters 125 (1986) 184.

55 T.Kobayashi, M.Futakami and O.Kajimoto,
Chem. Phys. Letters 141 (1987) 450.

56 K.Rotkiewicz and W.Rubaszewska,
J. Lumin. 27 (1982) 221.

57 J.Herbich, F.Perez-Salgado, R.P.H.Rettschnick,
Z.R.Grabowski and H.Wojtowicz,
Chem. Phys. (1990) submitted

58 T.Kobayashi, M.Futakami, and O.Kajimoto,
Chem. Phys. Letters 130 (1986) 63.

59 E.M.Gibson, A.C.Jones and D.Phillips,
Chem. Phys. Letters 136 (1987) 454.

60 E.M.Gibson, A.C.Jones, A.G.Taylor, W.G.Bouwmann,
D.Phillips and J.Sandell,
J. Phys. Chem. 92 (1988) 5449.

61 L.W.Peng, M.Dantus, A.H.Zewail, K.Kemnitz, J.M.Hicks and
K.B.Eisenthal,
J.Phys.Chem 91 (1987) 6162.

62 J.A.Warren, E.R.Bernstein and J.I.Seeman,
J. Chem. Phys. 88 (1988) 871.

63 V.H.Grassian, J.A.Warren, E.R.Bernstein and H.V.Secor,
J. Phys. Chem. 90 (1989) 3994.

64 O.Kajimoto, M.Futakami, T.Kobayashi and K.Yamasaki,
J. Phys. Chem. 92 (1988) 1347.

65 J.August, T.F.Palmer, J.P.simons, C.Jouvet, and W.Rettig
Chem. Phys. Letters 145 (1988) 273.

66 C.Belorgeut, P.Quintard, P.de Lorne and V.Lorenzelli,
Can. J. Spec. 21 (1976) 119.

67 E.M.Gibson,
University of London (1988) PhD Thesis.

68 M.J.S.Dewar and W.Thiel,
J. Am. chem. Soc. 99 (1977) 4899.

69 J.Christoffeson, J.M.Hollas and G.H.Kirby,
Mol. Phys. 16 (1969) 441.

70 T.Kobayashi, K.Homma, O.Kajimoto and S. Tsuchiya,
J. Chem. Phys. 86 (1987) 1111.

71 S.Kamei, H. Abe, N.Mikami and M.Ito,
J. Phys. Chem. 89 (1985) 3636.

72 P.R.Bunker,
Molecular symmetry and spectroscopy Acad. Press
New York (1979).

73 P.Wannier, P.M.Rentzepis and J.Jortner,
Chem. Phys. Letters 10 (1971) 1973.

74 A.Amirav, U.Even and J.Jortner,
Chem. Phys. Letters 69 (1980) 14.

75 A.Amirav, U.Even and J.Jortner,
J. Chem. Phys. 74 (1981) 3745.

76 H.Saigusa and M.Itoh,
J. Phys. Chem 89 (1985) 5486.

77 M. Itoh and Y.Morita,
J. Phys. Chem. 92 (1988) 5693.

78 M.Castella, P. Millie, F.Piuzzi, J.Caillet,
J. Langlet, P.Claverie and A.Tramer,
J. Phys. Chem. 93 (1989) 3949.

79 A.L.McClellan,
Tables of experimental dipole moments,
W.H.Freeman & Co., London, (1965).

80 C.R.C handbook of Chemistry and Physics
49 ed. (1968-69).

81 E.M.Kosower and H.Dodiuk,
J. Am. Chem. Soc. 98 (1976) 924.

82 S.Leutwyler and J.Bösiger,
Faraday Discuss. Chem. Soc. 86 (1988) paper.

CHAPTER FOUR: SPECTROSCOPY OF N-ETHYLCARBAZOLE DIMER

4.1 Introduction

Many aromatic molecules are known to form weakly bound molecular complexes including molecular homodimers in a supersonic jet environment. The molecule N-ethylcarbazole (NEC) forms such a ground state homodimer and in this chapter a study of the fluorescence properties of this system will be reported. The LIF excitation spectra and dispersed fluorescence spectra of N-ethylcarbazole dimer will be presented in sections 4.2.1 and 4.2.2 respectively, and these data will be discussed in section 4.3.

To date studies have been carried out on the homodimers of several aromatic molecules, some of these molecules are depicted in figure 4.1.

In solution phase and solid state, many molecules are known to form excimers, however in a supersonic expansion upon excitation most of the molecules studied to date exhibit structured fluorescence that is characteristic of the perturbed monomer species. There are however some exceptions to this,for example the $(fluorene)_2$ system, for which broad structureless excimer emission is observed, an observation which to date is very rare. In this section examples of both cases will be discussed.

The LIF spectroscopy of $(fluorene)_2$ was first reported by Itoh et al[1]. The excitation spectrum was characterised by a broad underlying feature with a complex series of transitions

Figure 4.1 Some molecules which form ground state homodimers in a supersonic environment

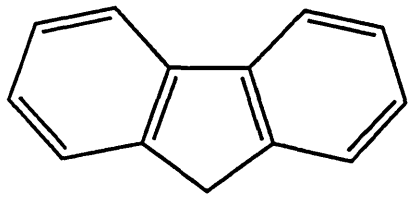

fluorene

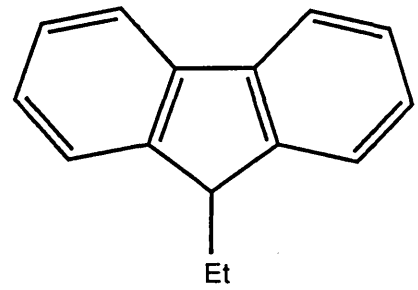

9-ethylfluorene

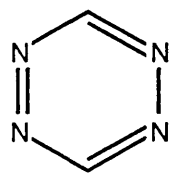

s-tetrazine

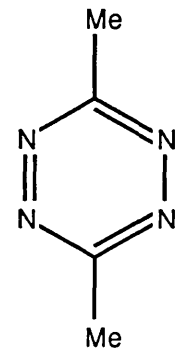

dimethyl s-tetrazine

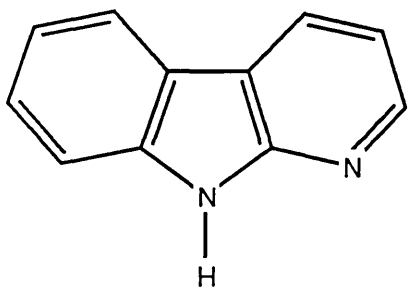

1-azacarbazole

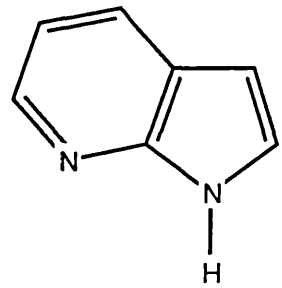

7-azaindole

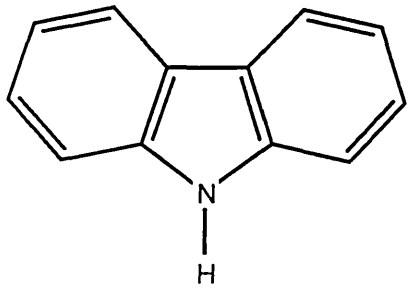

carbazole

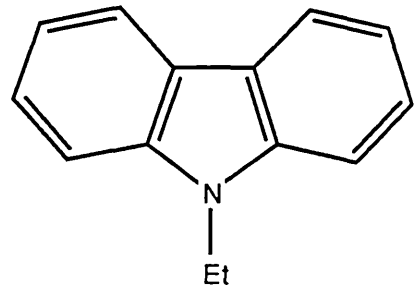

N-ethylcarbazole (NEC)

superimposed on this. These features were red shifted from the isolated molecule origin,the lowest energy transition occuring shifted some 227cm^{-1}. These red shifted features were attributed to the fluorene dimer due to the dependence of their intensity on the partial pressure of fluorene in the expansion. The low frequency structure was assigned as probably arising from intermolecular vibrations of the dimer species.

Broad structureless emission, maximising at 360nm, was observed following excitation of the dimer origin at 298nm. The fluorescence lifetime of this emission was found to be 70ns[2], in contrast to that of the isolated molecule emission, 15.6ns[3]. This broad emission band was assigned to an excimer state which arises when the initially excited dimer state undergoes a near barrierless and therefore rapid transformation to the excimer state, which then emits. The fluorescence lifetimes confirm that the emitting state differs greatly from the monomer excited state. The structure of the ground state dimer was postulated to have the two partner molecules lying parallel but slightly displaced[4], a facile reorganisation occuring on excitation to a less displaced structure with the two fluorene moieties in an 'eclipsed' configuration, allowing increased interaction in the excimer. However an antiparallel structure seems equally viable, allowing interaction of the two dipole moments of 0.6Debye. The 9-ethylfluorene homodimer exhibited a similar excimeric emission, as did the heterodimer of fluorene and 9-ethylfluorene[2].

Similar broad red shifted emission was reported in chapter 3 for the molecules DMABN, DMAMB and DMAEB, and this was also attributed to excimeric emission, although structure assignable to intermolecular vibrations was not observed in the excitation spectrum. The dimer structure in the ground state was predicted to be antiparallel sandwich conformation unlike that of fluorene. These molecules have a large dipole moment in addition to donor and acceptor groups. An antiparallel sandwich configuration allows close interaction between the donor group of one molecule and the acceptor group of the other, giving rise to a strongly bound ground state. Electronic excitation facilitates a partial electron transfer between the two molecules and gives rise to a strongly bound excimer state.

A system found to exhibit fluorescence characteristic of the perturbed monomer is that of (s-tetrazine)$_2$, which has been studied extensively by Levy et al[5-8]. The LIF excitation spectrum was characterised by sharp tansitions on a flat background which could be assigned as intramolecular and intermolecular fundamental vibrations. Three dimer electronic origin transitions were observed, and two different dimer structures were determined from the rotational contours of these transitions. The first electronic origin was determined to arise from a symmetric co-planar dimer structure, this was shifted bathochromically 28cm^{-1} from the monomer electronic origin transition, the dimer being slightly more strongly bound in the excited state. The other dimer electronic origins were found shifted from the monomer origin by 45cm^{-1} and 144cm^{-1} respectively These were determined to arise from

a T-shaped dimer with two near degenerate excited states. In both cases the two non equivalent chromophores experience a different solvent environment, from the partner molecule in the dimer, and hence show different spectral shifts. Emission spectra recorded following excitation of the origin transitions of both dimer states showed structured fluorescence from the initially excited state. This was also true for emission at higher excitation energies, however there was also evidence for intramolecular vibrational redistribution. There was no evidence for any large structural rearrangement such as excimer formation. At much higher excitation energies, fluorescence characteristic of the monomer was observed, and this was attributed to dissociation of the dimer species.

The related molecule dimethyl s-tetrazine was also studied. The LIF excitation spectrum revealed only one dimer origin transition, in contrast to s-tetrazine, which was bathochromically shifted from the bare molecule origin by $548cm^{-1}$. Rotational analysis of this origin transition confirmed the dimer structure to be a parallel configuration, with the two constituent molecules displaced with respect to each other so there is little direct overlap. Upon excitation the interaction between the dimer constituents becomes much stronger. As for s-tetrazine, excitation of the origin transition gave rise to well resolved vibronic features, but at higher energies the onset of IVR was at much lower energies than for s-tetrazine, in addition there was no evidence for emission from the initially pumped state. There was no evidence for dissociation of the dimer even at higher

excess energies. There are similarities between this structure and that proposed for $(fluorene)_2$ and, although there is no evidence of the typical red shifted emission, this system was termed a mild excimer[8].

Another system that is believed to form an excimer state, although no red shifted emission is observed, is the $(benzene)_2$ system. LIF studies[9] on this dimer showed a marked reduction in the quantum yield of fluorescence, and a reduced fluorescence lifetime in the dimer. These observations were attributed to the formation of an excimer state that was not emissive.

The structure of the ground state dimer is the subject of some controversy. Ab initio calculations[10-12] have predicted the structure to involve the two constituent molecules to be non parallel, with either a T-shaped structure[10,11], or a V-shaped structure as predicted by Carsky et al[12]. Semi empirical calculations[13-15] however have predicted a parallel structure where the two moieties are displaced such that the dihedral angle between them is 70-80°. The spectroscopy of $(benzene)_2$ has been investigated extensively [9,16-19], and the excitation spectrum reveals one allowed dimer origin transition $40cm^{-1}$ to the red of the monomer origin. This has been assigned[18] to a dimer with a displaced parallel stacked dimer of C_{2h} symmetry. More recently splitting of the origin transition by $1.7cm^{-1}$ has been observed[18], favouring a v-shaped structure of C_{2v} symmetry where the constituent molecules at a 70° angle to each other.

The dimer of 7-azaindole has been studied by Fuke et al[20]. Two electronic transitions were identified at ~33000cm^{-1} and assigned as the one photon allowed ^1B_u <- ^1A_g transition and 38cm^{-1} lower in energy the two photon allowed ^2A_g <- ^1A_g transition, arising from the electronic excited state of the dimer being split into Bu and Ag symmetry in the C_{2h} point group. These were studied by multiphoton ionisation (MPI) and LIF spectroscopy. The excitation spectrum of the ^1B_u <- ^1A_g transition showed a large number of well resolved features assigned as intermolecular and intramolecular vibrations. The fluorescence was characteristic of a perturbed monomer state and not an excimer state. The structure of the dimer was predicted to be 'cyclic' containing two strong hydrogen bonds between the pyrrolic hydrogen and the indolic nitrogen on opposite moieties. The excited state is therefore greatly stabilised due to a large increase in basicity of the indolic nitrogen and acidity of the pyrollic proton upon excitation. The absorption spectrum from the groundstate to the lower energy state vibronic levels exhibited a broad linewidth and excitation ofthese levels gave rise to unresolved red shifted emission, assigned as being due to double proton transfer reactions (DPTR) within the dimer causing tautomerisation.

In a later study[21] DPTR in 1-azacarbazole dimer and the 7-azaindole-1-azacarbazole heterodimer were investigated by MPI and LIF spectroscopy. In contrast to 7-azaindole the lowest excited state was found to be one photon allowed and undergo DPTR, the higher energy state being non reactive. Due to the dependence of the relative intensity of signal from the two states on the degree of cooling in the expansion, the two

transitions were assigned as two different isomers. The lowest energy state was assigned as being the co-planar isomer and the higher, non reactive state to an isomer distorted from planar. The key vibration was found to be the N-H··N intermolecular stretch. A further LIF study by Fuke et al[22] suggested a re-assignment of the two states in 7-azaindole as being due to two structural isomers, one of these isomers, of near coplanar structure, selectively undergoing DPTR in the excited state. Excitation of the symmetric stretch of the hydrogen bond promotes pronounced DPTR.

The carbazole chromophore is of interest for the following reasons: Firstly it is isoelectronic with fluorene, which has been shown to undergo facile excimer formation under jet-cooled conditions. Secondly in the restricted environment of polymer chains, for example poly(N-vinylcarbazole) and poly (N-ethyl-2-vinylcarbazole), carbazole chromophores are constrained in such a manner that they form excimeric pairs with neighbouring chromophores, these excimers being responsible for all the observed[23-25] emission. For poly (N-vinylcarbazole) two distinct excimer emissions were identified, and attributed[25] to an eclipsed sandwich structure in addition to a more weakly bound configuration in which only one aromatic ring from each constituent molecule is eclipsed.

In a recent study the LIF excitation and emission spectra of the jet cooled carbazole dimer were reported[26]. The LIF excitation spectrum contained a number of well resolved transitions built on a flat background, some of which could

be assigned as low frequency intermolecular vibrations, and the dimer origin occuring some 763cm^{-1} to the red of the monomer origin. The fluorescence spectrum of this dimer was found to arise from the initially excited dimer state, being characteristic of the perturbed carbazole monomer. No evidence of excimer formation was observed in contrast to the isoelectronic (fluorene)$_2$ system. This implies that the two freely interacting carbazole molecules form a structure that differs greatly from that enforced in polymer chains. The ability to form excimers was related to the differing intermolecular interactions which determine the ground state structure. On the basis of Austin Model 1 optimised geometry calculations the carbazole dimer was predicted to have a double hydrogen bonded, heavily displaced antiparallel sandwich structure with C_{2h} symmetry in which there is no overlap of the aromatic rings. This structure was thought to either preclude or produce a high barrier to rearrangement of the dimer to the overlapped sandwich structure necessary for excimer formation.

Ethylation of the carbazole nitrogen is of interest in respect of the above observations since this would eliminate the possibility of hydrogen bonding and thus prevent formation of the heavily displaced antiparallel stack confguration. Formation of an excimer state may occur more readily in this case as the more eclipsed sandwich structure could be expected to be the strongest interaction.

4.2 Results

The LIF excitation and dispersed fluorescence spectra presented here show that the supersonic expansion contained a mixture of both NEC monomer and dimer. The partial pressure of each of these species is determined by the sample oven temperature; the higher the oven temperature, the higher the number density of dimer in the expansion. Features that are attributed to the molecular dimer exhibited an approximate quadratic dependence of their intensity on features previously assigned to the monomer. The oven temperature used in all cases was ~150°C.

4.2.1 Excitation Spectra of N-ethylcarbazole dimer

The LIF excitation spectrum of jet cooled NEC dimer is presented as figure 4.2. The spectrum is characterised by a number of sharp vibronic transitions on a flat background. The energies, relative intensities and assignments of these bands are listed as table 4.1. The absolute energy value of the dimer origin transition was reproducible to ± 0.5cm^{-1}, and the spectral shifts from the dimer origin transition were reproducible to ± 0.2 cm^{-1}. The lowest energy transition occurs some 606.8cm^{-1} to lower energy than that of the isolated NEC monomer, at 29047cm^{-1} ± 2cm^{-1}. This feature is assigned as the vibrationless electronic origin of $(NEC)_2$. The monomer origin was found to be at 29654cm^{-1}, some 112cm^{-1} higher in energy than that reported by Auty et al[27] although there was good agreement between the relative

Figure 4.2 LIF excitation spectrum of jet cooled N-ethylcarbazole

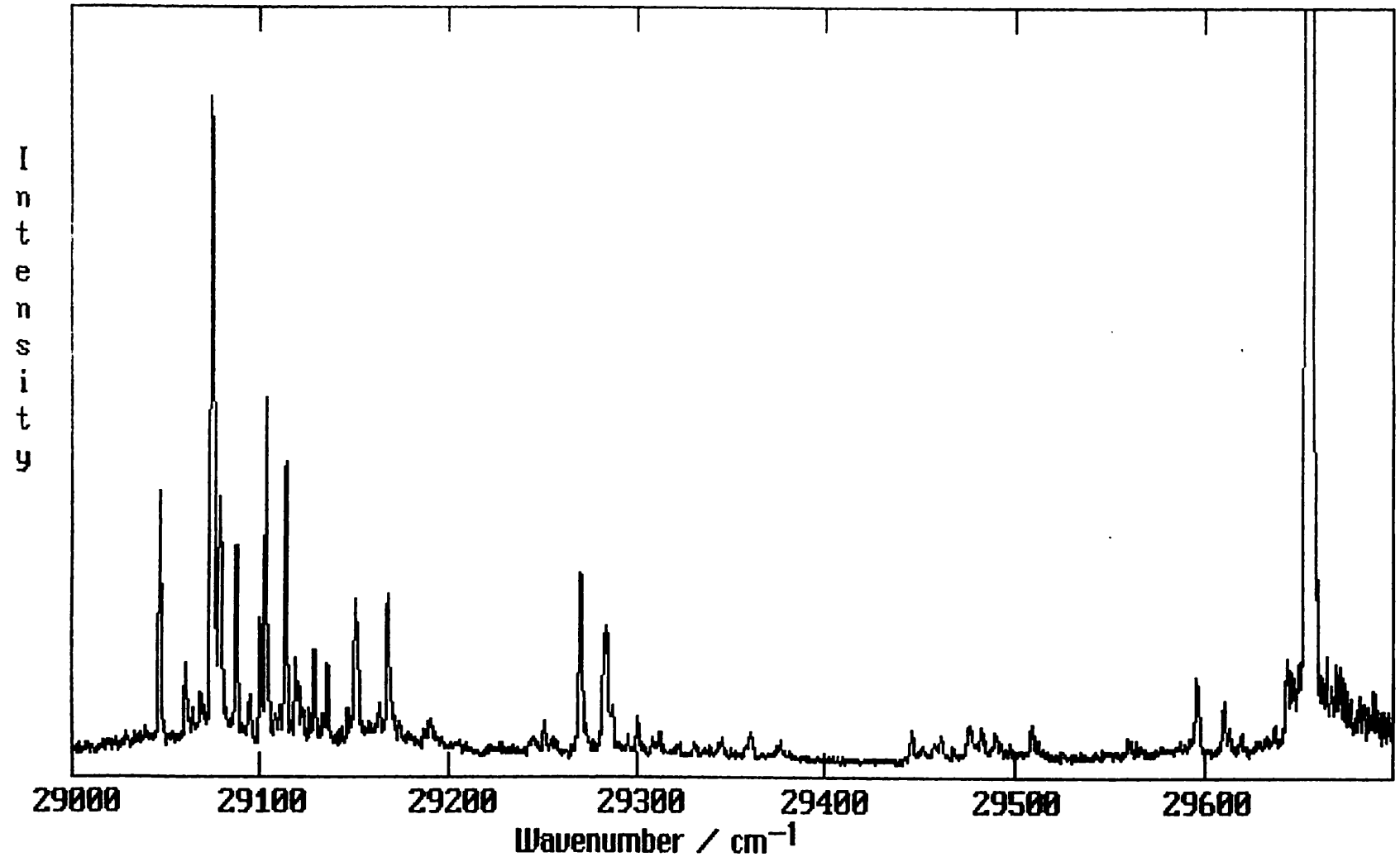

Table 4.1 Bands observed in the LIF excitation spectrum of a jet cooled N-ethylcarbazole monomer / dimer mixture.

Frequencies are quoted as wavenumber shift from the dimer origin transition, occuring at 29047 ± 2cm^{-1}

Relative shift from 29047cm^{-1} / cm^{-1}	Relative Intensity	Assignment
0.0	36	origin 0(0,0)
14.0	10	14
17.2	5	
21.6	8	
27.5	100	$\beta_a(0,1)$
31.6	33	31.6
40.2	28	$\beta_b(0,1)$
47.5	7	
53.3	18	
55.9	49	$\beta_a(0,2)$
63.0	5	
66.2	45	$\beta_a(0,1)+ \beta_b(0,1)$
71.6	10	$\beta_b(0,1) + 31.6$
78.8	5	$\beta_b(0,2)$
81.3	14	$\beta_a(0,3)$
88.3	11	$\beta_a(0,2) + 31.6$
99.0	5	$\beta_a(0,1) + \beta_b(0,1) + 31.6$
102.9	20	$\sigma(0,1)$
115.7	6	
120.3	22	$b_1(128)^*$
202.4	4	
221.7	27	$a_1(203)$
235.5	17	221.7 + 14
251.8	5	
263.9	3	
312.8	3	

Table 4.1 continued..

Relative shift from 29047cm^{-1} / cm^{-1}	Relative Intensity.	Assignment
328.7	2	
398.2	3	
413.6	2	
434.4	3	
442.8	2	
461	3	
512.5	1	
548.6	9	b_2(529)
562.9	7	548.6 + 14?
572.5	2	b_2(576)
596.4	12	
606.8	>200	monomer origin

Assignment notation:

i) ß = intermolecular bending vibration

σ = intermolecular stretching vibration

(x,y) x = ground state quanta

y = excited state quanta

ii) a_1 and b_2 refer to assignments of intramolecular modes in terms of monomer point group symmetry.

The values in parentheses are jet cooled monomer intramolecular fundamentals[3].

* The value in parentheses is that for the jet cooled carbazole dimer[26].

spectral shifts of monomer transitions. Intense features attributable to vibronic transitions occur at 221.7, 548.6 and 572.5cm^{-1} from the dimer origin transition. These can all be assigned by comparison to the monomer spectra previously recorded to intramolecular vibrations of the NEC molecules[3,27]. Additional intense transitions occur at 27.5, 40.2, 55.9, 66.2, 102.9 and 120.3cm^{-1} from the dimer origin transition which, since they have no counterparts in the monomer spectrum, cannot be assigned as NEC intramolecular fundamentals. Hence these transitions are assigned as intermolecular vibrations.

4.2.2 Dispersed Fluorescence Spectra

The dispersed fluorescence spectrum of NEC dimer following excitation at 29047cm^{-1}, excitation of the dimer electronic origin, is shown in figure 4.3. The resolution was ~8.5cm^{-1} fwhm at all excitation wavelengths used. The spectrum shows a number of transitions on a flat background. Table 4.2 gives the relative energies, intensities and assignments of these bands. Relative spectral shifts were reproducible to ± 2cm^{-1}. The intensity resonance band (emission at the same energy as excitation) contains a contribution of ~ 70% from scattered laser light, and the relative intensities of the transitions are normalised to account for this contribution. This contribution was determined by tuning the excitation slightly off the transition concerned and monitoring the intensity of the signal in resonance with the excitation wavelength, and

Figure 4.3 Emission spectrum of jet cooled N–ethylcarbazole after exciting into the origin transition

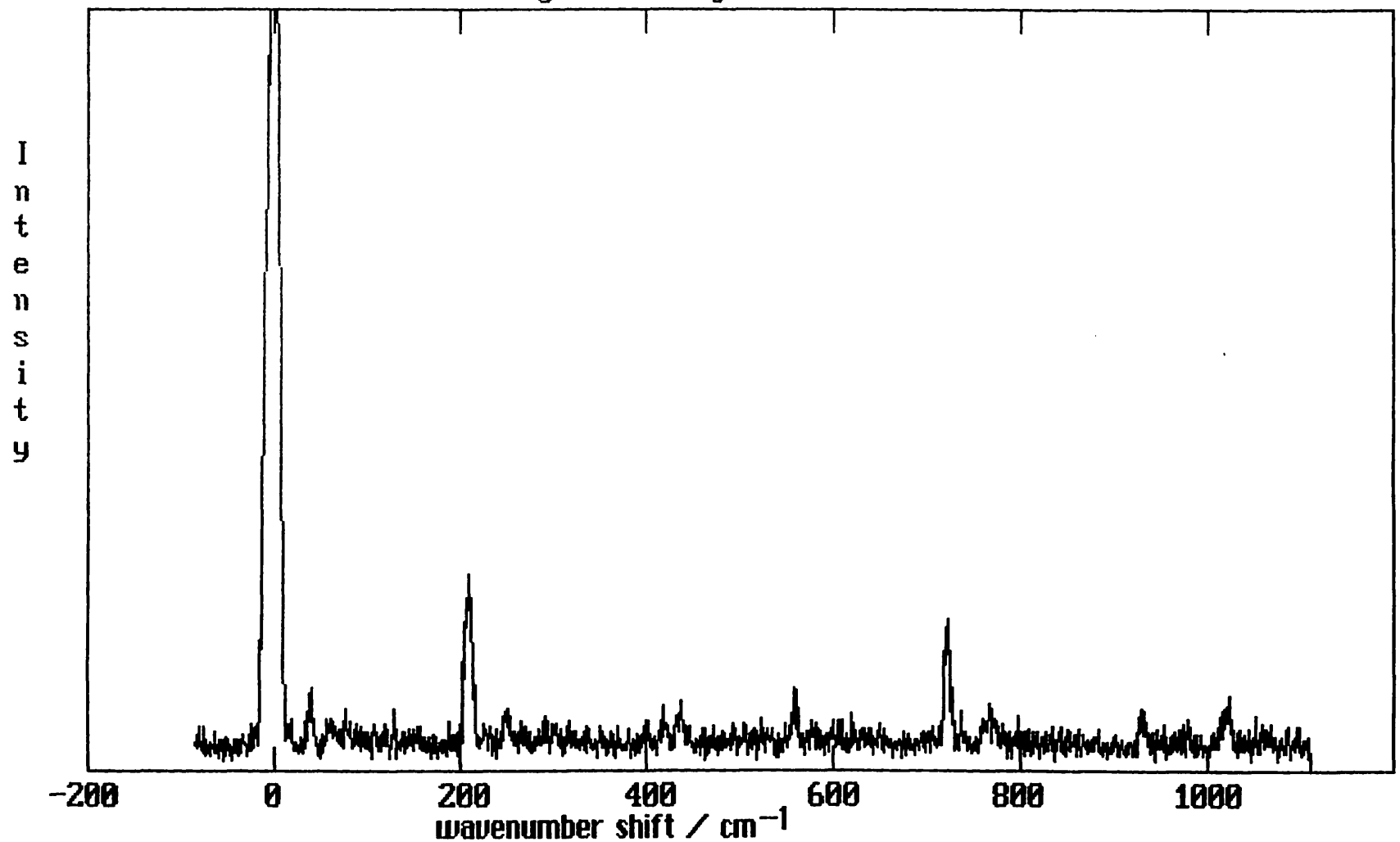

Table 4.2 Bands observed in the LIF emission spectrum of a jet cooled N-ethylcarbazole monomer / dimer mixture after excitation of the dimer origin transition at 29047cm^{-1}.

Relative shift from 29047cm^{-1} / cm^{-1}	Relative Intensity.	Assignment
0.0	100	origin
40.5	22	$ß_b(0,1)$
211.5	53	$a_1(206)$
251.5	15	211.5 + $ß_b(0,1)$
397.9	10	
417.4	15	2 x 211.5
436.3	17	$a_1(429)$
558.6	19	$b_2(554)$
721	45	$a_1(714)$
767.6	16	211.5 + 558.6
931.0	15	211.5 + 721
1023.1	19	$b_2(1014)$

then subtracting this intensity from the signal observed when exciting the transition.

The emission spectrum recorded following excitation of the intense feature at 27.5cm^{-1} from the origin transition is shown in figure 4.4. The spectrum is characterised by a large number of transitions built upon a flat background. The contribution from scattered light was ~50%. The relative shifts, intensities and assignments of the observed transitions are listed as table 4.3.

The emission spectrum recorded following excitation of the feature at 55.9cm^{-1} from the origin transition is shown in figure 4.5 and table 4.4 lists the relative shifts, intensities and assignments of the observed well resolved transitions. The scattered light contribution to the resonance band was ~65%. Red shifted emission was not observed at any of the excitation wavelengths used.

4.3 Discussion

The behaviour of the NEC monomer has been established to be very similar to that of carbazole[3] and behaves as though it were of C_{2v} point group symmetry although this is not strictly the case. The intramolecular vibrations observed in the NEC dimer excitation and emission spectra have consequently been assigned in these terms by comparison to the NEC monomer[27] and carbazole dimer[26] spectra. The intermolecular bending modes were assigned as β_a = 27.5cm^{-1} and β_b = 40.2cm^{-1}, and there was also an intermolecular symmetrical stretching motion σ=102.9cm^{-1}. The corresponding

Figure 4.4 Emission spectrum of jet cooled N-ethylcarbazole recorded after excitation of the intense transiton at 27.5cm^{-1}

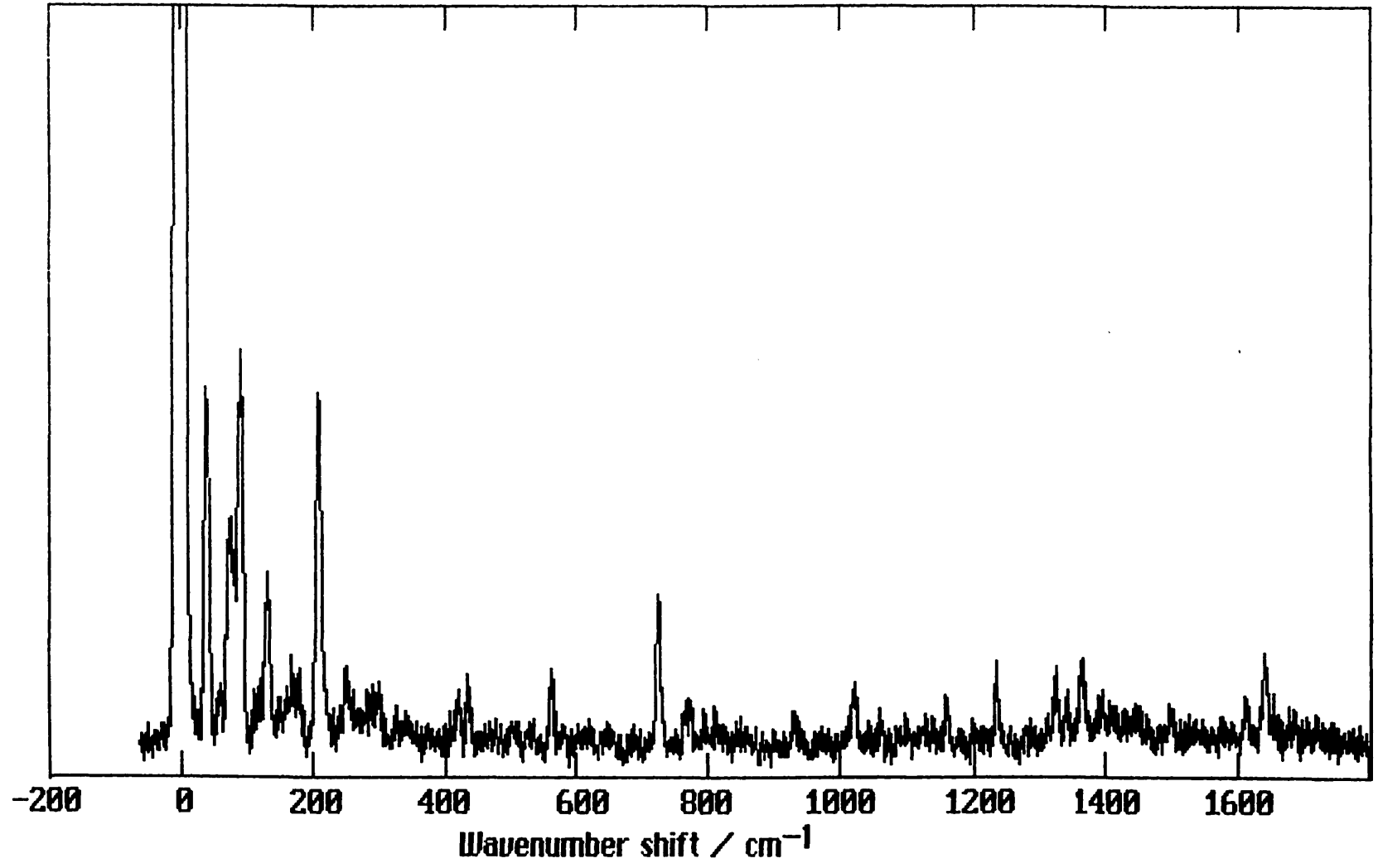

Table 4.3 Bands observed in the LIF emission spectrum of a jet cooled N-ethylcarbazole monomer / dimer mixture after excitation of the dimer intense transition at 27.5cm^{-1}.

Relative shift / cm^{-1}	Relative Intensity	Assignment
0.0	100	$\beta_a(0,1)$
39.5	34	$\beta_a(0,1)$ + $\beta_b(1,0)$
74.8	23	$\beta_a(0,1)$ + $\beta_b(2,0)$
91.0	39	$\beta_a(0,1)$ + $\sigma(1,0)$
130.8	17	$\beta_a(0,1)$ + $\beta_b(1,0)$+ $\sigma(1,0)$
179.8	8	
209.6	35	$\beta_a(0,1)$ + $a_1(206)$
250.7	8	$\beta_a(0,1)$ + $\beta_b(1,0)$ + 209.6
302.5	5	
420.4	6	$\beta_a(0,1)$ + 2 x 209.6
431.5	8	
562.3	8	$\beta_a(0,1)$ + $b_2(554)$
722.8	14	$\beta_a(0,1)$ + $a_1(714)$
771.5	5	
811.5	4	
933.2	4	$\beta_a(0,1)$ + 722.8 + 209.6
1023.0	7	$\beta_a(0,1)$ + $b_2(1014)$
1158.6	6	$\beta_a(0,1)$ + $b_2(1145)$
1233.4	8	$\beta_a(0,1)$ + 209.6 + 1023.0
1323.7	9	$\beta_a(0,1)$ + a1(1308)
1341.9	6	
1363.9	9	$\beta_a(0,1)$ + 209.6 + 1158.6

Figure 4.5 Emission spectrum of jet cooled N-ethylcarbazole after excitation into the 55.9cm $^{-1}$ transition.

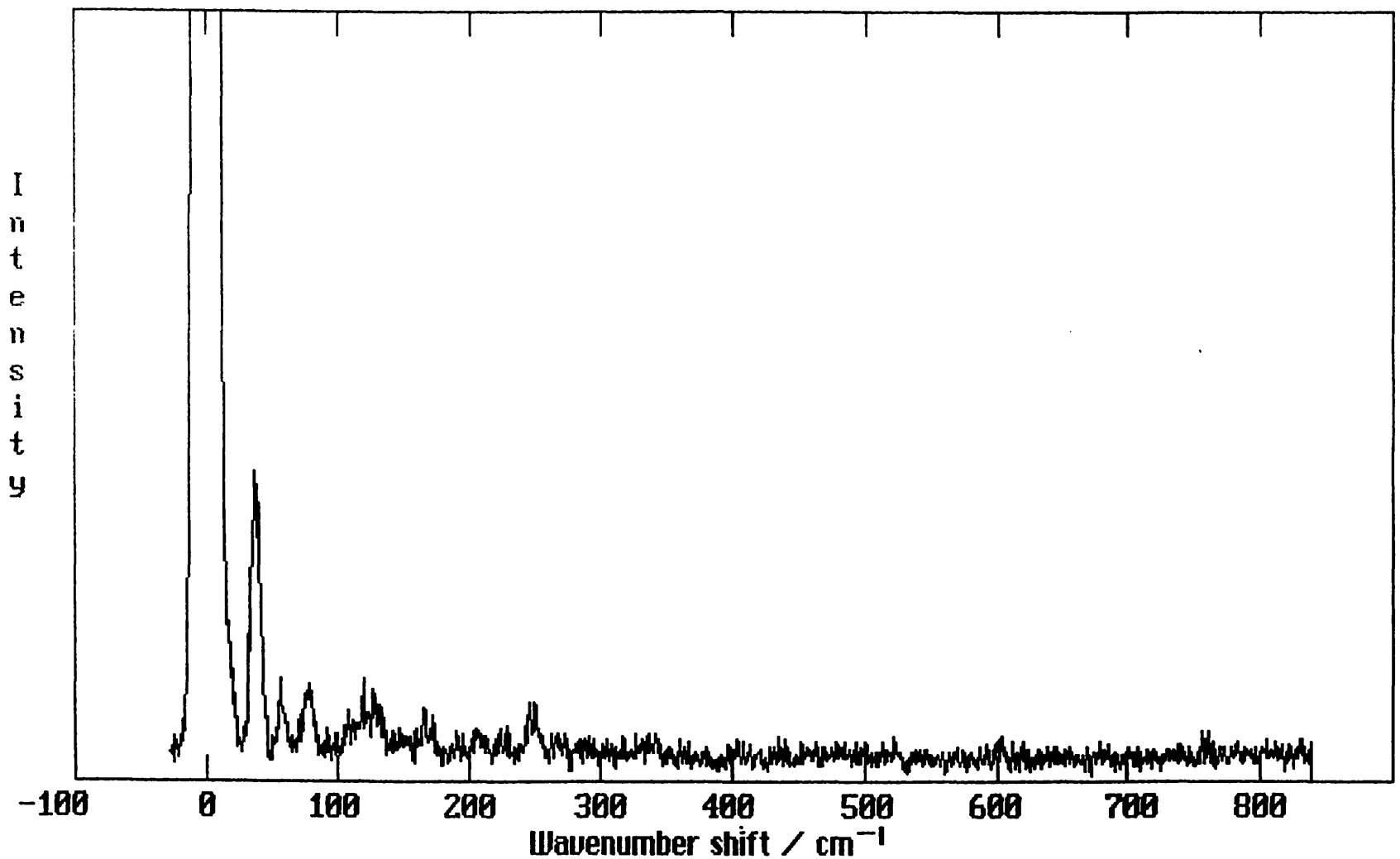

Table 4.4 Bands observed in the LIF emission spectrum of a jet cooled N-ethylcarbazole monomer / dimer mixture after excitation of the 55.9 cm^{-1} dimer transition.

Relative shift / cm^{-1}	Relative Intensity	Assignment
0.0	100	$\beta_a(0,2)$
37.5	16	$\beta_a(0,2) + \beta_b(1,0)$
56.0	5	$\beta_a(2,2)$
77.8	5	$\beta_a(0,2) + \beta_b(2,0)$
119.9	5	$\beta_a(0,2) + \sigma(1,0)$
129.6	4	$\beta_a(0,2) + \beta_b(1,0) + \sigma(1,0)$
168.5	3	$\beta_a(0,2) + \beta_b(2,0) + \sigma(1,0)$
248.9	4	$\beta_a(0,2) + \beta_b(1,0) + a_1(206)$

ground state values are β_a=28cm^{-1}, β_b = 40cm^{-1} and σ=91cm^{-1}. The values observed for the excited state intermolecular vibrations compare well with both the carbazole dimer bend =44cm^{-1}, stretch = 95cm^{-1} and the NEC alkyl cyanide complexes bend (13-22cm^{-1}) and stretch (161-235cm^{-1})[28].A point of interest is that all the observed bands are shifted slightly to higher energy than in the monomer. This was found to be the case for carbazole dimer cooled in a supersonic jet[26] and carbazole held in a fluorene matrix[29].

The excitation spectrum of NEC dimer shows only one origin transition, and the observed spectral shift of this from the monomer origin is 606.8cm^{-1}, which compares with 763cm^{-1} for carbazole)$_2$, 222cm^{-1} for fluorene dimer and 230cm^{-1} for the dimer of 9-ethylfluorene. Clearly the value is closest to that for carbazole and the increase in interaction for (NEC)$_2$ is similar to that in (carbazole)$_2$. From the observation of only one origin transition it can be determined that only one dimer structure exists. Also only one set of discernible transitions was observed, which is initially surprising since the excited states of dimers can often be split into two 'excitonic' states, the nature of this splitting will be outlined later.

Several possible structures of the NEC dimer seem feasible, namely i) antiparallel sandwich ii) T-shaped and iii) head to tail structure. The implications of the above spectroscopic observations on these possible dimer structures are as follows:

The antiparallel sandwich structure allows close interaction of the permanent dipole moments of both moieties and

therefore there is the opportunity for strong dipole-dipole and dipole-induced dipole interactions. In this structure both of the NEC moities are equivalent, experiencing the same solvation effect from the other chromophore therefore both moities would exhibit the same spectral shift from the monomer origin. This sandwich structure will be of C_{2h} symmetry, and therefore the $S_1(A_1)$ state of the monomer will be split into two excitonic states in the dimer. The A_1 state will split into B_u and A_g exciton states. The one photon transition to the B_u state would be allowed but to the A_g state would be disallowed. Therefore for this structure only one origin transition and one set of discernible vibronic transitions would be expected, which is in line with the above observations.

There are two possible T shaped configurations both of C_1 symmetry, one in which the two molecular long axes lie parallel and the other where the molecular long axes lie perpendicular. In each case the transition moments are perpendicular to each other and in the point group dipole approximation excitonic splitting is disallowed so there is only one exciton state and only one set of discernible transitions would be expected. In each case the respective chromophores experience different solvation and therefore multiple origin transitions are expected which is contrary to the observations here.

The head to tail structure, whilst allowing a close approach of dipoles does suffer considerable steric hindrance from the ethyl group. Excitonic splitting here for a dimer of C_{2v} symmetry is allowed, the A_1 state of the monomer correlating

with two allowed A_1 exciton states in the dimer, however one of these states, has zero transition moment in the point dipole approximation giving rise to a single spectrum. Nevertheless due to differing solvation of the respective chromophores two dimer origins with different solvent shifts would be expected, in contrast to the observations here.

All the observations here tend to support the sandwich structure similar to that observed for the carbazole dimer. In the carbazole dimer this assignment was also supported by the results of semi empirical Austin Model 1 calculations of optimised geometries[26]. Further support to this assignment for NEC dimer is the observation of the 120.3cm^{-1} transition which is similar to a b_1 mode observed at 128.6cm^{-1} in the carbazole dimer spectrum which is formally forbidden under the C_{2v} symmetry of the carbazole monomer but assigned from its observation at 128cm^{-1} in carbazole complexes with ammonia and water in which intensity was borrowed through Fermi-resonance[30]. Such a transition would be disallowed for the head to tail structure since the monomer C_{2v} symmetry is retained for this dimer structure and the b_1 mode is forbidden. Under the C_{2h} structure of the antiparallel sandwich structure postulated here the b_1 mode correlates to an a' mode and becomes allowed. Also for the T-shaped structure all intramolecular modes become allowed under the C_1 symmetry and a more complex spectrum would be expected.

The nature of the excitonic splitting is dependent on certain factors, namely the excitation energy of the free monomer, the change in symmetry on going from the monomer to the dimer and also the interaction between the two constituent

moieties. The relationship between these factors when considering a dimer $X_1(X_2)$ is given by[31]:

$$E = E_x + I_1\ 1/2(I_2 - I_1) \pm\{((I_2 - 1/2I_1)^2 + \Delta^2\}^{1/2} \quad (1)$$

where:

E = excitation energy of the two excitonic states

E_x = excitation energy of the free monomer

$I_1(I_2)$ = change in intermolecular interaction upon excitation of $X_1(X_2)$.

Δ = half exciton or Davydov splitting due to the excitation exchange interaction between the two identical chromophores.

The values of I_1 and I_2 can be thought of as the solvent shift that each moiety experiences due to the other moiety. For the displaced antiparallel sandwich structure of C_{2h} symmetry both molecules experience the same solvent shift and $I_1 = I_2$, so the equation becomes:

$$E = E_x + I \pm \Delta \quad (2)$$

For this structure the S_1 state is expected to be split into A_g and B_u states, and these can be represented by the wavefunction:

$$\Psi_g = (\Psi_1^*\Psi_2 + \Psi_1\Psi_{2*})/\sqrt{2}$$
$$\Psi_u = (\Psi_1^*\Psi_2 - \Psi_1\Psi_2^*)/\sqrt{2} \quad (3)$$

where Ψ_1^* refers to the locally excited state of moiety X_1 in the dimer, etc..

The transition moments of these two states are given by:

$$M_g = (M_1 + M_2)/\sqrt{2}$$
$$M_u = (M_1 - M_2)/\sqrt{2} \qquad (4)$$

In the point dipole model[32], the interaction between the two transitions can be expressed as:

$$H_{12} = \frac{1}{4\pi\epsilon_0}\left[\frac{M_1M_2}{R^3}\right] - \left[\frac{3(M_1R)(M_2R)}{R^5}\right] \qquad (5)$$

where:

R = vector separation of the dipole centres

ϵ_0 = permitivity of free space

The transition moments are related to the oscillator strength, f by:

$$f = 4.277\text{x}10^{52}\nu\ |M|^2 \qquad (6)$$

whwere ν is in cm^{-1}.

The half exciton splitting when the transition moments are equivalent (ie $M_1 = M_2$) is given by:

$$\Delta = \frac{(1-3\cos^2\theta)f}{4.703\text{x}10^{42}\nu R^3} \qquad (7)$$

In the A_g state $M_2 = -M_1$, and therefore the transition will be destabilised relative to the monomer, the B_u state will be stabilised and the observed origin transition is to this B_u state.

The spectroscopic red shift of the dimer from the monomer can be explained in terms of the increase in permanent dipole moment following excitation. This increase in carbazole is from 2.0D in the ground state[33] to 3.0D in the S_1 state. This increase in dipole moment causes a substantial increase

in dipole - dipole and dipole induced dipole forces and hence there is a stronger interaction in the excited state. In the absence of acccurate information on the oscillator strength of the transition and the structure of the dimer it is not possible to calculate what the observed excitonic splitting should be however it is unlikely to be larger than that calculated for the carbazole dimer[26]. Therefore the minimum value of the solvent shift must be 606.8 - 128 = 479cm^{-1}, though the true value is probably greater. Solvent shifts of similar magnitude were observed complexes of NEC with alkyl cyanides (354-427cm^{-1})[28] where the major attractive interaction is also of a dipole dipole nature.

Some of the features in the excitation spectrum of NEC cannot readily be assigned in terms of intramolecular or intermolecular vibrations, namely those at 14cm^{-1} and 235.5cm^{-1}. These bands are each shifted 14cm^{-1} from an intramolecular fundamental vibration of an NEC chromophore and are therefore tentatively assigned as arising from co-operative electronic vibrational excitation in which two zeroth order states exist, one with vibrational and electronic excitation of the same chromophore, and the second with vibrational excitation of the partner to the electronically excited chromophore. The carbazole dimer also exhibited similar features which were similarly assigned[26].

A number of combination bands built upon a transition at 31.6cm^{-1} were observed, however this mode could not redily be assigned.

The observation of extensive intermolecular vibrations provides evidence of considerable displacement along one of

the molecular co-ordinate following electronic excitation. In carbazole few intermolecular vibrations were observed and in fluorene there is extensive intermolecular activity. NEC dimer appears to lie somewhere between these two cases. The transition energy of the low frequency bending vibrations of the NEC dimer are affected to a lesser degree upon excitation than the intermolecular stretching vibration, implying that the gretest change is occuring along the intermolecular stretching coordinate.

As outlined in the introduction a number of types of behaviour have been observed for dimers cooled in a supersonic jet. These can be summarised as being characteristic of the perturbed monomer[5-8,25], exhibiting excited state proton transfer[20-22] or giving rise to broad red shifted emission attributeable to excimer formation[1,2]. In addition formation of excimers has been invoked to explain the reduction in fluorescence quantum yield for the benzene dimer[9-19]. For NEC dimer no evidence for any red shifted emission was observed, however relatively few bands were excited, the $55.9cm^{-1}$ being the highest energy transition excited, therefore excimer formation cannot be precluded but can be regarded as having an activation barrier of at least $55.9cm^{-1}$. Rearrangement of the displaced antiparallel sandwich structure postulated to a more eclipsed structure (as found for fluorene) is considered necessary for observation of excimer emission, and this process does not occur at the excitation energies used here.

In conclusion NEC has been shown to form a strongly bound molecular dimer of 1:1 stoichiometry, which is preferentially stabilised in the first electronic excited state as compared with the ground state. This increased interaction is brought about by the enhanced permanent dipole moment in the S_1 state and hence greater attractive dipole-dipole and dipole - induced dipole forces. The structure of the dimer is most probably anti-parallel sandwich and has a pseudo C_{2h} symmetry. Extensive intermolecular vibrational activity is observed in the electronic spectra suggesting considerable displacement along some intermolecular co-ordinate upon excitation. A contraction of this type is consistent with a large bathochromic shift of $606.8cm^{-1}$. In contrast to the dimers of fluorene and 9-ethylfluorene no excimeric emission was observed . Excimer formation cannot be completely ruled out for NEC but the experiments performed here show that the activation energy for excimer formation must be greater than $56cm^{-1}$, whereas in the aforementioned cases the transition to the excimer state was barrierless. In general NEC dimer behaves in a similar manner to that of carbazole despite the abiltity of carbazole to form strong hydrogen bonds, suggesting that dipole-dipole interactions can have a considerable degree of specificity and can therefore affect subsequent behaviour strongly.

4.4 References

1 H.Saigusa a.d M.Itoh
J. Phys. Chem. 89 (1985) 5486.

2 M.Itoh and Y.Morita,
J. Phys. Chem 92 (1988) 5693.

3 A.R.Auty,
PhD. University of London (1986).

4 F.L.Minn, J.P.Pinion and N.Filipesan,
J. Phys. Chem. 75 (1971) 563.

5 D.H.Levy, C.A.Haynam and D.V.Brumbaugh,
Faraday Discuss. Chem. Soc. 72 (1982) 137.

6 C.A.Haynam, D.V.Brumbaugh and D.H.Levy,
J. Chem. Phys. 79 (1983) 1581.

7 L.Young, C.A.Haynam and D.H.Levy,
J. Chem. Phys. 79 (1983) 1592.

8 C.A.Haynam, D.V.Brumbaugh and D.H,Levy,
J. Chem Phys. 81 (1984) 2282.

9 P.R.R.Langridge-Smith, D.V.Brumbaugh, C.A.Haynam and D.H.Levy,
J.Phys Chem. 85 (1981) 3742.

10 G.Karlstrom, P. Linse, A.Wallqvist and B.Johnson,
J. Am. Chem. Soc. 105 (1983) 3777.

11 J.Pawliszyn, M.M.Szczesniak and S.Scheiner,
J. Phys. Chem. 88 (1984) 1726.

12 P.Carsky, H.L.Selzle and E.W.Schlag,
Chem. Phys. 125 (1988) 165.

13 D.E.Williams,
Acta. Crystallogr. Sect. A. 32 (1980) 715.

14 B.W.van de Waal,
Chem. Phys. Letters 123 (1986) 69.

15 M.Schauer and E.R. Bernsiein,
J. Chem. Phys. 82 (1985) 3722.

16 J.B.Hopkins, D.E.Powers and R.E.Smalley,
J. Phys. Chem. 85 (1881) 3739.

17 K.H.Fung, H.L.Selzle and E.W.Schlag,
J. Phys. Chem. 87 (1983) 5113.

18 K.S.Law, M.Schauer and E.R. Bernsiein,
J. Chem. Phys. 81 (1984) 4871.

19 K.O.Bornsen, H.L.Selzle and E.W.Schlag,
J. Chem. Phys. 85 (1986) 1726.

20 K.Fuke, H.Yoshiuchi and K.Kaya,
J. Phys. Chem. 88 (1984) 5840.

21 K.Fuke, T.Yabe, N.Chiba, T.Kohida and K.Kaya,
J. Phys. Chem. 90 (1986) 2309.

22 K.Fuke and K.Kaya,
J. Phys. Chem. 93 (1989) 614.

23 G.E.Johnson,
J. Chem. Phys. 61 (1974) 3002.

24 G.E.Johnson,
J. Chem. Phys. 62 (1975) 4697.

25 F.Evers, K.Kobs, R.Memming and D.R.Terrell,
J. Am. Chem. Soc. 105 (1983) 5988.

26 A.G.Taylor, A.C.Jones and D.Phillips,
Chem. Phys. 138 (1989) 413.

27 A.R.Auty, A.C.Jones and D.Phillips,
J. Chem. Soc. Faraday Trans. 2 82 (1986) 1219.

28 A.G.Taylor, A.C.Jones, A.R.Auty and D.Phillips,
Chem. Phys. Letters 131 (1986) 534.

29 A.Bree and R.Zwarich,
J. Chem. Phys 49 (1968) 3344.

30 E. Hönnegger, R.Bombach and S.Leutwyler,
J. Chem. Phys. 85 (1986) 1234.

31 J.Jortner,
J. Chem. Soc. Faraday Discuss. 73 (1982) 173.

32 J.N.Murrell and J.Tanaka,
Mol. Phys. 7 (1964) 363.

33 W.Liptay,
Angew. Chem. Int. Engl. Ed. 8 (1969) 177.

CHAPTER FIVE: SPECTROSCOPY OF N-(4-CYANOPHENYL)CARBAZOLE

5.1 Introduction

In this chapter the LIF spectroscopy of isolated jet cooled N-(4-cyanophenyl)carbazole (CPC) is reported for the first time. The LIF excitation spectrum is presented in section 5.2.1 and dispersed fluorescence spectra of CPC are presented in section 5.2.2. In section 5.3 these data are discussed.

Spectroscopic studies of several jet cooled bi-aryls have been reported; these molecules are depicted in figure 5.1. Aromatic molecules of this type which are composed of two planar aromatic systems joined by a single carbon-carbon bond are flexible in the sense that the molecular conformation is sensitive to perturbations from the environment. These molecules can, upon excitation, easily adopt an energetically more favourable conformation by change of the interplanar angle. A classical example of this is the biphenyl molecule, where in the crystalline phase van der Waals forces dominate and the molecule is held planar with D_{2h} symmetry[1]. In the gas phase the molecule has been shown to have an interplanar angle of 42°[2]. The one and two photon electronic absorption spectra of jet cooled biphenyl-h_{10} and biphenyl-d_{10} have been reported[3]. For the deuterated molecule, two progressions were observed, each developing for more than 20 quanta with an almost constant spacings of ~61cm^{-1}. For the non deuterated case a similar but slightly more complicated spectrum was observed the spacing of the similar progressions

Figure 5.1 Some bi-aryls investigated in a supersonic jet.

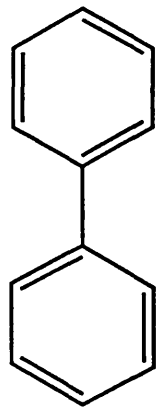

biphenyl

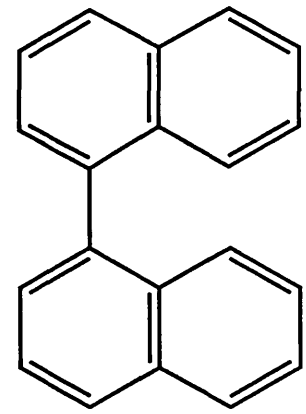

1,1' binaphthyl

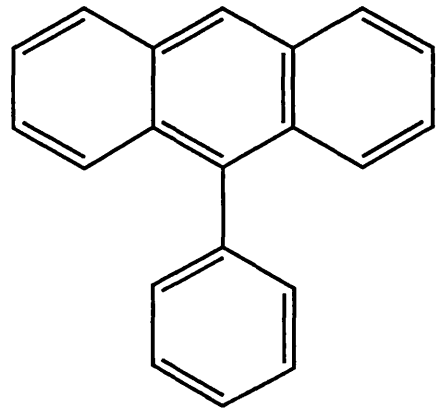

9-phenylanthracene

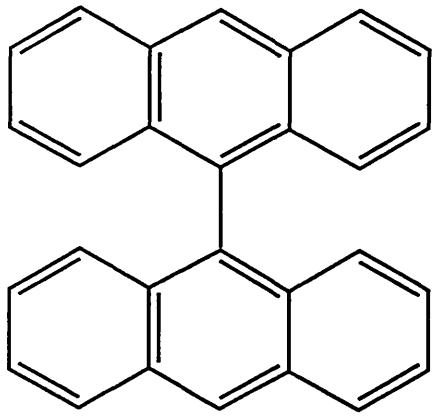

9,9' bianthryl

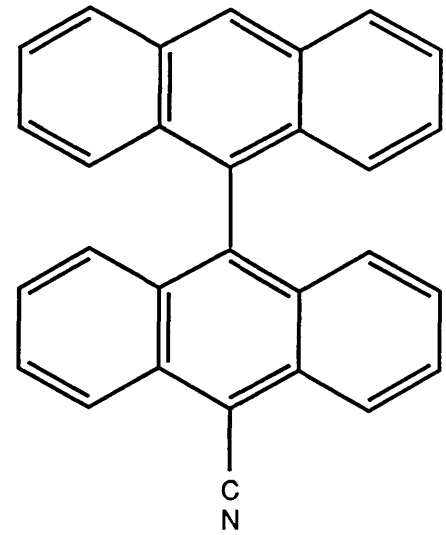

10-cyano-9,9' bianthryl

is ~67cm^{-1}, and these progressions were assigned as the torsional vibration of the phenyl rings. The vibrational spacings of the two progressions were found to differ very slightly, and the intensity ratio of the two progressions reverses from the one photon spectrum to two photon spectrum. This indicates the existence of two different excited electronic states. These observations were explained as follows: In the crystal there are two closely spaced electronic states: two photon allowed $B_{3g}(S_1)$ and one photon allowed $B_{2u}(S_2)$ under the planar D_{2h} symmetry. In the gas phase biphenyl has a twisted ground state structure of D2 symmetry, in which both S_1 (B_3 derived from B_{3g}) and S_2 (B_2 from B_{2u}) are theoretically both one and two photon allowed, however the one(S_2) and two photon(S_1) allowed nature still persists to a certain extent even in the twisted structure, resulting in the observed intensity ratio.

Jonkman and Wiersma[4] reported the LIF excitation and dispersed fluorescence spectra of another bi-aryl, namely 1,1'-binaphthyl(BN). A weak origin occurs at 31716cm^{-1}, in addition a 'false origin' group of lines commencing at 32122cm^{-1} was observed, reminiscent of that observed at 437cm^{-1} from the origin in the naphthalene spectrum. Two progressions were observed in the origin region of the excitation spectrum, one starting at 31716cm^{-1} in a low frequency, slightly anharmonic mode with a fundamental frequency of 30cm^{-1} and the other starting at 31737cm^{-1} with a lower frequency spacing (28cm^{-1}). The splitting (21cm^{-1}) between these two progressions was assigned as the exciton

splitting of the binaphthyl molecule and the low frequency mode as a molecular libration (torsion) that is connected with a rotation of one of the rings around the connecting carbon-carbon bond. The small exciton splitting suggests that the naphthalene rings are only weakly coupled. The total intensity in both progressions is identical, and from this it was concluded that in the state excited the rings are orthogonal with respect to one another. From the progression in the librational mode it was further concluded that the same holds for the ground state. From the structureless dispersed fluorescence spectra and lifetime of 50 ± 5ns it was concluded that, in the isolated molecule, efficient vibrational relaxation occurs through conversion of vibrational into librational (torsional) energy.

In a subsequent publication Jonkman and Wiersma[5] reported the LIF excitation and emission spectra of BN-h_{14} and BN-d_{14} which lead to a different interpretation of the spectra. Comparison of the two spectra reveals that each is composed of two strong and two weak progressions in modes of low frequency (~30cm^{-1}). The four transitions can be described in terms of excitations to levels of a weakly coupled dimer. This dimer exhibits a C_2 axis of symmetry and therefore all states of the dimer should be classified as either symmetric(A) or antisymmetric(B) with respect to this symmetry axis, consequently each single absorption line in the monomer spectrum will be split into two by the interchange-equivalent interaction between the rings. The observation of four origins indicates the presence of a *trans*-inclined and *cis*-inclined configuration, each

exhibiting two groups of lines. The Franck-Condon envelope of the librational progressions indicates that the potential energy surface for states of A and B symmetry are different, implying that the interplanar angle in each of the four excited states is different. From the intensities of the A and B progressions it was deduced that for the origin transitions the transition momemt in each subunit is oriented in the naphthalene plane at an angle of ~50° with respect to the long axis. It was further deduced that the change in torsional angle on excitation to the antisymmetric B double well potential energy surface is ~12° to the *trans* and ~6° to the *cis* side, and from this a maximum barrier of 150cm^{-1} was calculated. The emission spectrum was interpreted by assuming that very efficient vibrational relaxation occurs through conversion of vibrational into librational energy, and the molecule relaxes into the energetically most stable structure.

Werst et al[6] reported the LIF spectroscopy of jet cooled 9-phenylanthracene in the frequency range 26800-28000cm^{-1}. Seven vibrational modes of the first electronic excited singlet state were observed. The lowest frequency (49cm^{-1}) mode was assigned to torsional motion around the bond joining the two aromatic ring. This assignment was further confirmed by isotopic substitution of the phenyl ring. The lowest frequency mode was found to differ greatly between the two spectra when compared with the other modes. These other features were assigned to modes of anthracene, only weakly coupled to the phenyl ring. Torsional spacings fitted well to

a one dimensional double well potential with a maximum at ~90°and minima at ~60 and 120°. Torsional levels in the S_0 state were identified by raising the temperature of the jet to populate the low frequency S_0 states.

Formation of a twisted intramolecular charge transfer (TICT) state has been invoked to explain the unusual dual fluorescence characteristics of several molecules such as 9,9'bianthryl[7] this explanation has been discussed in detail in chapter 3. On the basis of several solution phase studies[8] the two anthracene moieties are considered to be orthogonal in the ground state. In order for formation of a TICT state almost a full electronic charge must be transferred from one moiety to the other, which can only occur when the orthogonal structure is relaxed, hence the term 'twisted'. Schneider and Lippert [9] concluded that the torsional angle of the S_1 state deviates from 90°, and was estimated at 78°.

Yamasaki et al[10] reported the LIF excitation spectrum of jet cooled 9,9'bianthryl between 355 and 375nm. A characteristic pattern of bands with 11-16cm^{-1} spacings was observed in the origin and vibronic region of the spectrum and was assigned as a progression due to the torsional motion of anthracence moieties around the 9-9' axis. From a simulation of the spectrum using a double well potential of internal rotation the torsional angle in the S_1 state was derived to be 67 ± 5°. The authors concluded that this study offers a firm basis for the proposed mechanism of CT formation. If the stable structure of the excited state were

orthogonal, charge transfer would be inhibited, the observed non orthogonal structure assures the relaxation into a less twisted form in which resonance between the two moieties becomes viable. However they further concluded that the energy level of the CT state would be high unless stabilised by surrounding polar molecules. Therefore the CT emission was not expected for the bare bianthryl even if the upper state is non-orthogonal.

In a concurrent publication Khundkar and Zewail[11] reported the LIF excitation and emission spectrum of jet cooled 9,9' bianthryl. The spectra were anthracene like, indicating that the rings are weakly coupled. Exciton effects were considered in assignment of the spectra, but it was assumed that only one exciton state was optically active. The torsional potential of the S_1 state was modelled as a double-well potential similar to those of biphenyl, binapthyl and 9-phenylanthracene with barriers to perpendicularity and planarity of ~30 and 1100cm^{-1} respectively. Anthracene modes in S_1 and S_0 were also assigned. Measurements of the fluorescence lifetimes of the S_1 state were made up to 6000cm^{-1} excess energy and showed no evidence of charge transfer.

Kajimoto et al[12] subsequently investigated the solvated 9,9'bianthryl molecule. The fluorescence spectra of both bare and solvated 9,9'bianthryl were recorded. For the bare molecule only emission from the locally excited S_1 state was observed, even on excitation to a high vibronic state. In contrast the excitation of the 0-0 band of bianthryl solvated by acetone gave fluorescence attributed to an intramolecular

CT state. The ratio of the intensity of the CT fluorescence to that of the locally excited fluorescence increased with increased degree of solvation. Solvation by the non polar cyclohexane did not give rise to CT emission. The stoichiometry of the bianthryl-acetone complex was required to be 1:n where n>1. If this band was due to intermolecular charge transfer the increase in emission with increasing solvation would not be so significant as that observed in these experiments.

In a recent publication[13] the LIF spectroscopy of 9,9'bianthryl and 10-(cyano)-9,9'bianthryl(CBA) was investigated. As previously mentioned bianthryl forms an intramolecular charge transfer state upon excitation when in polar surroundings. Another possible way to preferentially stabilise the charge transfer state with respect to the locally excited state is to introduce an acceptor substituent into bianthryl. This has been shown to favour formation of the CT state, and perhaps give rise to dual emission for the isolated jet cooled molecule. Therefore a comparative study of the above molecules was made. The torsional potentials in the S_0 and S_1 states of BA and CBA were determined by a fit procedure of a one dimensional model to the experimental data. The results show that the S_1 double minimum potential is shallower than for CBA, indicating a stronger interaction between the two moieties of the latter molecule. The dispersed fluorescence spectra of CBA was discussed in terms of intramolecular vibrational redistribution processes. The fluorescence decay rates were measured as a function of excess vibrational energy of CBA reflecting a saturation

behaviour already within the origin region in contrast to BA (saturation near 380cm^{-1}). This is tentatively assigned to the presence of a low lying dark background state possibly of charge transfer character.

In a preliminary solution phase study[14] the emission spectra of CPC and the related molecules N-phenylcarbazole(PC), 1'-napthylcarbazole(C1N) and 9'-phenanthrylcarbazole(C9P) (see figure 5.2) were reported. The molecules CPC, C1N and C9P were shown to have very large quantum yields of TICT fluorescence, and they exhibit only one emission band in polar solvents, arising from the TICT state. Steric effects in the ground state configuration cause torsion of the carbazole-benzonitrile bond, twisting the two moieties out of plane with each other, to near orthogonal conformation. On excitation in the presence of polar solvents the conformation is relaxed and this is accompanied, in the case of CPC, by charge transfer from the carbazole to the benzonitrile moiety. PC however, shows only normal emission from the locally excited state, and the effect of adding an acceptor group to the phenyl ring is to promote CT state formation and hence red shifted emission. The quantum yield of TICT fluorescence was found to be 0.38 for CPC in acetonitrile, 0.19 and 0.15 for C1N and C9P respectively. The ground state equilibrium twist angles were calculated to be 39, 55 and 55° for CB, C1N and C9P respectively. A value for CPC was not given but it was said to be substantially twisted in the ground state.

Figure 5.2 Some derivatives of carbazole studied in solution phase [14]

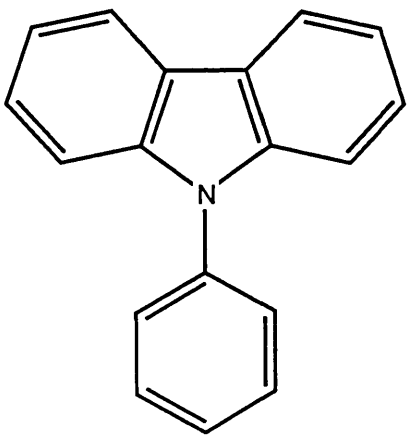

PC

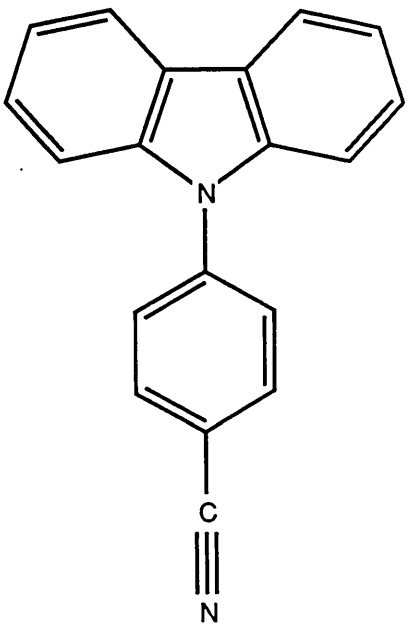

CPC

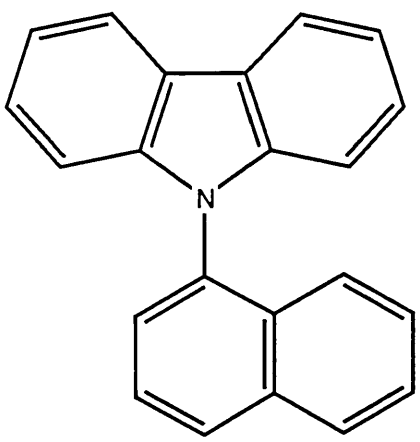

C1N

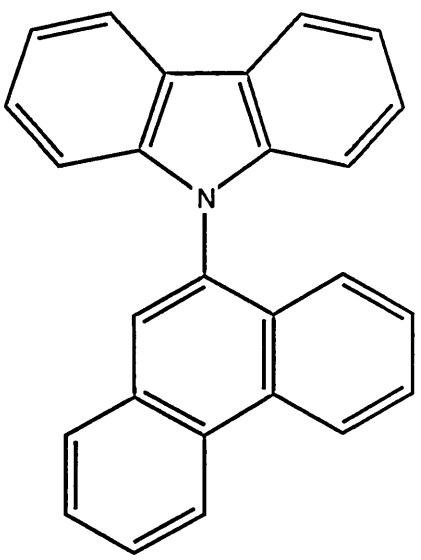

C9P

The hydrogen bound complex of carbazole with benzonitrile has also recently been studied[15]. This differs from CPC since the complex is hydrogen bound via the cyano group of the benzonitrile, whereas in CPC the two molecules are connected by a N-C bond to the *para* carbon atom of the benzonitrile moiety. LIF excitation spectra revealed a three membered low frequency progression in a mode of $21cm^{-1}$ assigned as being the excited state carbazole - benzonitrile intermolecular bending vibration. Another transition was observed at $154cm^{-1}$ and assigned as the corresponding intermolecular stretching vibration. In the emission spectra a similar progression was observed in a mode of $21cm^{-1}$ in addition to a transition at $141cm^{-1}$, these were assigned respectively as the corresponding ground state intermolecular bending and stretching vibrations.

To date no spectroscopic studies of the jet cooled CPC molecule have been made. In this chapter LIF excitation and emission spectra are presented and these spectra are discussed in terms of the molecules carbazole and benzonitrile, as well as in the light of the TICT state hypothesis.

5.2 Results

5.2.1 Excitation Spectra

The LIF excitation spectrum of jet cooled CPC is presented as figure 5.3, The spectrum is characterised by a

Figure 5.3 LIF excitation spectrum of jet cooled N-(4-cyanophenyl)carbazole

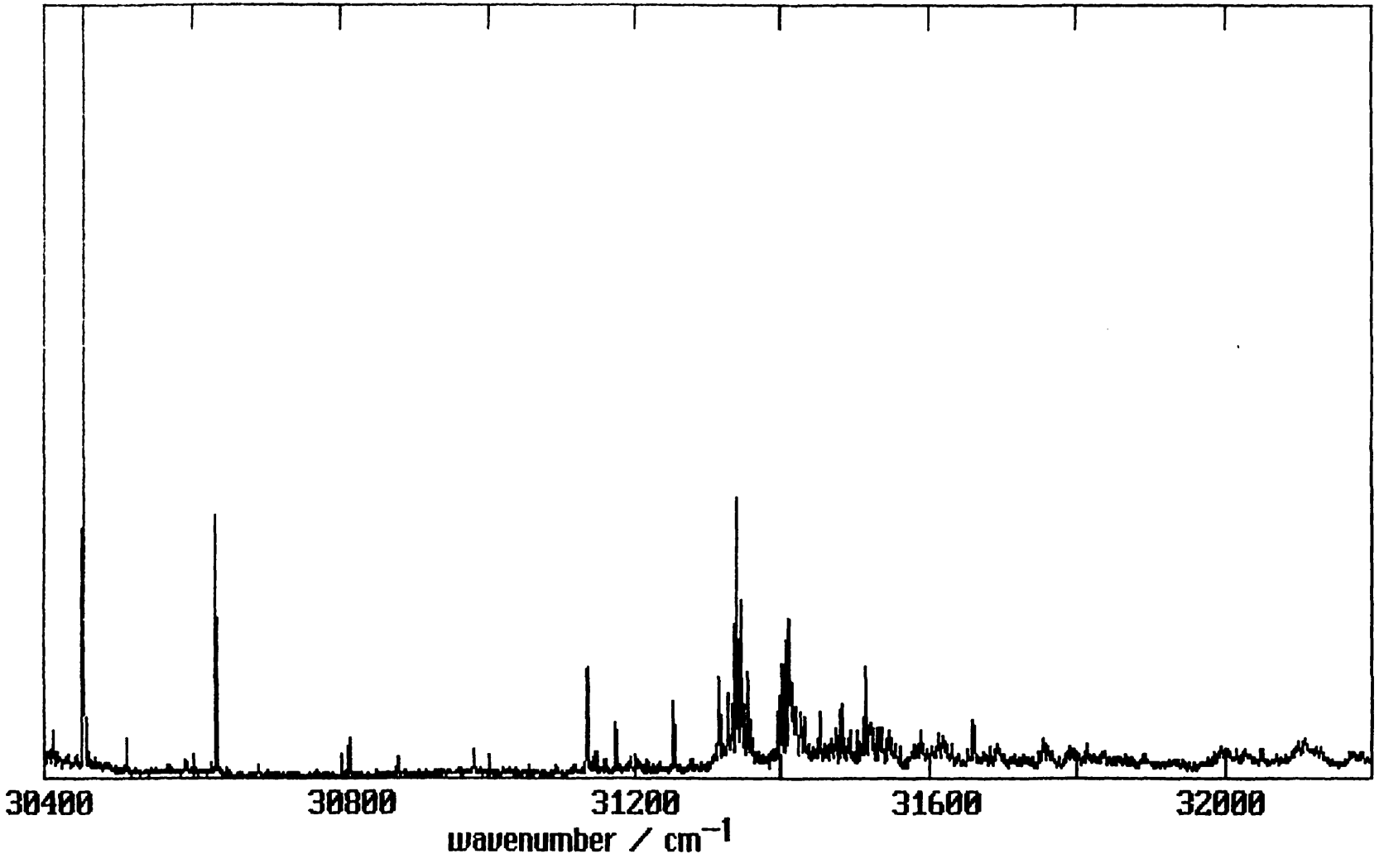

number of sharp vibronic transitions on a flat background. The lowest energy transition occurs at 30452.6cm^{-1} ± 2cm^{-1} and this feature is assigned as the vibrationless electronic origin of CPC. Relative shifts from the origin transition were reproducible to ± 0.5cm-1. An expanded spectrum of an observed dense region of transitions is depicted in figure 5.4. The energies, relative intensities and assignments of these observed transitions are listed as table 5.1.

5.2.2 Dispersed Fluorescence Spectra

The dispersed fluorescence spectrum of CPC following excitation at 30452.6cm^{-1}, ie excitation of the electronic origin, is shown in figure 5.5. The spectrum shows a number of sharp transitions on a flat background. Table 5.2 gives the relative energies, intensities and assignments of these bands. The resolution was ~10cm^{-1} fwhm. The intensity of the resonance band (emission at the same energy as excitation) contains a contribution of ~ 80% from scattered laser light, and the relative intensities of the transitions are normalised to account for this contribution. This contribution was determined by tuning the excitation slightly off the transition concerned and monitoring the intensity of the signal in resonance with the excitation wavelength, and then subtracting this intensity from the signal observed when exciting the transition. It has to be noted therefore that the relative intensities of the bands are accurate when compared to the first fluorescence band, but subject to large errors when compared with the resonance band. The emission

Figure 5.4 LIF excitation spectrum of CPC
expanded to show dense region of transitions

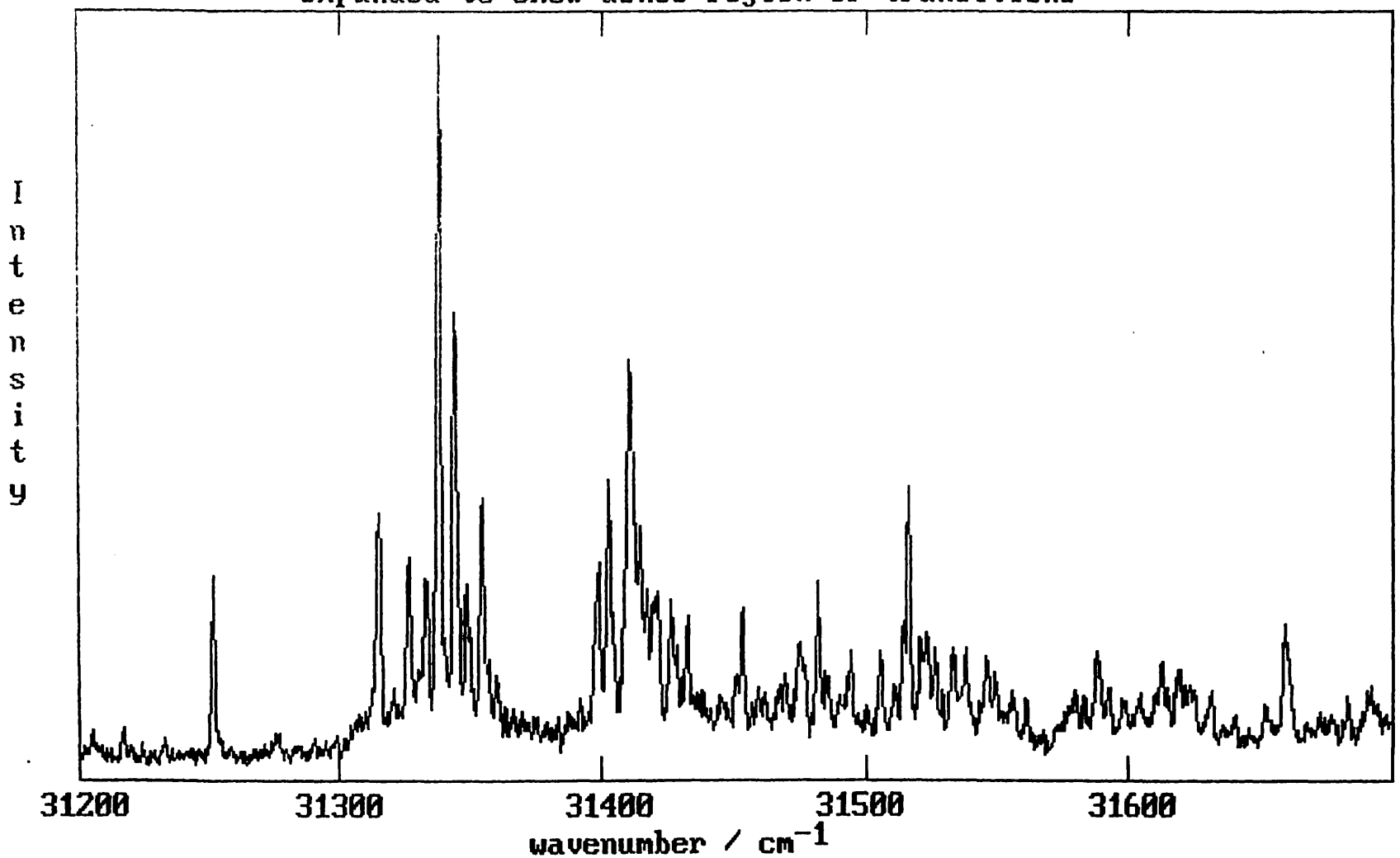

Table 5.1 Bands observed in the LIF excitation spectrum of jet cooled N-(4-cyanophenyl)carbazole.

Frequencies are quoted as wavenumber shift from the origin transition, occuring at 30452.6cm^{-1} ± 2cm^{-1}

Relative shift from 30452.6cm^{-1} / cm^{-1}	Relative Intensity.	Assignment
0.0	100	0(0,0)
57.2	6	τ
136.0	2	
172.4	2	
179.0	36	$a_1(203)$
235.4	1	$a_1(203) + \tau$?
357.8	5	2 x 179
424.1	2	$a_1(424)$
527.1	3	$b_2(529)$
682.7	12	$a_1(701)$
688.8	2	
694.7	2	
707.1	1	527.1 + 179
721.4	6	
741.0	1	
799.0	8	
861.6	10	682.7 + 179
873.0	8	
879.7	7	
884.2	30	$b_2(927)$
890.2	19	X
894.9	5	
900.5	11	X
944.3	8	
948.7	13	$a_1(982)$
956.3	19	$b_2(997)$?

Table 5.1 continued..

Relative shift from 30452.6cm^{-1} / cm^{-1}	Relative Intensity.	Assignment
960.1	11	X
966.9	7	
972.3	7	
1016.3	4	
1021.8	6	
1028.7	9	b_2(1033)
1041.1	6	682.7 + 2 x 179
1052.0	5	
1062.7	9	884.2 + 179
1068.7	6	890.2 + 179
1079.0	5	900.5 + 179
1084.5	5	
1092.6	5	
1102.3	4	
1107.8	3	
1126.8	3	948.7 + 179
1135.0	5	956.3 + 179
1159.4	5	
1166.1	4	
1177.8	3	
1206.3	8	1028.7 + 179
1229.8	4	
1239.1	4	
1301.9	5	

i) Values in parentheses refer to jet cooled N-ethylcarbazole intramolecular fundamentals[17]

ii) X denotes an intramolecular fundamental vibration that could not be assigned

iii) τ denotes a torsional mode of the N-C bond.

Figure 5.5 Dispersed fluorescence spectrum of jet cooled CPC after exciation of the origin transition

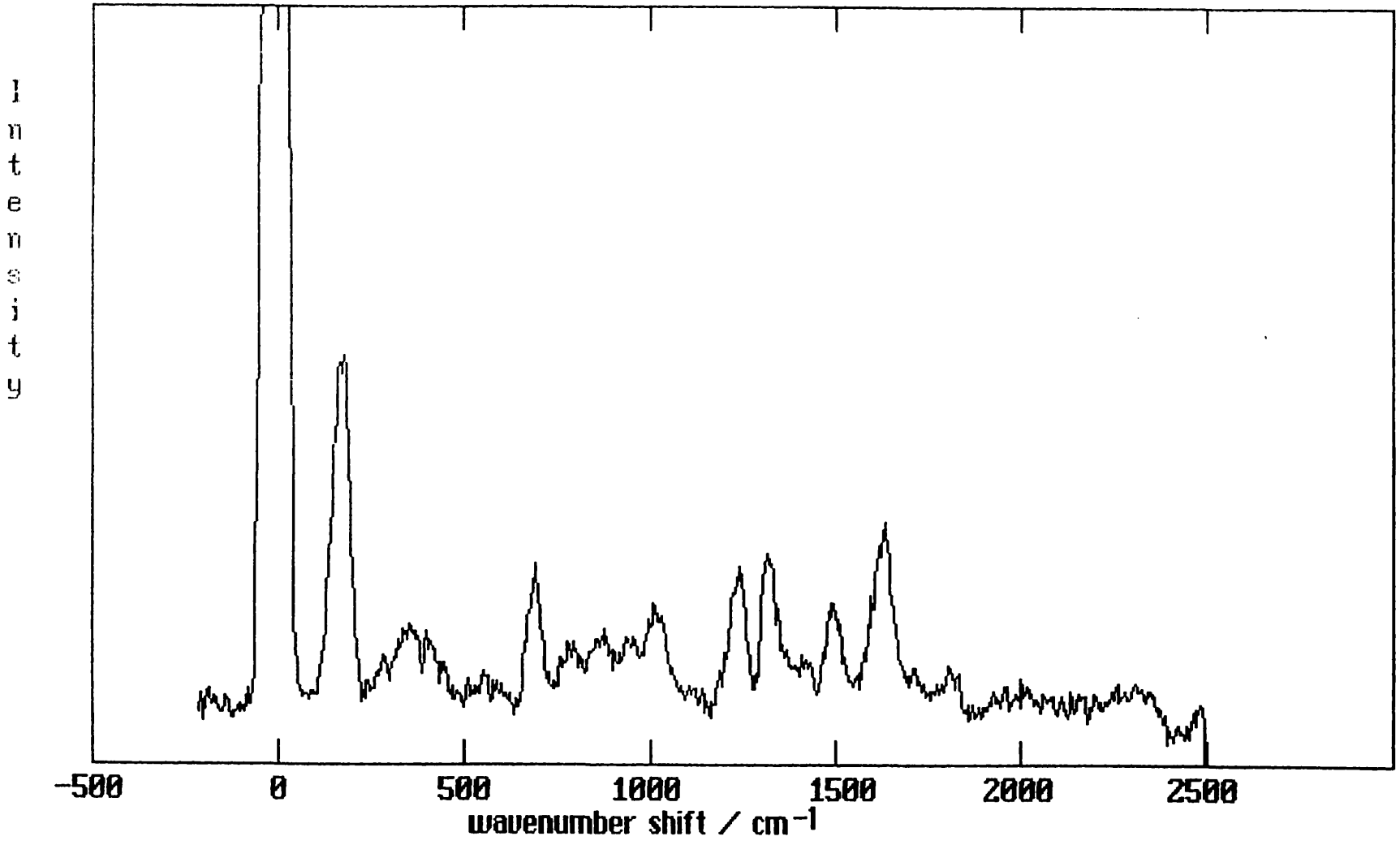

Table 5.2 Bands observed in the LIF emission spectrum of jet cooled N-(4-cyanophenyl)carbazole after excitation of the origin transition.

Relative shift / cm^{-1}	Relative Intensity.	Assignment
0.0	100	0(0,0)
180	20	$a_1(206)$
282	7	
358	8	2 x 179.6
405	7	$a_1(429)$
550	6	$b_2(554)$
581	4	
692	10	$a_1(714)$
791	8	
871	6	179.6 + 692.3
952	8	$b_2(967)$
1033	7	$b_2(1014)$
1236	9	
1317	10	$a_1(1308)$
1503	7	
1639	11	
1807	6	

spectrum recorded following excitation of the transition at 179cm^{-1} from the origin transition is shown in figure 5.6 and the relative shifts, intensities and assignments of the observed features are listed as table 5.3. The contribution to the resonance band from scattered light was ~60%.

The emission spectrum recorded following excitation of the feature at 884cm^{-1} from the origin transition, the most intense transition in the dense region of the spectrum, is shown in figure 5.7 and table 5.4 lists the relative shifts and intensities of the observed features. The shifts were reproducible only to ± 6cm^{-1} and at the resolution used it was not possible to assign any single vibrations. The contribution from scattered light in the resonance band was ~ 70%.

The emission spectrum recorded following excitation of the feature at 956cm^{-1} from the origin transition is shown in figure 5.8 and table 5.5 lists the relative shifts and intensities of the observed features. There was an estimated 70% contribution from scattered light, and at the resolution used it was not possible to resolve single vibronic level transitions and therefore assignments were not possible.

5.3 Discussion

The molecule CPC consists of a carbazole and a benzonitrile moiety connected via the carbazole nitrogen - benzonitrile carbon bond. The spectroscopy of CPC seems reminiscent of a perturbed carbazole spectrum rather than the spectrum for benzonitrile, indicating that the chromophore in CPC is

Figure 5.6 Dispersed fluorescence spectrum of jet cooled CPC after excitation of the 179cm^{-1} transition

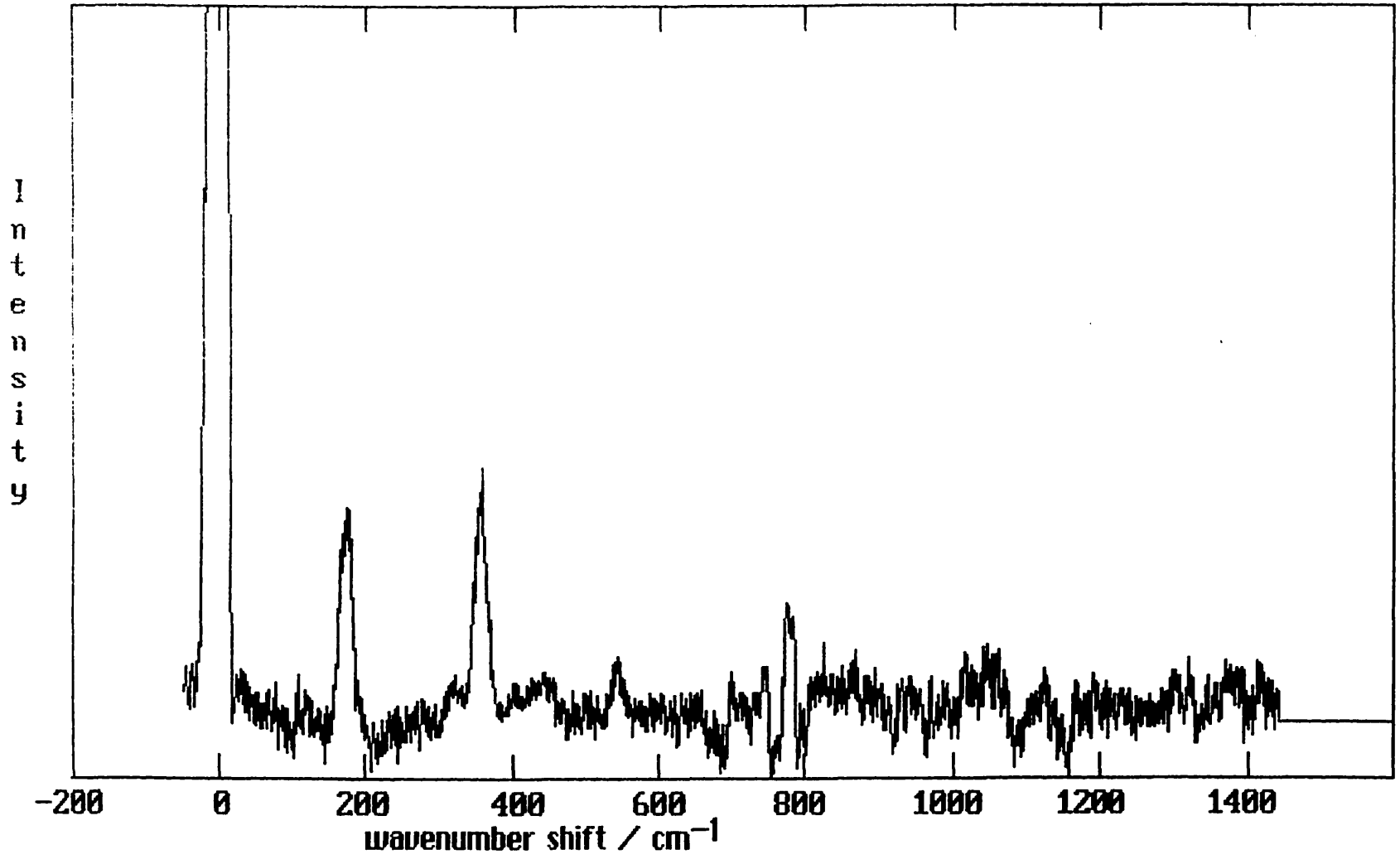

Table 5.3 Bands observed in the LIF emission spectrum of jet cooled N-(4-cyanophenyl)carbazole after excitation of the 179cm^{-1} transition.

Relative shift / cm^{-1}	Relative Intensity.	Assignment
0.0	100	
177	16	$a_1(206)$
358	18	2 x 177
544	5	$b_2(554)$
699	4	$a_1(714)$
744	4	
776	9	
1017	5	$b_2(1014)$
1051	5	
1125	4	

Figure 5.7 Dispersed Fluorescence Spectrum of jet cooled CPC after excitation of the 884cm^{-1} transition

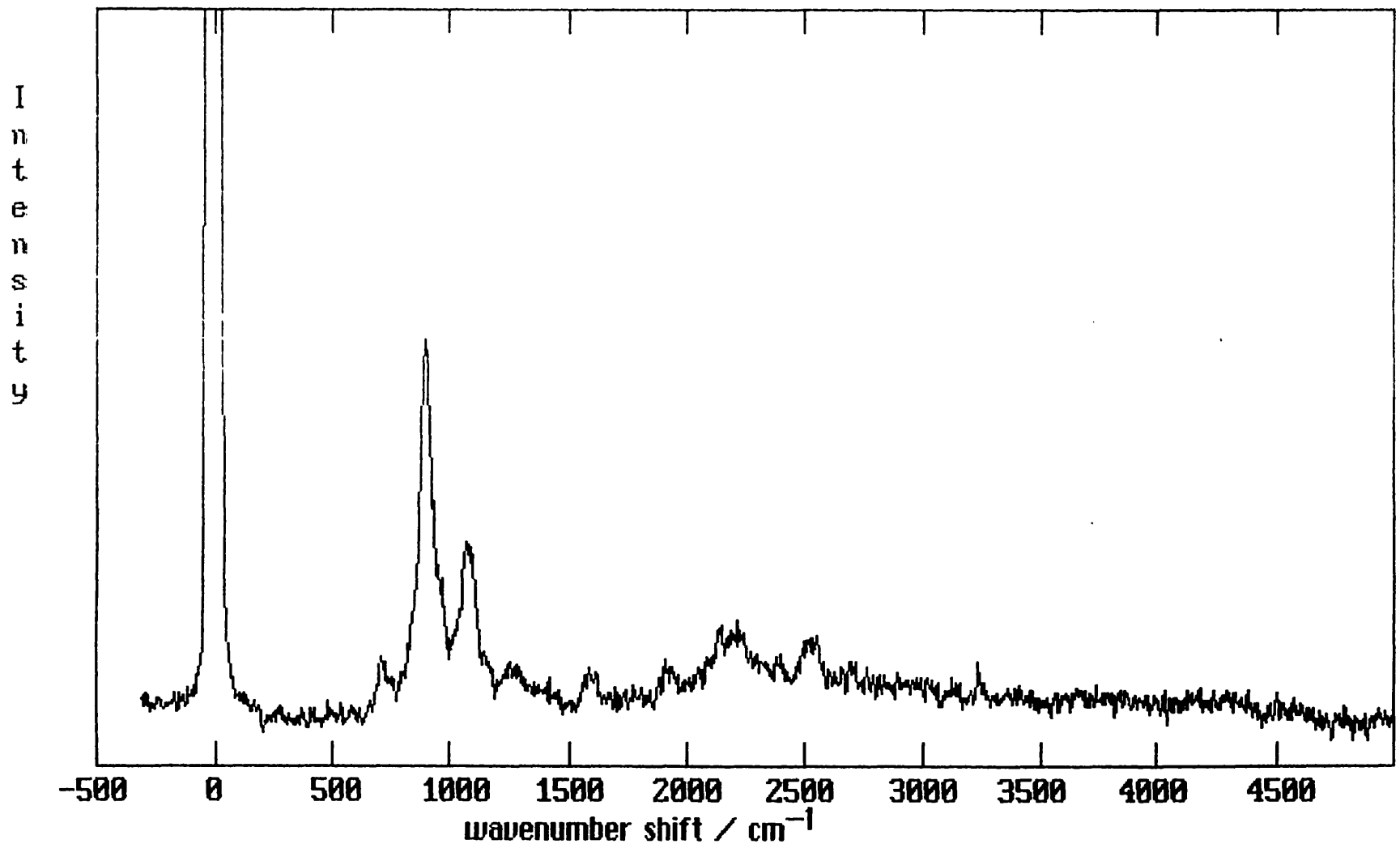

Figure 5.8 Dispersed Fluorescence Spectrum of jet cooled CPC after excitation of the 956cm^{-1} transition

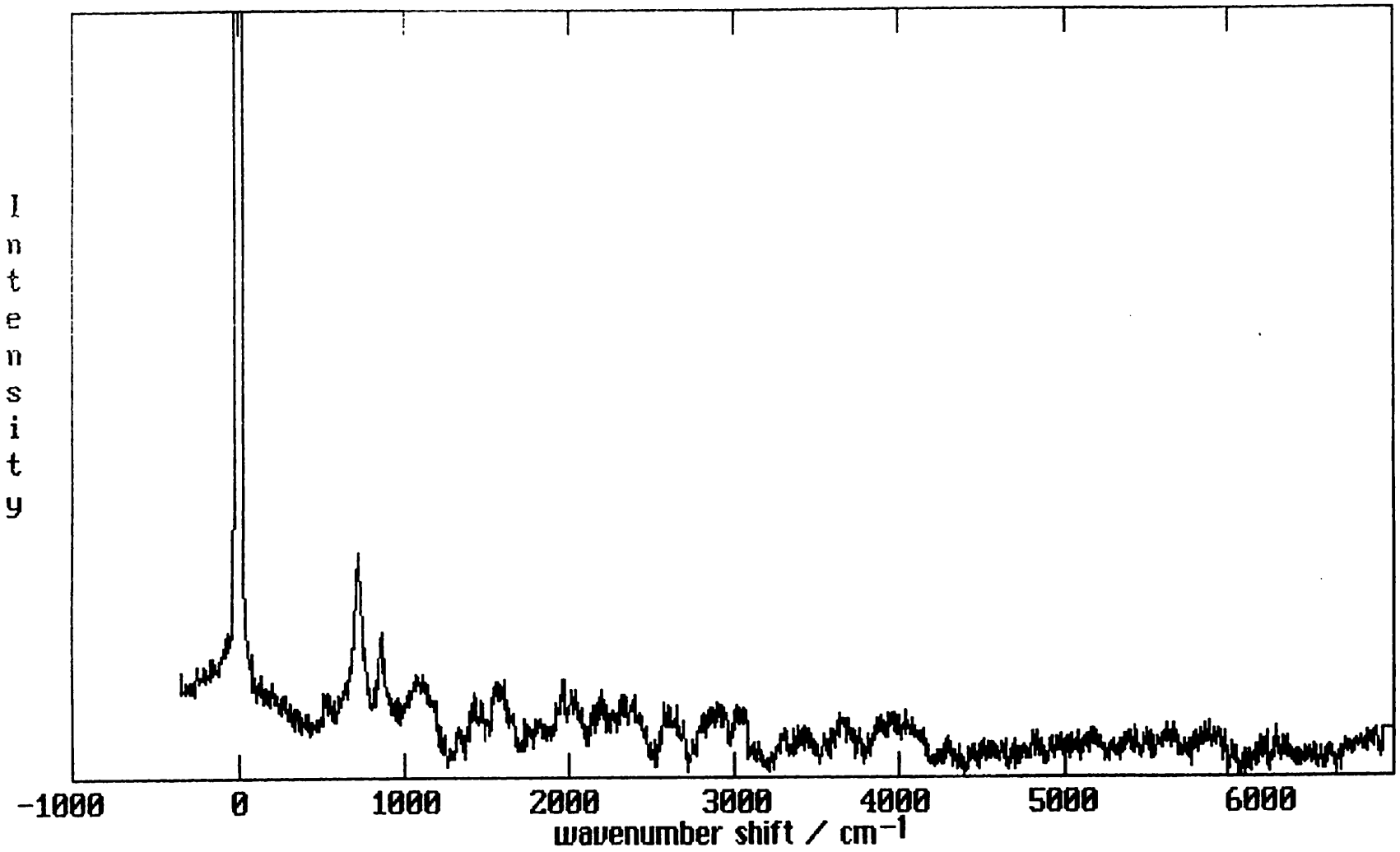

Table 5.4 Bands observed in the LIF emission spectrum of jet cooled N-(4-cyanophenyl)carbazole after excitation of the $884cm^{-1}$ transition.

Relative shift / cm_{-1}	Relative Intensity.	Assignment
0.0	100	
715	6	
894	31	
1088	14	
1268	5	
1919	5	
2196	8	
2552	7	

Table 5.5 Bands observed in the LIF emission spectrum of jet cooled N-(4-cyanophenyl)carbazole after excitation of the $956cm^{-1}$ transition.

Relative shift / cm^{-1}	Relative Intensity.	Assignment
0.0	100	
722	20	
864	11	
1097	4	
1593	4	

mainly associated with the carbazole moiety. The first electronic excited state of benzonitrile occurs at 36512cm^{-1} [16], and therefore cannot interact strongly with the S_1 state of carbazole occurring at 30809cm-1[15]. The S_2 state of carbazole lies ~4000cm^{-1} higher in energy[15] than the S_1 state so all the assignable features are due to the S_1 state, although b_2 symmetry features gain intensity through vibronic coupling to the S_2 state.

The similarity of the CPC spectra to those of carbazole and N-ethylcarbazole[17] leads to the assignment of the observed transitions in terms of the intramolecular fundamentals of these molecules. Similarly to carbazole[17] a progression is observed in the a_1 fundamental at 179cm^{-1} extending to two members. This vibration is strongly affected by phenyl substitution and is is shifted to a greater degree than for carbazole and N-ethylcarbazole. The excitation spectrum of CPC is characterised by a number of a_1 and b_2 symmetry fundamentals together with combination bands of these modes. The assignments are based on those of Auty et al[17] for carbazole and N-ethylcarbazole, which in turn are based upon the crystal work of Bree and Zwarich[18]. The electronic origin of CPC dominates the excitation spectrum, occurring at 30453cm^{-1}, which compares with 29654cm^{-1} for N-ethylcarbazole (obtained from chapter 4), and 30278cm^{-1} for the carbazole - benzonitrile complex origin[15]. The bathochromic shift of these relative to CPC implies that cyanophenyl substitution does not lower the S_1 excited state to such an extent as complexation or N-ethylation.

Unlike the spectra of other bi-aryls such as biphenyl and binapthyl there is a relative lack of low frequency torsional vibrations. This is believed to be due to the negligible change in molecular conformation upon excitation to the S_1 state of CPC. The ground state conformation of CPC is thought to be of C_{2v} symmetry where the two constituent moieties are orthogonal with respect to each other, and because of the similarity of the spectra to that of N-ethylcarbazole, CPC is thought to maintain C_{2v} symmetry upon excitation to the S_1 state. Any twisting of the molecule from an orthogonal conformation would reduce the symmetry to C_s and cause many more vibrations to become active in the spectrum. The relative lack of torsional vibrations is consistent with this conformation for the S_1 state, although there is one low frequency mode at $58cm^{-1}$ that is tentatively assigned as a torsion of the N-C bond. There is also some evidence that torsional modes become active at higher energies, as the excitation spectrum becomes considerably more complicated and very close vibrational spacings are observed. The spectrum in this region cannot readily be assigned in terms of intramolecular fundamentals. Some of the observed transitions are assigned as intramolecular fundamentals of CPC, the exact nature of which is uncertain, and these have been denoted X in the tables of assignments.

Under the expansion conditions used here there was no evidence of any red shifted emission attributable to TICT state formation, even at an excess excitation energy of $980cm^{-1}$. This leads to the conclusion that for the isolated CPC molecule charge transfer either does not occur, or there

is a high energy barrier, at least 980cm^{-1}, to CT state formation. As previously mentioned the lack of torsional information indicates the excited state conformation, which is the same as that in the ground state, is with the two moieties orthogonal so that there is no overlap between the π orbitals, disfavouring charge transfer. It is also worth noting that for carbazole electronic excitation results in charge transfer away from the nitrogen to the carbazole ring system[19], ie CT is in the opposite direction to that required for formation of a TICT state in CPC.

In summary the bichromophoric molecule N-(4-cyanophenyl)carbazole has spectroscopic behaviour that is characterised by that of a perturbed carbazole chromophore. In addition red shifted emission was not observed for the isolated jet cooled N-(4-cyanophenyl)carbazole, in contrast to that observed in solution phase experiments[14], implying that the role of the solvent is critical in affecting the conformation of the molecule and hence the formation of an intramolecular CT state. The work here represents only a preliminary study of CPC and an obvious extension to this work would be the investigation of the LIF excitation and emission spectra of CPC complexed with various solvents under jet cooled conditions.

5.4 References

1 A.Hargreaves and S.H.Rizvi,
Acta. Cryst. 15 (1962) 365.

2 H.Suzuki,
Bull. Chem. Soc. Japan 32 (1959) 1340.

3 J-I.Murakami, M.Ito and K.Kaya,
J. Chem. Phys. 74 (1981) 6505.

4 H.T.Jonkman and D.A.Wiersma,
Chem. Phys. Letters 97 (1983) 261.

5 H.T.Jonkman and D.A.Wiersma,
J. Chem. Phys. 81 (1984) 1573.

6 D.W.Werst, W.R.Gentry and P.F.Barbara,
J. Phys. Chem. 89 (1985) 729.

7 F.Schneider and E.Lippert,
Ber. Bunsenges. Phys. Chem. 72 (1968) 1155.

8 W.Liptay, G.Walz, W.Baumann, H.Schlosser,
H.Deckers and N.Detzer,
Z. Naturforsch. 26a (1971) 2020 and references therein.

9 F.Schneider and E.Lippert,
Ber. Bunsenges. Phys. Chem. 74 (1970) 624.

10 K.Yamasaki,K.Arita, O.Kajimoto and K.Hara,
Chem. Phys. Letters 123 (1986) 277.

11 L.R.Khundkar and A.H.Zewail,
J. Chem. Phys. 84 (1986) 1302.

12 O.Kajimoto, K.Yamasaki, K.Arita and K.Hara,
Chem. Phys. Letters 125 (1986) 184.

13 A.Subaric-Leitis, Ch.Monte, A.Roggan, W.Rettig,
P.Zimmermann and J.Heinze,
J. Chem. Phys. 93 (1990) 4543.

14 A.G.Taylor, PhD thesis, University of London (1989).

15 W.Rettig and M.Zander,
Chem. Phys. Letters 87 (1982) 229.

16 T.Kobayashi, K.Honma, O.Kajimoto and S.Tsuchiya,
J. Chem. Phys. 83 (1987) 1111.

17 A.R.Auty, PhD thesis, University of London (1986).

18 A.Bree and R.Zwarich,
J. Chem. Phys. 49 (1968) 3355.

19 W.Liptay
Mod. Quant. Chem. 3 Academic Press N.Y. (1965) p45.